The Development and Analysis of Atomistic-to-Continuum Coupling Methods

A DISSERTATION
SUBMITTED TO THE FACULTY OF THE GRADUATE SCHOOL
OF THE UNIVERSITY OF MINNESOTA
BY

Xingjie Helen Li

IN PARTIAL FULFILLMENT OF THE REQUIREMENTS
FOR THE DEGREE OF
Doctor of Philosophy

Mitchell Luskin, Advisor

June, 2012

Acknowledgements

My deepest gratitude goes to my advisor, Dr. Mitchell Luskin. During the past five years, he has built up my self-confidence, encouraged my dreams, and given me tremendous help in all aspects of my professional life, as well as personal development. I feel it is a privilege working and collaborating with him. His wisdom, advice, patience and trust has been a blessing during my graduate studies, and will have a profound influence in my future career. The research work in this dissertation is inspired by his ideas, and driven forward by his input and timely feedback through numerous meetings, discussions, and email correspondence.

I am also grateful to many faculty members in the School of Mathematics . I wish to thank Dr. Richard McGehee, Dr. Bryan Mosher, Dr. Christoph Ortner and Dr. Ellad Tadmor for their advice and help on my job application. I also thank Dr. Maria-Carme Calderer for writing various recommendation letters to support my Doctoral Dissertation Fellowship, AMS-Simons Travel Grants application, and job application.

I am grateful to Dr. Christoph Ortner and Dr. Alexander Shapeev for their great help on my research and professional life, and I appreciate Brian VanKoten, Alexander Miller, Liping Li and Dr. Chenyan Wu for their great help on my research and job application. I thank Denis A. Bashkirov and Dr. Hui Li for helping me revise the slides and presentations. Many staff and members of the University of Minnesota also brightened my days. I thank Ms. Bonny Fleming for helping me with the Doctoral Dissertation Fellowship application and all the required forms for the PhD program, and I thank Ms. Diane Trager for helping me collect and notice all the package and mails.

There are also many friends and family that have earned my gratitude. I thank Dr. Hui Li, Qixuan Wang, Yi Wang and Dr. Chenyan Wu for being my best friends for more than a decade: standing with me, offering me a shoulder that I can cry on, and

sharing joy in my accomplishments. I thank Dr. Ming Fang and Hsi-Wei Shih for taking me grocery shopping and keeping me away from hunger. In particular, I would like to thank my great friends from the Club of Amazing Mathematics & Engineering Ladies (CAMEL) at UMN, including Hao Zhu (Co-founder), Huiqiong Deng, Xiaoqing He, Hui Li, Zhihua Su, Yi Wang, and Lin Yang. My special thanks goes to my parents, who brought me up, provided me with excellent foods and education, and supported me learning abroad. Their unconditional love is always a harbor in my heart.

Dedication

To my mother Yuejuan Chen and my father Jisheng Li.

Abstract

Atomistic-to-continuum coupling methods (a/c methods) have been proposed to increase the computational efficiency of atomistic computations involving the interaction between local crystal defects with long-range elastic fields [1, 2, 3, 4, 5, 6, 7, 8]. The need for a more accurate atomistic-to-continuum (a/c) coupling method led me to develop and analyze several consistent multiscale models for my dissertation work.

With my advisor Dr. Mitchell Luskin, we gave a new formulation of the consistent a/c model for an atomistic chain that allows its extension to arbitrary finite range interactions for pair-interaction potentials. We also gave an analysis of the stability and accuracy of a linearization of the generalized quasi-nonlocal method that holds for strains up to lattice instabilities.

The Embedded Atom Method (EAM) model is a general empirical multi-body interatomic potential that was developed to model the behavior of metals such as copper and aluminum. I formulated a one-dimensional consistent EAM a/c method based on an aspect different from Shimokawa *et al.* [4] and W.E. *et al.* [5], and gave an analysis of the sharp stability and optimal accuracy for the model [9]. Furthermore, I have rigorously compared the lattice stability for atomistic chains modeled by the embedded atom method (EAM) with their approximation by local Cauchy–Born models in [10]. I find that a lattice modeled by the EAM undergoes a finite wave length instability at smaller strains than the expected long wave continuum instability.

Besides the energy-based models, an alternative approach to a/c couplings is the force-based quasicontinuum (QCF) approximation [11, 12, 1, 3, 13], first investigated mathematically by M. Dobson and M. Luskin. However, proving stability of the force-based quasicontinuum (QCF) model [14] remains an open problem [15, 12, 16]. In 1D and 2D, we show that by *blending* atomistic and Cauchy–Born continuum forces (instead of a sharp transition as in the QCF method) one obtains positive-definite blended force-based quasicontinuum (B-QCF) models. We establish sharp conditions on the required blending width.

Potential future development in the area of the a/c coupling models is also explored and discussed.

Contents

List of Figures

Chapter 1

Introduction to the Atomistic-to-Continuum Coupling Methods

Atomistic-to-continuum coupling methods (a/c methods) have been proposed to increase the computational efficiency of atomistic computations involving the interaction between local crystal defects with long-range elastic fields [1, 2, 3, 4, 5, 6, 7, 8]. Energy-based methods in this class, such as the quasicontinuum model (denoted QCE [17]) exhibit spurious interfacial forces ("ghost forces") even under uniform strain [18, 14]. The effect of the ghost force on the error in computing the deformation and the lattice stability by the QCE approximation has been analyzed in [14, 19, 20, 21]. The development of more accurate energy-based a/c methods is an ongoing process [4, 5, 22, 23, 24, 25]. The quasi-nonlocal energy (QNL) was the first quasicontinuum energy without ghost forces in the atomistic-to-continuum interface for a uniformly strained lattice [4]. The developers of the QNL method introduced interfacial atoms, which interacted with the atomistic region using the atomistic model and interacted with the continuum region using the continuum model. However, for a one dimensional chain, the original QNL method is restricted to next-nearest-neighbor interactions. Several papers extend the QNL model to more general cases [22, 26, 23, 9].

An alternative approach to a/c coupling is the force-based quasicontinuum (QCF)

approximation [11, 12, 1, 3, 13], but the non-conservative and indefinite equilibrium equations make the iterative solution and the determination of lattice stability more challenging [15, 12, 16]. Indeed, it is an open problem whether the (sharp-interface) QCF method is stable in dimension greater than one. The need for a more accurate atomistic-to-continuum (a/c) coupling method led me to develop and investigate several consistent multiscale models, which are discussed in the following.

The rest of this dissertation is organized as follows.

- The rest of Chapter 1 is to describe the notation used in the thesis.

- In Chapter 2, we formulate the one-dimensional QNL energy in terms of interactions rather than the energy contributions of individual atoms [21], which allows us to generalize the original QNL energy to arbitrary finite range interactions. A closely related method has been independently proposed and studied numerically for two and three dimensional problems by Shapeev in [22, 26].

  We also give an analysis of the stability and accuracy of a linearization of the generalized quasi-nonlocal method in the one dimensional case. The stability and optimal order error analysis for a linearization of the original QNL model with second nearest-neighbor interaction was analyzed for the one dimensional case in [27]. A nonlinear *a priori* and *a posteriori* error analysis for the QNL model with second nearest-neighbor interaction in one dimension was given in [28].

- Chapter 3 introduces a one-dimensional QNL energy for the embedded atom model (EAM) following [4]. The embedded atom model [29, 30, 31] is an empirical many-body potential that is widely used to model FCC metals such as copper and aluminum. We then give an analysis of the stability and error for the EAM-QNL approximation in the next-nearest neighbor case for a periodic chain.

  We identify conditions for the pair potential, electron density function, and embedding function so that the lattice stability of the atomistic and the EAM-QNL models are asymptotically equal. We also show in Remark 3.3.4 that the atomistic and EAM-QNL models can be less stable than the local quasicontinuum model (EAM-QCL), which is the EAM-QNL model with no atomistic region, if the above

conditions on the pair potential, electron density function, and embedding function are not satisfied.

- Material failure such as crack propagation and ductile fracture is due to lattice instability, and the prediction of the conditions that lead to material failure is the most important goal of many large-scale materials computations. In chapter 4, we have rigorously compared the lattice stability for atomistic chains modeled by the embedded atom method (EAM) with their approximation by local Cauchy–Born models. By computing the minimum eigenvalue of each linearized model, we find that a lattice modeled by the EAM undergoes a finite wave length instability at smaller strains than the expected long wave continuum instability. We also identify the critical assumptions for the pair potential, electron density function, and embedding function for the lattice stability. Both the volume-based local model and the reconstruction-based local model can give O(1) errors for the critical strain since the embedding energy density generally has positive curvature (see figures in [29, 30]). These observations reveal some unexpected results that may have significant consequences for the reliability of computational results obtained with the EAM model.

- Many blended a/c coupling methods have been proposed in the literature, e.g., [32, 33, 34, 35, 36, 37, 38, 39, 40]. In chapter 5, we formulate a blended force-based quasicontinuum (B-QCF) method, similar to the method proposed in [13], which smoothly blends the forces of the atomistic and continuum model instead of the sharp transition in the QCF method. In 1D and 2D, we establish sharp conditions under which a linearized B-QCF operator is positive definite.

  Our results have three advantages over the stability result proven in [13]. Firstly, we establish H^1-stability (instead of H^2-stability) which opens up the possibility to include defects in the analysis, along the lines of [41, 16]. Secondly, our conditions for the positive definiteness of the linearized B-QCF operator are needed to ensure the convergence of several popular iterative solution methods for the B-QCF equations [15]. We note that the convergence of these popular iterative solution methods for the QCF equations cannot be guaranteed because of its indefinite linearized operator [15]. Thirdly, our results admit much narrower blending

regions, which is crucial for the computational efficiency of the method.

- Chapter 6 points out possible future developments in the area of a/c coupling methods.

1.1 Notation

In this section, we present the notation used in the thesis. We define the scaled reference lattice

$$\epsilon\mathbb{Z} := \{\epsilon\ell : \ell \in \mathbb{Z}\},$$

where $\epsilon > 0$ scales the reference atomic spacing and $\mathbb{Z}$ is the set of integers. We then deform the reference lattice $\epsilon\mathbb{Z}$ uniformly into the lattice

$$F\epsilon\mathbb{Z} := \{F\epsilon\ell : \ell \in \mathbb{Z}\}$$

where $F > 0$ is the macroscopic deformation gradient, and we define the corresponding deformation $\mathbf{y}_F$ by

$$(\mathbf{y}_F)_\ell := F\epsilon\ell \quad \text{for } -\infty < \ell < \infty.$$

For simplicity, we consider the space $\mathcal{U}$ of $2N$-periodic zero mean displacements $\mathbf{u} = (u_\ell)_{\ell\in\mathbb{Z}}$ given by

$$\mathcal{U} := \left\{\mathbf{u} : u_{\ell+2N} = u_\ell \text{ for } \ell \in \mathbb{Z}, \text{ and } \sum_{\ell=-N+1}^{N} u_\ell = 0\right\},$$

and we thus admit deformations $\mathbf{y}$ from the space

$$\mathcal{Y}_F := \{\mathbf{y} : \mathbf{y} = \mathbf{y}_F + \mathbf{u} \text{ for some } \mathbf{u} \in \mathcal{U}\}.$$

We set $\epsilon = 1/N$ throughout so that the reference length of the periodic domain is fixed.

We define the discrete differentiation operator, $D\mathbf{u}$, on periodic displacements by

$$(D\mathbf{u})_\ell := \frac{u_\ell - u_{\ell-1}}{\epsilon}, \quad -\infty < \ell < \infty.$$

We note that $(D\mathbf{u})_\ell$ is also $2N$-periodic in ℓ and satisfies the zero mean condition. We will denote $(D\mathbf{u})_\ell$ by Du_ℓ. We then define

$$\left(D^{(2)}\mathbf{u}\right)_\ell := \frac{Du_\ell - Du_{\ell-1}}{\epsilon}, \qquad -\infty < \ell < \infty,$$

and we define $\left(D^{(3)}\mathbf{u}\right)_\ell$ and $\left(D^{(4)}\mathbf{u}\right)_\ell$ in a similar way. To make the formulas concise and more readable, we sometimes denote Du_ℓ by u'_ℓ, $D^{(2)}u_\ell$ by u''_ℓ, etc., when there is no confusion in the expressions.

For a displacement $\mathbf{u} \in \mathcal{U}$ and its discrete derivatives, we define the discrete ℓ^2_ϵ norms by

$$\|\mathbf{u}\|_{\ell^2_\epsilon} := \left(\epsilon \sum_{\ell=-N+1}^{N} |u_\ell|^2\right)^{1/2}, \qquad \|\mathbf{u}'\|_{\ell^2_\epsilon} := \left(\epsilon \sum_{\ell=-N+1}^{N} |u'_\ell|^2\right)^{1/2}, \text{ etc.}$$

Finally, for smooth real-valued functions $\mathcal{E}(\mathbf{y})$ defined for $\mathbf{y} \in \mathcal{Y}_F$, we define the first and second derivatives (variations) by

$$\langle \delta\mathcal{E}(\mathbf{y}), \mathbf{w}\rangle := \sum_{\ell=-N+1}^{N} \frac{\partial \mathcal{E}}{\partial y_\ell}(\mathbf{y}) w_\ell \qquad \text{for all } \mathbf{w} \in \mathcal{U},$$

$$\langle \delta^2\mathcal{E}(\mathbf{y})\mathbf{v}, \mathbf{w}\rangle := \sum_{\ell,\, m=-N+1}^{N} \frac{\partial^2 \mathcal{E}}{\partial y_\ell \partial y_m}(\mathbf{y}) v_\ell w_m \qquad \text{for all } \mathbf{v},\, \mathbf{w} \in \mathcal{U}.$$

Chapter 2

The QNL Approximation for Finite Range Interactions

2.1 Chapter Overview

In this chapter, we give a new formulation of the quasi-nonlocal method in one space dimension that allows its extension to arbitrary finite range interactions. We also give an analysis of the stability and accuracy of a linearization of our generalized quasi-nonlocal method that holds for strains up to lattice instabilities.

2.2 The Local QC Approximation and its Error

In this section, we first briefly describe the 1D atomistic chain model. We give the fully atomistic energy, $\mathcal{E}^a(\mathbf{Y})$, and then use linear interpolation to derive the coarse-grained local QC energy, $\mathcal{E}^{qc}(\mathbf{Y})$. We next compute and analyze the difference between these two energies. We then rescale the model and conclude that the coarse-grained local QC energy is formally a second order approximation (where the small parameter is lattice spacing scaled by the size of the macroscopic domain) to the fully atomistic energy when the strain gradient is small.

For simplicity, we assume that the infinite atomistic chain with positions $y_\ell < y_{\ell+1}$

has period $2N$, that is,

$$y_{\ell+1+2N} - y_{\ell+2N} = y_{\ell+1} - y_\ell \quad \forall \ell \in \mathbb{Z},$$

where $\mathbb{Z}$ is the set of integers. The total stored atomistic energy per period for an interaction potential, $\tilde{\phi}(r)$, with up to sth nearest-neighbor interactions is given by

$$\mathcal{E}^a(\mathbf{y}) := \sum_{k=1}^{s} \sum_{\ell=-N+1}^{N} \tilde{\phi}(y_{\ell+k-1} - y_{\ell-1}). \tag{2.1}$$

We note that $\mathcal{E}^a(\mathbf{y})$ can be rewritten as

$$\begin{aligned}
\mathcal{E}^a(\mathbf{y}) &= \sum_{k=1}^{s} \sum_{\ell=-N+1}^{N} \tilde{\phi}\big(k(y_\ell - y_{\ell-1})\big) \\
&\quad + \sum_{k=2}^{s} \sum_{\ell=-N+1}^{N} \left\{ \tilde{\phi}(y_{\ell+k-1} - y_{\ell-1}) - \frac{1}{k} \sum_{t=0}^{k-1} \tilde{\phi}\big(k(y_{\ell+t} - y_{\ell+t-1})\big) \right\} \\
&= \sum_{\ell=-N+1}^{N} \tilde{\phi}_{cb}(y_\ell - y_{\ell-1}) \\
&\quad + \sum_{k=2}^{s} \sum_{\ell=-N+1}^{N} \left\{ \tilde{\phi}(y_{\ell+k-1} - y_{\ell-1}) - \frac{1}{k} \sum_{t=0}^{k-1} \tilde{\phi}\big(k(y_{\ell+t} - y_{\ell+t-1})\big) \right\}
\end{aligned} \tag{2.2}$$

where

$$\tilde{\phi}_{cb}(\tilde{r}) := \sum_{k=1}^{s} \tilde{\phi}(k\,\tilde{r})$$

is the *Cauchy–Born* energy density [17, 27].

Intuitively, we can reduce the total amount of computation by first choosing $2M$, $M << N$, representative atoms in one period, linearly interpolating the positions of the remaining atoms, and then computing the total atomistic energy by using the interpolated positions. More precisely, we introduce the representative atoms with positions Y_j such that

$$Y_j = y_{\ell_j}, \quad j = -M, \ldots, M,$$

where the subindex ℓ_j for $j = -M, \ldots, M$ satisfies

$$-N = \ell_{-M} < \cdots < \ell_{j-1} < \ell_j < \cdots < \ell_M = N.$$

The representative atoms thus satisfy

$$Y_{-M} < \cdots < Y_{j-1} < Y_J < \cdots < Y_M.$$

We denote the number of atoms between Y_{j-1} and Y_j as $\tilde{\nu}_j$, and the distance separating the $\tilde{\nu}_j$ equally spaced atoms between Y_{j-1} and Y_j as $\tilde{r}_j$, that is,

$$\tilde{\nu}_j := \ell_j - \ell_{j-1} \quad \text{and} \quad \tilde{r}_j = (Y_j - Y_{j-1})/\tilde{\nu}_j \quad \text{for } j = -M+1, \ldots, M.$$

Then the positions of the atoms between Y_{j-1} and Y_j can be approximated by

$$y_{\ell_{j-1}+i} = y_{\ell_j - (\tilde{\nu}_j - i)} = Y_{j-1} + i\,\tilde{r}_j = \frac{\tilde{\nu}_j - i}{\tilde{\nu}_j} Y_{j-1} + \frac{i}{\tilde{\nu}_j} Y_j, \qquad 0 \le i \le \tilde{\nu}_j. \tag{2.3}$$

We thus have that

$$Y_{j-1} = y_{\ell_{j-1}} < y_{\ell_{j-1}+1} < \cdots < y_{\ell_j - (\tilde{\nu}_j - 1)} < y_{\ell_j} = Y_j, \qquad 0 \le i \le \tilde{\nu}_j.$$

We further assume that each $\tilde{\nu}_j$ is sufficiently large, i.e., $\tilde{\nu}_j \ge s$ for $j = -M+1, \ldots, M$. We can then observe for the atomistic deformations given by the interpolation (2.3) that

$$\tilde{\phi}(y_{\ell+k-1} - y_{\ell-1}) - \frac{1}{k}\sum_{t=0}^{k-1} \tilde{\phi}(k(y_{\ell+t} - y_{\ell+t-1}))$$
$$= \begin{cases} 0, & \ell_{j-1} < \ell < \ell_j - (k-2), \\ \tilde{\phi}\big((p+1)\tilde{r}_j + (k-p-1)\tilde{r}_{j+1}\big) - \frac{p+1}{k}\tilde{\phi}(k\tilde{r}_j) - \frac{k-p-1}{k}\tilde{\phi}(k\tilde{r}_{j+1}), & \ell = \ell_j - p,\ 0 \le p \le k-2. \end{cases}$$

Rearranging the terms in (2.2) and applying the equalities above, we can rewrite the total atomistic energy $\mathcal{E}^a(\mathbf{Y})$ as the sum of a coarse-grained local QC energy, $\mathcal{E}^{qc}(\mathbf{Y})$, and an interfacial energy:

$$\begin{aligned} \mathcal{E}^a(\mathbf{Y}) &= \sum_{k=1}^{s} \sum_{\ell=-N+1}^{N} \tilde{\phi}\big(k(y_\ell - y_{\ell-1})\big) \\ &\quad + \sum_{k=2}^{s} \sum_{\ell=-N+1}^{N} \left\{ \tilde{\phi}(y_{\ell+k-1} - y_{\ell-1}) - \frac{1}{k}\sum_{t=0}^{k-1} \tilde{\phi}\big(k(y_{\ell+t} - y_{\ell+t-1})\big) \right\} \\ &= \mathcal{E}^{qc}(\mathbf{Y}) + \sum_{j=-M+1}^{M} \mathcal{P}_j, \end{aligned} \tag{2.4}$$

where the coarse-grained local QC model is

$$\mathcal{E}^{qc}(\mathbf{Y}) := \sum_{j=-M+1}^{M} \tilde{\nu}_j \, \tilde{\phi}_{cb}(\tilde{r}_j), \tag{2.5}$$

and where the interfacial energy is

$$\mathcal{P}_j := \sum_{k=2}^{s} \sum_{p=1}^{k-1} \left\{ \tilde{\phi}\left(p\tilde{r}_j + (k-p)\tilde{r}_{j+1}\right) - \frac{p}{k}\tilde{\phi}(k\,\tilde{r}_j) - \frac{k-p}{k}\tilde{\phi}(k\,\tilde{r}_{j+1}) \right\}, \quad j = -M+1, \ldots, M.$$

We note that we have used the periodicity for the representative atoms chosen in one period. Therefore, we have that $\tilde{r}_{M+1} = \tilde{r}_{-M+1}$ and the definition of $\mathcal{P}_M$ makes sense.

To understand the difference between the atomistic energy $\mathcal{E}^a(\mathbf{Y})$ and the coarse-grained local QC energy $\mathcal{E}^{qc}(\mathbf{Y})$, we first evaluate the interfacial energy terms, namely $\mathcal{P}_j$, $j = -M+1, \ldots, M$. Using the Taylor expansion about $\frac{k}{2}(\tilde{r}_j + \tilde{r}_{j+1})$, we can estimate $\mathcal{P}_j$ by

$$\begin{aligned} \mathcal{P}_j = \sum_{k=2}^{s} \Bigg\{ & \frac{-k^3+k}{12}\tilde{\phi}''\left(\frac{k}{2}(\tilde{r}_j + \tilde{r}_{j+1})\right)(\tilde{r}_{j+1} - \tilde{r}_j)^2 \\ & + \mathtt{C}(k)\phi^{(4)}(k\eta_j)(\tilde{r}_{j+1} - \tilde{r}_j)^4 \Bigg\}, \quad j = -M+1, \ldots, M, \end{aligned} \tag{2.6}$$

where $\mathtt{C}(k)$ is calculated by

$$\mathtt{C}(k) = \frac{1}{384}\left[\sum_{p=1}^{k-1}(k-2p)^4 - k^4(k-1)\right],$$

and η_j is some number in the interval $[\tilde{r}_j, \tilde{r}_{j+1}]$.

2.2.1 Scaled Models

We next consider a scaled version of the atomistic and local QC energies. Thus, we define the two scaled interaction potentials $\phi(r)$ and $\phi_{cb}(r)$ by

$$\phi(r) = \frac{1}{\epsilon}\tilde{\phi}(r\epsilon) \quad \text{and} \quad \phi_{cb}(r) = \frac{1}{\epsilon}\tilde{\phi}_{cb}(r\epsilon)$$

where $\epsilon > 0$ scales the reference lattice. We can now convert (2.6) to the scaled form:

$$\begin{aligned} \mathcal{P}_j &\approx \sum_{k=2}^{s} \left\{ \frac{-k^3+k}{12}\tilde{\phi}''\left(\frac{k}{2}(\tilde{r}_j + \tilde{r}_{j+1})\right)(\tilde{r}_{j+1} - \tilde{r}_j)^2 \right\} \\ &= \epsilon \sum_{k=2}^{s} \left\{ \frac{-k^3+k}{12}\phi''\left(\frac{k}{2}(r_j + r_{j+1})\right)(r_j - r_{j+1})^2 \right\} \end{aligned} \tag{2.7}$$

where $r_j := \tilde{r}_j/\epsilon$.

Therefore, the total atomistic energy (2.4) has the scaled form

$$\begin{aligned}\mathcal{E}^a(\mathbf{Y}) &= \sum_{j=-M+1}^{M} \tilde{\nu}_j\, \tilde{\phi}_{cb}(\,\tilde{r}_j) + \sum_{j=-M+1}^{M} \mathcal{P}_j \\ &\approx \sum_{j=-M+1}^{M} \nu_j\, \phi_{cb}(r_j) + \epsilon \sum_{j=-M+1}^{M} (r_j - r_{j+1})^2 \sum_{k=2}^{s} \left\{ \frac{-k^3+k}{12} \phi''\left(\frac{k}{2}(r_j + r_{j+1})\right)\right\} \\ &= \mathcal{E}^{qc}(\mathbf{Y}) + \sum_{j=-M+1}^{M} H_{j+1} C_j \left[\epsilon H_{j+1} (Y''_{j+1})^2\right] \qquad (2.8)\end{aligned}$$

where

$$C_j := \sum_{k=2}^{s} \left\{ \frac{-k^3+k}{12} \phi''\left(\frac{k}{2}(Y'_j + Y'_{j+1})\right)\right\}$$

and

$$\begin{aligned} X_j &:= \epsilon \ell_j, & H_j &:= (X_j - X_{j-2})/2, \\ \nu_j &:= \epsilon \tilde{\nu}_j, & Y'_j &:= \frac{Y_j - Y_{j-1}}{X_j - X_{j-1}} = r_j, \\ Y''_j &:= \frac{Y'_j - Y'_{j-1}}{H_j}. \end{aligned}$$

Proposition 2.2.1 *The coarse-grained local QC energy $\mathcal{E}^{qc}(\mathbf{Y})$ is formally a second order approximation to the fully atomistic energy $\mathcal{E}^a(\mathbf{Y})$, or more precisely,*

$$\begin{aligned}\mathcal{E}^a(\mathbf{Y}) &= \mathcal{E}^{qc}(\mathbf{Y}) + \sum_{j=-M+1}^{M} H_{j+1} C_j \left[\epsilon H_{j+1} (Y''_{j+1})^2\right] + O\left(\sum_{j=-M+1}^{M} \epsilon H_{j+1}^4 (Y''_{j+1})^4\right), \\ &= \mathcal{E}^{qc}(\mathbf{Y}) + \sum_{j=-M+1}^{M} H_{j+1} C_j \left[\epsilon H_{j+1} (Y''_{j+1})^2\right] + O\left(\epsilon H^3\right)\end{aligned}$$

where $H = \max_j H_j$.

2.3 The Generalized Quasi-Nonlocal Approximation

From (2.8), we find that the difference between the atomistic energy and the coarse-grained local QC energy is formally of second order, i.e., $\max_j O(\epsilon H_j)$. However, when

the strain gradient is large in some regions, namely where $\epsilon H_j(Y_j'')^2$ is large, this error can be unacceptable. Hence, to maintain both accuracy and efficiency, we should use the atomistic model where the strain gradient is large and the local QC model where the strain gradient is moderate. In this section, we propose a hybrid atomistic-continuum coupling model that extends the quasi-nonlocal model [4] to include finite-range interactions. To simplify our analysis, we will propose and study our quasi-nonlocal model without coarsening, although the local QC region can be coarse-grained.

According to our assumption in Section 2.2, the total stored energy of the atomistic model per period (that includes up to the sth nearest neighbor pair interactions) in dimensionless form is

$$\mathcal{E}^a(\mathbf{y}) = \epsilon \sum_{\ell=-N+1}^{N} \sum_{k=1}^{s} \phi\left(\sum_{j=0}^{k-1} y'_{\ell+j}\right). \tag{2.9}$$

Here, the atomistic energy is a sum over the contributions from each bond and we can also rewrite it in terms of energy contributions of each atom,

$$\mathcal{E}^a(\mathbf{y}) = \epsilon \sum_{\ell=-N+1}^{N} E_\ell^a(\mathbf{y}), \quad \text{where}$$

$$E_\ell^a(\mathbf{y}) := \frac{1}{2}\sum_{k=1}^{s} \phi(\sum_{j=1}^{k} y'_{\ell+j}) + \frac{1}{2}\sum_{k=1}^{s} \phi(\sum_{j=0}^{k-1} y'_{\ell-j}).$$

If $\mathbf{y}$ is "smooth" near y_ℓ, i.e., $y'_{\ell+j}$ and $y'_{\ell-j}$ vary slowly near y_ℓ, then we can accurately approximate the distance between kth nearest-neighbors of y_ℓ by that of first nearest-neighbors to approximate $E_\ell^a(\mathbf{y})$ by $E_\ell^c(\mathbf{y})$, where

$$E_\ell^c(\mathbf{y}) := \frac{1}{2}\sum_{k=1}^{s} \left[\phi(k\, y'_\ell) + \phi(k\, y'_{\ell+1})\right] = \frac{1}{2}\left[\phi_{cb}(y'_\ell) + \phi_{cb}(y'_{\ell+1})\right].$$

If y'_ℓ is "smooth" outside of a region $\{-K, \ldots, K\}$, where $1 < K < N$, then the original quasicontinuum energy (denoted QCE)[17] uses the atomistic energy E_ℓ^a in the atomistic region $\mathcal{A} := \{-K, \ldots, K\}$ and the local QC energy E_ℓ^c in the continuum region $\mathcal{C} := \{-N+1, \ldots, N\} \setminus \mathcal{A}$ to obtain

$$\mathcal{E}^{qce}(\mathbf{y}) := \epsilon \sum_{\ell=-N+1}^{-K+1} E_\ell^c(\mathbf{y}) + \epsilon \sum_{\ell=-K}^{K} E_\ell^a(\mathbf{y}) + \epsilon \sum_{\ell=K+1}^{N} E_\ell^c(\mathbf{y}).$$

Although the idea of the QCE method is simple and appealing, there are interfacial forces (called ghost forces) even for uniform strain [3, 14]. The subsequent low order of consistency for the QCE method has been analyzed in [19, 20, 21].

The first quasicontinuum energy without a ghost force, the quasi-nonlocal energy (QNL), was proposed in [4]. The QNL energy introduced in [4] was restricted to next-nearest neighbor interactions which in 1D are next-nearest interactions. By understanding this method in terms of interactions rather than the energy contributions of "quasi-nonlocal" atoms, we have been able to extend the QNL energy (for pair potentials) to arbitrarily finite-range interactions while maintaining the uniform strain as an equilibrium (that is, there are no ghost forces). A generalization of the QNL energy to finite-range interactions from the point view of atoms was proposed in [5], but the construction requires the solution of large systems of linear equations that have so far not permitted a feasible general implementation. The interaction-based approach that we give here has been generalized to two space dimensions in [22, 26].

In our QNL energy, the nearest-neighbor interactions are left unchanged. A kth-nearest neighbor interaction $\phi\left(\sum_{j=0}^{k-1} y'_{\ell+j}\right)$ where $k \geq 2$ is left unchanged if at least one of the atoms $\ell + j : j = -1, \ldots, k-1$ belong to the atomistic region and is replaced by a Cauchy-Born approximation

$$\phi\left(\sum_{j=0}^{k-1} y'_{\ell+j}\right) \approx \frac{1}{k}\sum_{j=0}^{k-1} \phi\left(k\, y'_{\ell+j}\right) \tag{2.10}$$

if all atoms $\ell + j : j = -1, \ldots, k-1$ belong to the continuum region. We define

$$\begin{aligned} \mathcal{A}_{qnl}(k) &:= \{-K-k+1, -K-k+2, \ldots, K, K+1\}, \\ \mathcal{C}_{qnl}(k) &:= \{-N+1, \ldots, -K-k\} \bigcup \{K+2, \ldots, N\} \end{aligned} \tag{2.11}$$

for $k = 2, \ldots, s$. Then the our generalized QNL energy is given by

$$\begin{aligned} \mathcal{E}^{qnl}(\mathbf{y}) :=& \epsilon \sum_{\ell=-N+1}^{N} \phi(y'_\ell) + \epsilon \sum_{k=2}^{s} \sum_{\ell \in A_{qnl}(k)} \phi\left(\sum_{j=0}^{k-1} y'_{\ell+j}\right) \\ &+ \epsilon \sum_{k=2}^{s} \sum_{\ell \in C_{qnl}(k)} \frac{1}{k}\sum_{j=0}^{k-1} \phi\left(k y'_{\ell+j}\right). \end{aligned} \tag{2.12}$$

Since the forces at the atoms for the Cauchy-Born approximation (2.10) are unchanged for uniform strain, the QNL energy does not have ghost forces.

Proposition 2.3.1 *The QNL energy defined in* (2.12) *is consistent under a uniform deformation, i.e., it does not have a ghost force.*

Proof. The force at atom ℓ is defined to be $-\frac{\partial \mathcal{E}^{qnl}(\mathbf{y})}{\partial y_\ell}$, so from (2.12), we only need to verify that the approximation (2.10) is consistent under a uniform deformation. We note that

$$\frac{\partial}{\partial y_{\ell+m}}\phi\left(\sum_{j=0}^{k-1} y'_{\ell+j}\right)\Big|_{\mathbf{y}=\mathbf{y}_F} = \frac{\partial}{\partial y_{\ell+m}}\left[\frac{1}{k}\sum_{j=0}^{k-1}\phi\left(k y'_{\ell+j}\right)\right]\Big|_{\mathbf{y}=\mathbf{y}_F}, \qquad \forall m = -1,\ldots,k.$$

Therefore, the QNL energy is consistent. □

We note that the negative of the QNL forces for a general deformation $\mathbf{y}^{qnl} \in \mathcal{Y}_F$ is given by

$$\begin{aligned}\langle \delta\mathcal{E}^{qnl}(\mathbf{y}^{qnl}), \mathbf{w}\rangle = \epsilon \sum_{\ell=-N+1}^{N} \phi'(y'_\ell) w'_\ell + \epsilon \sum_{k=2}^{s}\sum_{\ell\in A_{qnl}(k)} \phi'\left(\sum_{t=0}^{k-1} y'_{\ell+j}\right)\left(\sum_{j=0}^{k-1} w'_{\ell+j}\right) \\ + \epsilon \sum_{k=2}^{s}\sum_{\ell\in C_{qnl}(k)}\sum_{j=0}^{k-1}\phi'\left(k\, y'_{\ell+j}\right) w'_{\ell+j} \quad \forall \mathbf{w}\in\mathcal{U}. \end{aligned} \tag{2.13}$$

2.4 Sharp Stability Analyses of Atomistic and QNL model

A sharp stability analysis for both the atomistic and QNL models are needed to determine whether the QNL approximation is accurate for strains near the limits of lattice stability. In this section, we will thus give stability analyses for both models. In order to provide clear statements and proofs, we first apply a similar method given in [21] to a third nearest-neighbor interaction range problem and then generalize the results to the finite range case.

2.4.1 Atomistic Model with Third Nearest-Neighbor Interaction Range

The total energy for the atomistic model given by a third nearest-neighbor interaction without external forces is

$$\mathcal{E}^a(\mathbf{y}) = \epsilon \sum_{\ell=-N+1}^{N} \phi(y'_\ell) + \phi(y'_\ell + y'_{\ell+1}) + \phi(y'_\ell + y'_{\ell+1} + y'_{\ell+2}). \tag{2.14}$$

It is easy to see that the uniform deformation $\mathbf{y}_F$ is an *equilibrium* of the atomistic model, that is,

$$\langle \delta \mathcal{E}^a(\mathbf{y}_F), \mathbf{w} \rangle = 0 \quad \forall \mathbf{w} \in \mathcal{U}.$$

We will say that the equilibrium $\mathbf{y}_F$ is *stable* for the atomistic model if $\delta^2 \mathcal{E}^a(\mathbf{y}_F)$ is positive definite, that is, if

$$\begin{aligned} \langle \delta^2 \mathcal{E}^a(\mathbf{y}_F)\mathbf{u}, \mathbf{u} \rangle = \epsilon \sum_{\ell=-N+1}^{N} \big(& \phi''_F |u'_\ell|^2 + \phi''_{2F} |u'_\ell + u'_{\ell+1}|^2 \\ & + \phi''_{3F} |u'_\ell + u'_{\ell+1} + u'_{\ell+2}|^2 \big) > 0 \quad \forall \mathbf{u} \in \mathcal{U} \setminus \{\mathbf{0}\} \end{aligned} \tag{2.15}$$

where

$$\phi''_F := \phi''(F), \ \phi''_{2F} := \phi''(2F), \dots, \phi''_{sF} := \phi''(sF).$$

We observe that

$$\begin{aligned} |u'_\ell + u'_{\ell+1}|^2 &= 2|u'_\ell|^2 + 2|u'_{\ell+1}|^2 - |u'_{\ell+1} - u'_\ell|^2, \\ |u'_\ell + u'_{\ell+1} + u'_{\ell+2}|^2 &= 3|u'_\ell|^2 + 3|u'_{\ell+1}|^2 + 3|u'_{\ell+2}|^2 \\ &\quad - 3\epsilon^2 |u''_{\ell+1}|^2 - 3\epsilon^2 |u''_{\ell+2}|^2 + \epsilon^2 |u''_{\ell+2} - u''_{\ell+1}|^2. \end{aligned} \tag{2.16}$$

Because of the periodicity of u'_ℓ, u''_ℓ in ℓ, we note that the sum of $u'_{\ell+1}$ from $-N+1$ to N is equal to the sum of u'_ℓ and the sum of $u''_{\ell+1}$ is equal to the sum of u''_ℓ, etc. So we can rewrite (2.15) and get the lower bound

$$\begin{aligned} \langle \delta^2 \mathcal{E}^a(\mathbf{y}_F)\mathbf{u}, \mathbf{u} \rangle &= \epsilon \sum_{\ell=-N+1}^{N} \big(\phi''_F + 4\phi''_{2F} + 9\phi''_{3F} \big) |u'_\ell|^2 - \epsilon \sum_{\ell=-N+1}^{N} \big(\epsilon^2 \phi''_{2F} + 6\epsilon^2 \phi''_{3F} \big) |u''_\ell|^2 \\ &\quad + \epsilon \sum_{\ell=-N+1}^{N} \big(\epsilon^2 \phi''_{3F} \big) |u''_{\ell+1} - u''_\ell|^2 \\ &= \big(\phi''_F + 4\phi''_{2F} + 9\phi''_{3F} \big) \|\mathbf{u}'\|^2_{\ell^2_\epsilon} - \big(\epsilon^2 \phi''_{2F} + 2\epsilon^2 \phi''_{3F} \big) \|\mathbf{u}''\|^2_{\ell^2_\epsilon} \\ &\quad - \epsilon \big(\epsilon^2 \phi''_{3F} \big) \sum_{\ell=-N+1}^{N} \big[4|u''_\ell|^2 - |u''_{\ell+1} - u''_\ell|^2 \big] \\ &\geq \big(\phi''_F + 4\phi''_{2F} + 9\phi''_{3F} \big) \|\mathbf{u}'\|^2_{\ell^2_\epsilon} - \epsilon^2 \big(\phi''_{2F} + 2\phi''_{3F} \big) \|\mathbf{u}''\|^2_{\ell^2_\epsilon} \end{aligned} \tag{2.17}$$

and since

$$\sum_{\ell=-N+1}^{N} 4|u''_\ell|^2 \geq \sum_{\ell=-N+1}^{N} \big[4|u''_\ell|^2 - |u''_{\ell+1} - u''_\ell|^2 \big] = \sum_{\ell=-N+1}^{N} \big[2|u''_\ell|^2 - 2u''_{\ell+1} u''_\ell \big] \geq 0,$$

the upper bound of $\langle \delta^2 \mathcal{E}^a(\mathbf{y}_F)\mathbf{u}, \mathbf{u}\rangle$ is

$$\langle \delta^2 \mathcal{E}^a(\mathbf{y}_F)\mathbf{u}, \mathbf{u}\rangle \le \big(\phi_F'' + 4\phi_{2F}'' + 9\phi_{3F}''\big)\|\mathbf{u}'\|_{\ell_\epsilon^2}^2 - \epsilon^2\big(\phi_{2F}'' + 6\phi_{3F}''\big)\|\mathbf{u}''\|_{\ell_\epsilon^2}^2. \tag{2.18}$$

We thus define

$$A_F^{(3)} := \phi_F'' + 4\phi_{2F}'' + 9\phi_{3F}'', \quad \mu_\epsilon := \inf_{\Psi\in\mathcal{U}\setminus\{\mathbf{0}\}} \frac{\|\Psi''\|_{\ell_\epsilon^2}}{\|\Psi'\|_{\ell_\epsilon^2}} = \frac{2\sin(\pi\epsilon/2)}{\epsilon}, \tag{2.19}$$

where the equality $\mu_\epsilon = \frac{2\sin(\pi\epsilon/2)}{\epsilon}$ is given in [21]. We then obtain the following stability result for the atomistic model.

Theorem 2.4.1 *Suppose $\phi_{2F}'' \le 0$, $\phi_{3F}'' \le 0$ and $\phi_{kF}'' = 0$ for $k \ge 4$. Then $\mathbf{y}_F$ is a stable equilibrium of the atomistic model if and only if $A_F^{(3)} - \epsilon^2\mu_\epsilon^2\big(\phi_{2F}'' + \eta\phi_{3F}''\big) > 0$ for $2 \le \eta \le 6$, where $A_F^{(3)}$ and μ_ϵ are defined in* (2.19).

2.4.2 The QNL Model with Third Nearest-Neighbor Interaction Range

The total energy for the QNL model given by a third nearest-neighbor interaction model without external forces is

$$\begin{aligned}\mathcal{E}^{qnl}(\mathbf{y}) = \epsilon\sum_{\ell=-N+1}^{N}\phi(y_\ell') + \epsilon\sum_{\ell\in A_{qnl}(2)}\phi\left(y_\ell' + y_{\ell+1}'\right) + \epsilon\sum_{\ell\in C_{qnl}(2)}\frac{1}{2}\big\{\phi(2y_\ell') + \phi(2y_{\ell+1}')\big\}\\ + \epsilon\sum_{\ell\in A_{qnl}(3)}\phi\left(y_\ell' + y_{\ell+1}' + y_{\ell+2}'\right) + \epsilon\sum_{\ell\in C_{qnl}(3)}\frac{1}{3}\big\{\phi(3y_\ell') + \phi(3y_{\ell+1}') + \phi(3y_{\ell+2}')\big\}.\end{aligned} \tag{2.20}$$

Since the QNL model does not have ghost forces, the uniform deformation $\mathbf{y}_F$ is still an equilibrium for (2.20). We thus focus on $\langle \delta^2 \mathcal{E}^{qnl}(\mathbf{y}_F)\mathbf{u}, \mathbf{u}\rangle$ to analyze the stability of the QNL model. We note that $\langle \delta^2 \mathcal{E}^{qnl}(\mathbf{y}_F)\mathbf{u}, \mathbf{u}\rangle$ can be written as

$$\begin{aligned}\langle \delta^2 \mathcal{E}^{qnl}(\mathbf{y}_F)\mathbf{u}, \mathbf{u}\rangle = \epsilon\sum_{\ell=-N+1}^{N}\phi_F''|u_\ell'|^2\\ + \epsilon\sum_{\ell\in A_{qnl}(2)}\phi_{2F}''|u_\ell' + u_{\ell+1}'|^2 + \epsilon\sum_{\ell\in C_{qnl}(2)}4\phi_{2F}''\left\{\frac{1}{2}|u_\ell'|^2 + \frac{1}{2}|u_{\ell+1}'|^2\right\}\\ + \epsilon\sum_{\ell\in A_{qnl}(3)}\phi_{3F}''|u_\ell' + u_{\ell+1}' + u_{\ell+2}'|^2\\ + \epsilon\sum_{\ell\in C_{qnl}(3)}9\phi_{3F}''\left\{\frac{1}{3}|u_\ell'|^2 + \frac{1}{3}|u_{\ell+1}'|^2 + \frac{1}{3}|u_{\ell+2}'|^2\right\}.\end{aligned} \tag{2.21}$$

Applying (2.16) to (2.21), we obtain

$$\begin{aligned}\langle \delta^2 \mathcal{E}^{qnl}(\mathbf{y}_F)\mathbf{u},\mathbf{u}\rangle &= A_F^{(3)}\|\mathbf{u}'\|_{\ell^2_\epsilon}^2 - \epsilon^3 \sum_{\ell\in A_{qnl}(2)} \phi''_{2F}|u''_{\ell+1}|^2 \\ &\quad - \epsilon^3 \sum_{\ell\in A_{qnl}(3)} \phi''_{3F}\left\{|u''_{\ell+1}|^2 + |u''_{\ell+2}|^2 + |u''_{\ell+2}-u''_{\ell+1}|^2\right\} \qquad (2.22)\\ &\geq A_F^{(3)}\|\mathbf{u}'\|_{\ell^2_\epsilon}^2.\end{aligned}$$

Since the lower bound in (2.22) is achieved by any displacement supported in the local region (which exists unless $K \in \{N-2, N-1, N\}$), it follows that $\mathbf{y}_F$ is stable in the generalized QNL model if and only if $A_F^{(3)} > 0$.

Theorem 2.4.2 *Suppose $\phi''_{2F} \leq 0$, $\phi''_{3F} \leq 0$ and $\phi''_{kF} = 0$ for $k \geq 4$. Then $\mathbf{y}_F$ is a stable equilibrium of the QNL model if and only if $A_F^{(3)} > 0$.*

We have given above a stability analyses of the atomistic model and the QNL model with a third-nearest neighbor interaction range. We now study the general case.

2.4.3 The Atomistic Model with sth Nearest-Neighbor Interaction Range

In the case of sth nearest neighbor interactions, the total energy for the atomistic model without external forces is

$$\mathcal{E}^a(\mathbf{y}) = \epsilon \sum_{\ell=-N+1}^{N}\sum_{k=1}^{s} \phi\left(\sum_{j=0}^{k-1} y'_{\ell+j}\right). \qquad (2.23)$$

The uniform deformation $\mathbf{y}_F$ is still its equilibrium, so the stability condition is

$$\langle \delta^2 \mathcal{E}^a(\mathbf{y}_F)\mathbf{u},\mathbf{u}\rangle = \epsilon \sum_{\ell=-N+1}^{N}\sum_{k=1}^{s} \phi''_{kF}\left(\sum_{j=0}^{k-1} u'_{\ell+j}\right)^2 > 0 \qquad \forall \mathbf{u}\in\mathcal{U}\setminus\{\mathbf{0}\}. \qquad (2.24)$$

We assume that $\phi''_F > 0$ and $\phi''_{kF} \leq 0$ for $k = 2, \ldots, s$. We first consider $\phi''_{kF}\left(\sum_{j=0}^{k-1} u'_{\ell+j}\right)^2$ for $k \geq 2$:

$$\begin{aligned}\phi''_{kF}\left(\sum_{j=0}^{k-1} u'_{\ell+j}\right)^2 &= \phi''_{kF}\sum_{j=0}^{k-1}\left(u'_{\ell+j}\right)^2 + \phi''_{kF}\sum_{j=0}^{k-2}\sum_{i=j+1}^{k-1} 2u'_{\ell+j}\,u'_{\ell+i} \qquad (2.25)\\ &= \phi''_{kF}\sum_{j=0}^{k-1}\left(u'_{\ell+j}\right)^2 + \phi''_{kF}\sum_{j=0}^{k-2}\sum_{i=j+1}^{k-1}\left\{\left(u'_{\ell+j}\right)^2 + \left(u'_{\ell+i}\right)^2 - \left(u'_{\ell+i}-u'_{\ell+j}\right)^2\right\}.\end{aligned}$$

Recalling that $u''_\ell := \frac{u'_\ell - u'_{\ell-1}}{\epsilon}$, we can further simplify (2.25) and get

$$\begin{aligned}\phi''_{kF}\left(\sum_{j=0}^{k-1} u'_{\ell+j}\right)^2 &= \phi''_{kF}\sum_{j=0}^{k-1}\left(u'_{\ell+j}\right)^2 + \phi''_{kF}\sum_{j=0}^{k-2}\sum_{i=j+1}^{k-1}\left\{\left(u'_{\ell+j}\right)^2 + \left(u'_{\ell+i}\right)^2\right\} \\ &\quad - \phi''_{kF}\epsilon^2\sum_{j=0}^{k-2}\sum_{i=j+1}^{k-1}\left(\sum_{t=j+1}^{i} u''_{\ell+t}\right)^2 \\ &\geq \phi''_{kF}\sum_{j=0}^{k-1}\left(u'_{\ell+j}\right)^2 + \phi''_{kF}\sum_{j=0}^{k-2}\sum_{i=j+1}^{k-1}\left\{\left(u'_{\ell+j}\right)^2 + \left(u'_{\ell+i}\right)^2\right\} \\ &\quad - \phi''_{kF}\epsilon^2\sum_{j=0}^{k-2}\left(u''_{\ell+j+1}\right)^2.\end{aligned} \tag{2.26}$$

The last inequality comes from the fact that $-\phi''_{kF}\epsilon^2 \geq 0$ for $k = 2, \ldots, s$, so we determine that the terms $i = j+2, \ldots, k-1$ in the third expression above are all nonnegative. Therefore, (2.24) becomes

$$\begin{aligned}&\langle \delta^2\mathcal{E}^a(\mathbf{y}_F)\mathbf{u}, \mathbf{u}\rangle \\ &\quad\geq \epsilon\sum_{\ell=-N+1}^{N}\phi''_F\left(u'_\ell\right)^2 \\ &\qquad + \sum_{k=2}^{s}\epsilon\sum_{\ell=-N+1}^{N}\phi''_{kF}\left\{\sum_{j=0}^{k-1}\left(u'_{\ell+j}\right)^2 + \sum_{j=0}^{k-2}\sum_{i=j+1}^{k-1}\left[\left(u'_{\ell+j}\right)^2 + \left(u'_{\ell+i}\right)^2\right] - \epsilon^2\sum_{j=0}^{k-2}\left(u''_{\ell+j+1}\right)^2\right\} \\ &\quad= \sum_{k=1}^{s} k^2\phi''_{kF}\|u'\|^2_{\ell^2_\epsilon} - \sum_{k=2}^{s}\epsilon^2\phi''_{kF}(k-1)\|u''\|^2_{\ell^2_\epsilon}.\end{aligned} \tag{2.27}$$

On the other hand, we can further study the third term in the fist line of (2.26) and rewrite it as:

$$\begin{aligned}&-\phi''_{kF}\epsilon^2\sum_{j=0}^{k-2}\sum_{i=j+1}^{k-1}\left(\sum_{t=j+1}^{i} u''_{\ell+t}\right)^2 \\ &\qquad= -\phi''_{kF}\epsilon^2\sum_{j=0}^{k-2}\sum_{i=j+1}^{k-1}\left[\sum_{t=j+1}^{i} {u''_{\ell+t}}^2 + \sum_{t=j+1}^{i-1}\sum_{s=t+1}^{i}\left({u''_{\ell+t}}^2 + {u''_{\ell+s}}^2\right)\right] \\ &\qquad\quad + \phi''_{kF}\epsilon^2\sum_{j=0}^{k-2}\sum_{i=j+1}^{k-1}\sum_{t=j+1}^{i-1}\sum_{s=t+1}^{i}\left(u''_{\ell+t} - u''_{\ell+s}\right)^2.\end{aligned}$$

Thus, we can use the first line of (2.26) and $\phi''_{kF} \le 0$, $k = 2, \dots, s$ to obtain an upper bound of $\phi''_{kF}\left(\sum_{j=0}^{k-1} u'_{\ell+j}\right)^2$:

$$\begin{aligned}\phi''_{kF}\left(\sum_{j=0}^{k-1} u'_{\ell+j}\right)^2 \le \phi''_{kF}\sum_{j=0}^{k-1}\left(u'_{\ell+j}\right)^2 + \phi''_{kF}\sum_{j=0}^{k-2}\sum_{i=j+1}^{k-1}\left\{\left(u'_{\ell+j}\right)^2 + \left(u'_{\ell+i}\right)^2\right\} \\ - \phi''_{kF}\epsilon^2\sum_{j=0}^{k-2}\sum_{i=j+1}^{k-1}\left[\sum_{t=j+1}^{i} {u''_{\ell+t}}^2 + \sum_{t=j+1}^{i-1}\sum_{s=t+1}^{i}\left({u''_{\ell+t}}^2 + {u''_{\ell+s}}^2\right)\right].\end{aligned} \tag{2.28}$$

Observing the last term of (2.28) and because of the periodicity condition of u''_ℓ, for each fixed k, we have that $\sum_{j=0}^{k-2}\sum_{i=j+1}^{k-1}\left[\sum_{t=j+1}^{i} {u''_{\ell+t}}^2 + \sum_{t=j+1}^{i-1}\sum_{s=t+1}^{i}\left({u''_{\ell+t}}^2 + {u''_{\ell+s}}^2\right)\right]$ is equivalent to $\sum_{j=0}^{k-2}\sum_{i=j+1}^{k-1}(i-j)^2|u''_\ell|^2 = \frac{k^4-k^2}{12}|u''_\ell|^2$. Thus, we can obtain the following upper bound of $\langle \delta^2\mathcal{E}^a(\mathbf{y}_F)\mathbf{u}, \mathbf{u}\rangle$:

$$\begin{aligned}\langle \delta^2\mathcal{E}^a(\mathbf{y}_F)\mathbf{u}, \mathbf{u}\rangle &\le \sum_{k=1}^{s} k^2\phi''_{kF}\|u'\|^2_{\ell^2_\epsilon} - \sum_{k=2}^{s}\epsilon^2\phi''_{kF}\sum_{j=0}^{k-1}\sum_{i=j+1}^{k-1}(i-j)^2\sum_{\ell=-N+1}^{N}\epsilon|u''_\ell|^2 \\ &= \sum_{k=1}^{s} k^2\phi''_{kF}\|u'\|^2_{\ell^2_\epsilon} - \sum_{k=2}^{s}\epsilon^2\phi''_{kF}\frac{k^4-k^2}{12}\|u''\|^2_{\ell^2_\epsilon}.\end{aligned} \tag{2.29}$$

Note that when $k = 2$, we have $\frac{k^4-k^2}{12} = 1 = k-1$, which means that the upper bound equals the lower bound if $s = 2$.

We next define

$$A^s_F := \sum_{k=1}^{s} k^2\phi''_{kF}, \tag{2.30}$$

and use the same notation for μ_ϵ defined in (2.19). We then obtain the following sharp stability estimate:

Theorem 2.4.3 *Suppose $\phi''_{kF} \le 0$ for $k = 2, \dots, s$. There exists a constant $B = B_F$ satisfying*

$$\sum_{k=2}^{s}(k-1)\phi''_{kF} \ge B_F \ge \phi''_{2F} + \sum_{k=3}^{s}\frac{k^4-k^2}{12}\phi''_{kF},$$

such that $\mathbf{y}_F$ is a stable equilibrium of the atomistic model if and only if $A^s_F - \epsilon^2\mu_\epsilon^2 B_F > 0$, where A^s_F is defined in (2.30) *and μ_ϵ is defined in* (2.19).

2.4.4 The QNL Model with sth Nearest-Neighbor Interaction Range

We now consider the stability of the QNL model in the general case. Again $\mathbf{y}_F$ is an equilibrium of the QNL model (2.13) when there is no external force, so we need to check whether

$$\langle \delta^2 \mathcal{E}^{qnl}(\mathbf{y}_F)\mathbf{u}, \mathbf{u}\rangle > 0, \quad \forall \mathbf{u} \in \mathcal{U} \setminus \{\mathbf{0}\},$$

where $\langle \delta^2 \mathcal{E}^{qnl}(\mathbf{y}_F)\mathbf{u}, \mathbf{u}\rangle$ is

$$\begin{aligned}
\langle \delta^2 \mathcal{E}^{qnl}(\mathbf{y}_F)\mathbf{u}, \mathbf{u}\rangle &= \epsilon \sum_{\ell=-N+1}^{N} \phi_F''(u_\ell')^2 + \epsilon \sum_{k=2}^{s} \sum_{\ell \in A_{qnl}(k)} \phi_{kF}'' \left(\sum_{j=0}^{k-1} u_{\ell+j}' \right)^2 \\
&\quad + \epsilon \sum_{k=2}^{s} \sum_{\ell \in C_{qnl}(k)} k \sum_{j=0}^{k-1} \phi_{kF}'' \left(u_{\ell+j}'\right)^2 \\
&= \epsilon \sum_{\ell=-N+1}^{N} \phi_F''(u_\ell')^2 \qquad (2.31) \\
&\quad + \epsilon \sum_{k=2}^{s} \sum_{\ell \in A_{qnl}(k)} \phi_{kF}'' \left\{ \sum_{j=0}^{k-1} \left(u_{\ell+j}'\right)^2 + \sum_{j=0}^{k-2} \sum_{i=j+1}^{k-1} \left[\left(u_{\ell+j}'\right)^2 + \left(u_{\ell+i}'\right)^2 \right] \right. \\
&\qquad \left. - \sum_{j=0}^{k-2} \sum_{i=j+1}^{k-1} \epsilon^2 \left(\sum_{t=j+1}^{i} u_{\ell+t}'' \right)^2 \right\} + \epsilon \sum_{k=2}^{s} \sum_{\ell \in C_{qnl}(k)} k \sum_{j=0}^{k-1} \phi_{kF}'' \left(u_{\ell+j}'\right)^2,
\end{aligned}$$

and for $k \geq 2$

$$\begin{aligned}
A_{qnl}(k) &= \{-K-k+1, -K-k+2, \ldots, K, K+1\}, \\
C_{qnl}(k) &= \{-N+1, \ldots, -K-k\} \bigcup \{K+2, \ldots, N\}.
\end{aligned}$$

Since $\phi''_{kF} \le 0$ when $k \ge 2$, (2.31) becomes

$$\begin{aligned}
\langle \delta^2 \mathcal{E}^{qnl}(\mathbf{y}_F)\mathbf{u}, \mathbf{u}\rangle &= \epsilon \sum_{\ell=-N+1}^{N} \phi''_F (u'_\ell)^2 + \epsilon \sum_{k=2}^{s} \sum_{\ell \in A_{qnl}(k)} \phi''_{kF} \left\{ \sum_{j=0}^{k-1} \left(u'_{\ell+j}\right)^2 \right. \\
&\qquad \left. + \sum_{j=0}^{k-2} \sum_{i=j+1}^{k-1} \left[\left(u'_{\ell+j}\right)^2 + \left(u'_{\ell+i}\right)^2 \right] - \sum_{j=0}^{k-2} \sum_{i=j+1}^{k-1} \epsilon^2 \left(\sum_{t=j+1}^{i} u''_{\ell+t} \right)^2 \right\} \\
&\qquad + \epsilon \sum_{k=2}^{s} \sum_{\ell \in C_{qnl}(k)} k \sum_{j=0}^{k-1} \phi''_{kF} \left(u'_{\ell+j}\right)^2 \\
&= A_F^s \|u'\|_{\ell^2_\epsilon}^2 - \epsilon \sum_{k=2}^{s} \epsilon^2 \phi''_{kF} \sum_{\ell \in A_{qnl}(k)} \sum_{j=0}^{k-2} \sum_{i=j+1}^{k-1} \epsilon^2 \left(\sum_{t=j+1}^{i} u''_{\ell+t} \right)^2 \\
&\ge A_F^s \|u'\|_{\ell^2_\epsilon}^2, \qquad (2.32)
\end{aligned}$$

where A_F^s is defined in (2.30). Since the lower bound in (2.32) is achieved by any displacement supported in the local region (which exists unless $K \in \{N-s+1, \ldots, N\}$), it follows that $\mathbf{y}_F$ is stable in the QNL model if and only if $A_F^s > 0$.

Theorem 2.4.4 *Suppose that $K < N - s + 1$ and that $\phi''_{kF} \le 0$ for $k = 2, \ldots, s$. Then $\mathbf{y}_F$ is a stable equilibrium of the QNL model if and only if $A_F^s > 0$.*

Remark 2.4.1 *From Theorem 2.4.3 and Theorem 2.4.4, we conclude that the difference between the sharp stability conditions of the fully atomistic and the QNL models is of order $O(\epsilon^2)$. This result is the same as for the pair potential case [11].*

2.5 Convergence of the QNL model

So far, we have investigated the stability of the fully atomistic model and the QNL model. In this section, we will give an optimal order error analysis for the QNL model. We compare the QNL solution with the atomistic solution and give an error estimate in terms of the deformation in the continuum region.

2.5.1 The Atomistic Model with External Dead Load

The total atomistic energy with an external dead load $\mathbf{f}$ is

$$\mathcal{E}^a_{tot}(\mathbf{y}) := \mathcal{E}^a(\mathbf{y}) + \mathcal{F}(\mathbf{y}) \qquad \forall \mathbf{y} \in \mathcal{Y}_F,$$

where

$$\mathcal{F}(\mathbf{y}) := -\sum_{\ell=-N+1}^{N} \epsilon f_\ell y_\ell.$$

To guarantee the existence of energy-minimizing deformations, we assume that the external loading force $\mathbf{f}$ is in $\mathcal{U}$. The equilibrium solution $\mathbf{y}^a \in \mathcal{Y}_F$ of the atomistic model with external force $\mathbf{f}$ then satisfies

$$-\langle \delta\mathcal{E}^a(\mathbf{y}^a), \mathbf{w}\rangle = \langle \delta\mathcal{F}(\mathbf{y}^a), \mathbf{w}\rangle \quad \forall \mathbf{w} \in \mathcal{U}, \tag{2.33}$$

where

$$\langle \delta\mathcal{E}^a(\mathbf{y}^a), \mathbf{w}\rangle = \epsilon \sum_{\ell=-N+1}^{N} \sum_{k=1}^{s} \sum_{j=0}^{k-1} \phi'\left(\sum_{t=0}^{k-1} Dy^a_{\ell+t}\right) w'_{\ell+j}, \tag{2.34}$$

and the external force is given by

$$\langle \delta\mathcal{F}(\mathbf{y}), \mathbf{w}\rangle := \sum_{\ell=-N+1}^{N} \frac{\partial \mathcal{F}}{\partial y_\ell}(\mathbf{y}) w_\ell = -\sum_{\ell=-N+1}^{N} \epsilon f_\ell w_\ell.$$

2.5.2 The General QNL Model with External Dead Load

The total energy of the QNL model corresponding to a deformation $\mathbf{y} \in \mathcal{Y}_F$ is

$$\mathcal{E}^{qnl}_{tot}(\mathbf{y}) := \mathcal{E}^{qnl}(\mathbf{y}) + \mathcal{F}(\mathbf{y})$$

So, the equilibrium solution $\mathbf{y}^{qnl} \in \mathcal{Y}_F$ satisfies

$$-\langle \delta\mathcal{E}^{qnl}(\mathbf{y}^{qnl}), \mathbf{w}\rangle = \langle \delta\mathcal{F}(\mathbf{y}^{qnl}), \mathbf{w}\rangle \quad \forall \mathbf{w} \in \mathcal{U}, \tag{2.35}$$

where

$$\begin{aligned}\langle \delta\mathcal{E}^{qnl}(\mathbf{y}^{qnl}), \mathbf{w}\rangle = \epsilon \sum_{\ell=-N+1}^{N} \phi'(y'_\ell) w'_\ell + \epsilon \sum_{k=2}^{s} \sum_{\ell \in A_{qnl}(k)} \phi'\left(\sum_{t=0}^{k-1} y'_{\ell+t}\right)\left(\sum_{j=0}^{k-1} w'_{\ell+j}\right) \\ + \epsilon \sum_{k=2}^{s} \sum_{\ell \in C_{qnl}(k)} \sum_{j=0}^{k-1} \phi'\left(k\, y'_{\ell+j}\right) w'_{\ell+j} \quad \forall \mathbf{w} \in \mathcal{U}.\end{aligned} \tag{2.36}$$

Setting $\mathbf{y}^{qnl} = \mathbf{y}_F + \mathbf{u}^{qnl}$ and $\mathbf{y}^a = \mathbf{y}_F + \mathbf{u}^a$, where both $\mathbf{u}^{qnl}$ and $\mathbf{u}^a$ belong to $\mathcal{U}$, we define the quasicontinuum error to be

$$\mathbf{e}^{qnl} := \mathbf{y}^a - \mathbf{y}^{qnl} = \mathbf{u}^a - \mathbf{u}^{qnl}.$$

To simplify the error analysis, we consider the linearization of the atomistic equilibrium equations (2.33) and the associated QNL equilibrium equations (2.35) about the uniform deformation $\mathbf{y}_F$. The linearized atomistic equation is

$$-\langle \delta^2 \mathcal{E}^a(\mathbf{y}_F)\,\mathbf{u}^a, \mathbf{w}\rangle = \langle \delta \mathcal{F}(\mathbf{y}_F), \mathbf{w}\rangle \quad \text{for all } \mathbf{w} \in \mathcal{U}, \tag{2.37}$$

and the linearized QNL equation is

$$-\langle \delta^2 \mathcal{E}^{qnl}(\mathbf{y}_F)\,\mathbf{u}^{qnl}, \mathbf{w}\rangle = \langle \delta \mathcal{F}(\mathbf{y}_F), \mathbf{w}\rangle \quad \text{for all } \mathbf{w} \in \mathcal{U}. \tag{2.38}$$

We thus analyze the linearized error equation

$$\langle \delta^2 \mathcal{E}^{qnl}(\mathbf{y}_F)\,\mathbf{e}^{qnl}, \mathbf{w}\rangle = \langle \mathbf{T}^{qnl}, \mathbf{w}\rangle \quad \text{for all } \mathbf{w} \in \mathcal{U}, \tag{2.39}$$

where the linearized consistency error is given by

$$\langle \mathbf{T}^{qnl}, \mathbf{w}\rangle := \langle \delta^2 \mathcal{E}^{qnl}(\mathbf{y}_F)\,\mathbf{u}^a, \mathbf{w}\rangle - \langle \delta^2 \mathcal{E}^{a}(\mathbf{y}_F)\,\mathbf{u}^a, \mathbf{w}\rangle. \tag{2.40}$$

To obtain an optimal order consistency error estimate, we extend the negative norm method given in [14, 28] to the sth nearest-neighbor truncation error functional

$$\langle \mathbf{T}^{qnl}, \mathbf{w}\rangle = \epsilon \sum_{k=2}^{s} \sum_{\ell \in C_{qnl}(k)} \phi''_{kF} \sum_{j=0}^{k-1} \left(kDu_{\ell+j} - \sum_{t=0}^{k-1} Du_{\ell+t} \right) Dw_{\ell+j}, \qquad \forall \mathbf{w} \in \mathcal{U}. \tag{2.41}$$

For each fixed k, we define $\mathbf{T}^{qnl}_k := \epsilon \phi''_{kF} \sum_{\ell \in C_{qnl}(k)} \sum_{j=0}^{k-1} \left(kDu_{\ell+j} - \sum_{t=0}^{k-1} Du_{\ell+t} \right)$. Then we have

$$\begin{aligned} \langle \mathbf{T}^{qnl}_k, \mathbf{w}\rangle &= \epsilon \phi''_{kF} \sum_{\ell=-N+1}^{-K-k} \sum_{j=0}^{k-1} \left(kDu_{\ell+j} - \sum_{t=0}^{k-1} Du_{\ell+t} \right) Dw_{\ell+j} \\ &\quad + \epsilon \phi''_{kF} \sum_{\ell=K+2}^{N} \sum_{j=0}^{k-1} \left(kDu_{\ell+j} - \sum_{t=0}^{k-1} Du_{\ell+t} \right) Dw_{\ell+j} \\ &= \epsilon \phi''_{kF} \sum_{\ell=K+2}^{2N-K-k} \sum_{j=0}^{k-1} \left(kDu_{\ell+j} - \sum_{t=0}^{k-1} Du_{\ell+t} \right) Dw_{\ell+j}. \end{aligned} \tag{2.42}$$

The last equality comes from the $2N$ periodicity of the model.

Note that we can change the indices, rearrange the order of summation of the sums in the last equality of (2.42), and rewrite it as the following expression

$$\begin{aligned}\langle \mathbf{T}_k^{qnl}, \mathbf{w}\rangle = \epsilon\phi''_{kF} \sum_{\ell=K+k+1}^{2N-K-k} \sum_{j=1}^{k} (k-j)\left(-Du_{\ell-j} + 2Du_\ell - Du_{\ell+j}\right) Dw_\ell \\ + \epsilon\phi''_{kF} \sum_{\ell=K+2}^{K+k} \sum_{j=0}^{\ell-(K+2)} \left(kDu_\ell - \sum_{t=0}^{k-1} Du_{\ell-j+t}\right) Dw_\ell \\ + \epsilon\phi''_{kF} \sum_{\ell=2N-K-2k+2}^{2N-K-k} \sum_{j=2N-K-k+1-\ell}^{k-1} \left(kDu_{\ell+j} - \sum_{t=0}^{k-1} Du_{\ell+t}\right) Dw_{\ell+j}.\end{aligned} \tag{2.43}$$

The first term of (2.43) corresponds to the inner continuum region, which is of second-order because of the symmetries of the interaction. The second and the third terms are the interfacial terms. They are only of first-order since they lose the symmetries of the interaction.

Now we will give an estimate of the consistency error $\langle \mathbf{T}^{qnl}, \mathbf{w}\rangle$ in the following theorem. We first define the following semi-norms:

$$\|\mathbf{v}\|^2_{\ell^2_\epsilon(\tilde{\mathcal{C}}_{qnl}(k))} := \epsilon \sum_{\ell\in\tilde{\mathcal{C}}_{qnl}(k)} v_\ell^2 \quad \text{and} \quad \|\mathbf{v}\|^2_{\ell^2_\epsilon(\mathcal{I}_{qnl}(k))} := \epsilon \sum_{\ell\in\mathcal{I}_{qnl}(k)} v_\ell^2,$$

where $\mathcal{I}_{qnl}(k) := \{-K-k+1, \ldots, -K-1\} \bigcup \{K+2, \ldots, K+k\}$ is the interface between the continuum and atomistic regions, $\tilde{\mathcal{C}}_{qnl}(k) := \mathcal{C}_{qnl}(k) \bigcup \mathcal{I}_{qnl}(k)$.

Theorem 2.5.1 *The consistency error $\langle \mathbf{T}^{qnl}, \mathbf{w}\rangle$, given in* (2.41)*, satisfies the following negative norm estimate*

$$\begin{aligned}\left|\langle \mathbf{T}^{qnl}, \mathbf{w}\rangle\right| \le \Bigg\{ \sum_{k=2}^{s} \epsilon^2 \mathtt{C}_1(k) |\phi''_{kF}| \|D^{(3)}\mathbf{u}\|_{\ell^2_\epsilon(\tilde{\mathcal{C}}_{qnl}(k))} \\ + \sum_{k=2}^{s} \epsilon \mathtt{C}_2(k) |\phi''_{kF}| \left(\sqrt{2s\epsilon}\right) \|D^{(3)}\mathbf{u}\|_{\ell^\infty_\epsilon(\mathcal{I}_{qnl}(k))} \Bigg\} \|D\mathbf{w}\|_{\ell^2_\epsilon},\end{aligned} \tag{2.44}$$

where $\mathtt{C}_1(k)$, $\mathtt{C}_2(k)$ are positive constants independent of ϵ.

Proof. From (2.43), we have

$$\left|\langle \mathbf{T}_k^{qnl}, \mathbf{w}\rangle\right| \le \epsilon^2 \mathtt{C}_1(k) |\phi''_{kF}| \|D^{(3)}\mathbf{u}\|_{\ell^2_\epsilon(\tilde{\mathcal{C}}_{qnl}(k))} \|D\mathbf{w}\|_{\ell^2_\epsilon} + \epsilon \mathtt{C}_2(k) |\phi''_{kF}| \|D^{(2)}\mathbf{u}\|_{\ell^2_\epsilon(\mathcal{I}_{qnl}(k))} \|D\mathbf{w}\|_{\ell^2_\epsilon}. \tag{2.45}$$

Therefore, we obtain an optimal order estimate for (2.41)

$$\left|\langle \mathbf{T}^{qnl}, \mathbf{w}\rangle\right| \leq \left[\sum_{k=2}^{s} \epsilon^2 \mathtt{C}_1(k)|\phi''_{kF}| \|D^{(3)}\mathbf{u}\|_{\ell^2_\epsilon(\tilde{\mathcal{C}}_{qnl}(k))} + \sum_{k=2}^{s} \epsilon \mathtt{C}_2(k)|\phi''_{kF}|\, \|D^{(2)}\mathbf{u}\|_{\ell^2_\epsilon(\mathcal{I}_{qnl}(k))}\right] \|D\mathbf{w}\|_{\ell^2_\epsilon}. \tag{2.46}$$

We note that we have

$$\begin{aligned}\|D^{(2)}\mathbf{u}\|^2_{\ell^2_\epsilon(\mathcal{I}_{qnl}(k))} &= \epsilon \sum_{\ell\in I(k)} \left(D^{(2)}\mathbf{u}_\ell\right)^2 \leq \epsilon \|D^{(2)}\mathbf{u}\|^2_{\ell^\infty_\epsilon(\mathcal{I}_{qnl}(k))} \sum_{\ell\in\mathcal{I}_{qnl}(k)} 1 \\ &\leq \epsilon\, 2s\, \|D^{(2)}\mathbf{u}\|^2_{\ell^\infty_\epsilon(\mathcal{I}_{qnl}(k))}.\end{aligned}$$

Thus, we can obtain from (2.46) the more concise (be weaker) estimate

$$\begin{aligned}\left|\langle \mathbf{T}^{qnl}, \mathbf{w}\rangle\right| \leq \Bigg\{&\sum_{k=2}^{s} \epsilon^2 \mathtt{C}_1(k)|\phi''_{kF}| \|D^{(3)}\mathbf{u}\|_{\ell^2_\epsilon(\tilde{\mathcal{C}}_{qnl}(k))} \\ &+ \sum_{k=2}^{s} \epsilon \mathtt{C}_2(k)|\phi''_{kF}|\, \left(\sqrt{2s\epsilon}\right) \|D^{(3)}\mathbf{u}\|_{\ell^\infty_\epsilon(\mathcal{I}_{qnl}(k))}\Bigg\} \|D\mathbf{w}\|_{\ell^2_\epsilon}.\end{aligned} \tag{2.47}$$

□

Theorem 2.5.2 *Suppose that $A^s_F > 0$, where A^s_F is defined in* (2.30)*. Then the linearized atomistic problem* (2.37) *as well as the linearized QNL approximation* (2.38) *have unique solutions, and they satisfy the error estimate*

$$\begin{aligned}\|D\mathbf{u}^a - D\mathbf{u}^{qnl}\|_{\ell^2_\epsilon} \leq &\frac{\sum_{k=2}^{s} \epsilon^2 \mathtt{C}_1(k)|\phi''_{kF}| \|D^{(3)}\mathbf{u}\|_{\ell^2_\epsilon(\tilde{\mathcal{C}}_{qnl}(k))}}{A^s_F} \\ &+ \frac{\sum_{k=2}^{s} \epsilon^{3/2}\left(\sqrt{2s}\right) \mathtt{C}_2(k)|\phi''_{kF}|\, \|D^{(3)}\mathbf{u}\|_{\ell^\infty_\epsilon(\mathcal{I}_{qnl}(k))}}{A^s_F}.\end{aligned}$$

Proof. This error estimate for the generalized QNL model follows from the error equation (2.39), the stability result (2.32), and the estimate of the truncation error (2.47). □

2.6 Conclusion

We propose a generalization of the one-dimensional QNL method to allow for arbitrary finite range interactions. We study the stability and convergence of a linearization of

the generalized QNL energy with arbitrary sth nearest-neighbor interaction range. We extend the methods given in [21, 11] to give sharp conditions under which the atomistic model and the QNL model are stable. The difference of the stability conditions between the QNL and atomistic model is shown to be of order $\mathrm{O}(\epsilon^2)$.

We then give a negative norm estimate for the truncation error and generalize the conclusions in [27] to the finite-range interaction case. We compare the equilibria of the generalized QNL model and the atomistic model and give an optimal order $\mathrm{O}(\epsilon^{3/2})$ error estimate for the strain in terms of the deformation in the continuum region.

Chapter 3

The QNL Approximation of the Embedded Atom Model

3.1 Chapter Overview

The Embedded Atom Model (EAM) is an empirical many-body potential which is widely used for FCC metals such as copper and aluminum. In this chapter, we consider the QNL method for EAM potentials, and we give a stability and error analysis for a chain with next-nearest neighbor interactions. We identify conditions for the pair potential, electron density function, and embedding function so that the lattice stability of the atomistic and the EAM-QNL models are asymptotically equal.

3.2 The Embedded Atom Model and Its QNL Approximation

We first give a description of the next-nearest neighbor EAM Model.

3.2.1 The Next-Nearest-Neighbor Embedded Atom Model

The total energy per period of the next-nearest neighbor EAM model is

$$\mathcal{E}^a_{tot}(\mathbf{y}) := \mathcal{E}^a(\mathbf{y}) + \mathcal{F}(\mathbf{y}) \tag{3.1}$$

for deformations $\mathbf{y} \in \mathcal{Y}_F$ where $\mathcal{E}^a(\mathbf{y})$ is the total atomistic energy and $\mathcal{F}(\mathbf{y})$ is the total external potential energy. The total atomistic energy is the sum of the *embedding energy*, $\hat{\mathcal{E}}^a(\mathbf{y})$, and the *pair potential energy*, $\tilde{\mathcal{E}}^a(\mathbf{y})$:

$$\mathcal{E}^a(\mathbf{y}) := \hat{\mathcal{E}}^a(\mathbf{y}) + \tilde{\mathcal{E}}^a(\mathbf{y}). \tag{3.2}$$

The embedding energy is

$$\hat{\mathcal{E}}^a(\mathbf{y}) := \epsilon \sum_{\ell=-N+1}^{N} G\left(\bar{\rho}^a_\ell(\mathbf{y})\right)$$

where $G(\bar{\rho})$ is the embedding energy function, the total electron density $\bar{\rho}^a_\ell(\mathbf{y})$ at atom ℓ is

$$\bar{\rho}^a_\ell(\mathbf{y}) := \rho(y'_\ell) + \rho(y'_\ell + y'_{\ell-1}) + \rho(y'_{\ell+1}) + \rho(y'_{\ell+1} + y'_{\ell+2}),$$

and $\rho(r/\epsilon)$ is the electron density contributed by an atom at distance r. The pair potential energy is

$$\tilde{\mathcal{E}}^a(\mathbf{y}) := \epsilon \sum_{\ell=-N+1}^{N} \frac{1}{2}\left[\phi(y'_\ell) + \phi(y'_\ell + y'_{\ell-1}) + \phi(y'_{\ell+1}) + \phi(y'_{\ell+1} + y'_{\ell+2})\right]$$

where $\epsilon\phi(r/\epsilon)$ is the pair potential interaction energy [29]. Our formulation allows general nonlinear external potential energies $\mathcal{F}(\mathbf{y})$ defined for $\mathbf{y} \in \mathcal{Y}_F$, but we note that the total external potential energy for periodic dead loads $\mathbf{f}$ is given by

$$\mathcal{F}(\mathbf{y}) := -\sum_{\ell=-N+1}^{N} \epsilon f_\ell y_\ell.$$

The equilibrium solution $\mathbf{y}^a$ of the EAM atomistic model (3.1) then satisfies

$$-\langle \delta\mathcal{E}^a(\mathbf{y}^a), \mathbf{w}\rangle = -\langle \delta\hat{\mathcal{E}}^a(\mathbf{y}^a), \mathbf{w}\rangle - \langle \delta\tilde{\mathcal{E}}^a(\mathbf{y}^a), \mathbf{w}\rangle = \langle \delta\mathcal{F}(\mathbf{y}^a), \mathbf{w}\rangle \quad \forall \mathbf{w} \in \mathcal{U}. \tag{3.3}$$

Here the negative of the embedding force of (3.3) is given by

$$\begin{aligned}\langle \delta\hat{\mathcal{E}}^a(\mathbf{y}^a), \mathbf{w}\rangle = \epsilon \sum_{\ell=-N+1}^{N} G'\Big(\bar{\rho}^a_\ell(\mathbf{y}^a)\Big) \cdot \Big[&\rho'(Dy^a_\ell)w'_\ell + \rho'(Dy^a_\ell + Dy^a_{\ell-1})(w'_\ell + w'_{\ell-1}) \\ &+ \rho'(Dy^a_{\ell+1})w'_{\ell+1} + \rho'(Dy^a_{\ell+1} + Dy^a_{\ell+2})(w'_{\ell+1} + w'_{\ell+2})\Big],\end{aligned}$$

the negative of the pair potential force of (3.3) is given by

$$\langle \delta\tilde{\mathcal{E}}^a(\mathbf{y}^a), \mathbf{w}\rangle = \epsilon \sum_{\ell=-N+1}^{N} \frac{1}{2}\Big[\phi'(Dy_\ell^a)w'_\ell + \phi'(Dy_\ell^a + Dy_{\ell-1}^a)(w'_\ell + w'_{\ell-1}) + \phi'(Dy_{\ell+1}^a)w'_{\ell+1} + \phi'(Dy_{\ell+1}^a + Dy_{\ell+2}^a)(w'_{\ell+1} + w'_{\ell+2})\Big]$$

and the external force is given by

$$\langle \delta\mathcal{F}(\mathbf{y}), \mathbf{w}\rangle = \sum_{\ell=-N+1}^{N} \frac{\partial \mathcal{F}}{\partial y_\ell}(\mathbf{y}) w_\ell \qquad \text{for all } \mathbf{w} \in \mathcal{U}.$$

3.2.2 The EAM-QNL Model for Next-Nearest-Neighbor Interactions

Hybrid atomistic-to-continuum methods can give an accurate and efficient solution if the deformation $\mathbf{y} \in \mathcal{Y}_F$ is "smooth" in most of the computational domain, but not in the remaining domain where defects occur [28, 14]. The goal of QC methods is to decompose the reference lattice into an atomistic region with defects and a continuum region with long-range elastic effects. It applies an atomistic model to the atomistic region for accuracy and a continuum model to the continuum region for efficiency.

In this paper, we will consider an atomistic region defined by the atoms with reference positions x_ℓ for $\ell = -K, \ldots, K$, and a continuum region for $\ell \in \{-N+1, \ldots, -(K+3)\} \cup \{(K+3), \ldots, N\}$. To eliminate the ghost force that energy-based quasicontinuum approximations can have [4, 3, 17, 27], we define the remaining atoms, $\pm(K+1), \pm(K+2)$, to be quasi-nonlocal atoms [4, 27]. For the pair potential energy, the quasi-nonlocal atoms $\pm(K+1), \pm(K+2)$ interact without approximation with atoms in the atomistic region, but interact through the continuum Cauchy-Born approximation with all other atoms [4]. The interactions of the quasi-nonlocal atoms for the embedding energy is slightly more complex, as given in [4] and below.

The atomistic energy associated with each atom is given by

$$\mathcal{E}_\ell^a(\mathbf{y}) := \hat{\mathcal{E}}_\ell^a(\mathbf{y}) + \tilde{\mathcal{E}}_\ell^a(\mathbf{y}) = G\left(\bar{\rho}_\ell^a(\mathbf{y})\right) + \frac{1}{2}\left[\phi(y'_\ell) + \phi(y'_\ell + y'_{\ell-1}) + \phi(y'_{\ell+1}) + \phi(y'_{\ell+1} + y'_{\ell+2})\right]$$

where $\hat{\mathcal{E}}_\ell^a(\mathbf{y})$ denotes the embedding energy at atom ℓ and $\tilde{\mathcal{E}}_\ell^a(\mathbf{y})$ denotes the pair potential energy at atom ℓ ($\hat{\mathcal{E}}_\ell^c(\mathbf{y})$, $\hat{\mathcal{E}}_\ell^{qnl}(\mathbf{y})$, $\tilde{\mathcal{E}}_\ell^c(\mathbf{y})$ and $\tilde{\mathcal{E}}_\ell^{qnl}(\mathbf{y})$ will be defined analogously

below), and the continuum energy associated with each atom is given by

$$\begin{aligned}\mathcal{E}^c_\ell(\mathbf{y}) := \hat{\mathcal{E}}^c_\ell(\mathbf{y}) + \tilde{\mathcal{E}}^c_\ell(\mathbf{y}) =& \frac{1}{2}G\left(\bar{\rho}^c_\ell(\mathbf{y})\right)) + \frac{1}{2}G\left(\bar{\rho}^c_{\ell+1}(\mathbf{y})\right) \\ &+ \frac{1}{2}\left[\phi(y'_\ell) + \phi(2y'_\ell) + \phi(y'_{\ell+1}) + \phi(2y'_{\ell+1})\right]\end{aligned}$$

where the total continuum electron density at atom ℓ is

$$\bar{\rho}^c_\ell(\mathbf{y}) := 2\rho(y'_\ell) + 2\rho(2y'_\ell).$$

To define the QNL energy for the quasi-nonlocal atoms, we define the QNL electron density at atom ℓ by

$$\bar{\rho}^{qnl}_\ell(\mathbf{y}) := 2\rho(y'_\ell) + 2\rho(y'_\ell + y'_{\ell-1}).$$

We then define the QNL energy for the quasi-nonlocal atoms by

$$\begin{aligned}\mathcal{E}^{qnl}_{K+1}(\mathbf{y}) :&= \hat{\mathcal{E}}^{qnl}_{K+1}(\mathbf{y}) + \tilde{\mathcal{E}}^{qnl}_{K+1}(\mathbf{y}) \\ &= \frac{1}{2}G\Big(\bar{\rho}^{qnl}_{K+1}(\mathbf{y})\Big) + \frac{1}{2}G\Big(\bar{\rho}^c_{K+2}(\mathbf{y})\Big) \\ &\quad + \frac{1}{2}\left[\phi(y'_{K+1}) + \phi(y'_{K+2}) + \phi(y'_{K+1} + y'_K) + \phi(2y'_{K+2})\right]\end{aligned}$$

and

$$\begin{aligned}\mathcal{E}^{qnl}_{K+2}(\mathbf{y}) :&= \hat{\mathcal{E}}^{qnl}_{K+2}(\mathbf{y}) + \tilde{\mathcal{E}}^{qnl}_{K+2}(\mathbf{y}) \\ &= \frac{1}{2}G\Big(\bar{\rho}^{qnl}_{K+2}(\mathbf{y})\Big) + \frac{1}{2}G\Big(\bar{\rho}^c_{K+3}(\mathbf{y})\Big) \\ &\quad + \frac{1}{2}\left[\phi(y'_{K+2}) + \phi(y'_{K+3}) + \phi(y'_{K+2} + y'_{K+1}) + \phi(2y'_{K+3})\right].\end{aligned}$$

We define the QNL energy in a symmetric way and so only give the formulas for $0 \leq \ell \leq N$.

The total energy per period of the QNL model is then given by

$$\begin{aligned}\mathcal{E}^{qnl}_{tot}(\mathbf{y}) &:= \epsilon \sum_{\ell=-N+1}^{N} \mathcal{E}^{qnl}_\ell(\mathbf{y}) + \mathcal{F}(\mathbf{y}) \\ &= \mathcal{E}^{qnl}(\mathbf{y}) + \mathcal{F}(\mathbf{y}) = \hat{\mathcal{E}}^{qnl}(\mathbf{y}) + \tilde{\mathcal{E}}^{qnl}(\mathbf{y}) + \mathcal{F}(\mathbf{y}),\end{aligned} \tag{3.4}$$

where

$$\mathcal{E}^{qnl}_\ell(\mathbf{y}) := \begin{cases} \mathcal{E}^a_\ell(\mathbf{y}) \quad \text{for} \quad 0 \leq \ell < K+1, \\ \mathcal{E}^{qnl}_\ell(\mathbf{y}) \quad \text{for} \quad \ell = K+1,\, K+2, \\ \mathcal{E}^c_\ell(\mathbf{y}) \quad \text{for} \quad K+2 < \ell < N. \end{cases}$$

The equilibrium solution $\mathbf{y}^{qnl}$ of the EAM-QNL model (3.4) then satisfies

$$-\langle \delta\mathcal{E}^{qnl}(\mathbf{y}^{qnl}), \mathbf{w}\rangle = -\langle \delta\hat{\mathcal{E}}^{qnl}(\mathbf{y}^{qnl}), \mathbf{w}\rangle - \langle \delta\tilde{\mathcal{E}}^{qnl}(\mathbf{y}^{qnl}), \mathbf{w}\rangle = \langle \delta\mathcal{F}(\mathbf{y}^{qnl}), \mathbf{w}\rangle \qquad \text{for all } \mathbf{w} \in \mathcal{U}, \tag{3.5}$$

where the negative of the embedding force is given by

$$\begin{aligned}
\langle \delta\hat{\mathcal{E}}^{qnl}(\mathbf{y}^{qnl}), \mathbf{w}\rangle = \ldots \\
&+ \epsilon \sum_{\ell=0}^{K} G'\big(\bar{\rho}_\ell^a(\mathbf{y}^{qnl})\big) \cdot \Big[\rho'(Dy_\ell^{qnl})w'_\ell + \rho'(Dy_\ell^{qnl} + Dy_{\ell-1}^{qnl})(w'_\ell + w'_{\ell-1}) \\
&\qquad\qquad + \rho'(Dy_{\ell+1}^{qnl})w'_{\ell+1} + \rho'(Dy_{\ell+1}^{qnl} + Dy_{\ell+2}^{qnl})(w'_{\ell+1} + w'_{\ell+2})\Big] \\
&+ \epsilon G'\big(\bar{\rho}_{K+1}^{qnl}(\mathbf{y}^{qnl})\big) \cdot \Big[\rho'(Dy_{K+1}^{qnl})w'_{K+1} + \rho'(Dy_{K+1}^{qnl} + Dy_K^{qnl})(w'_{K+1} + w'_K)\Big] \\
&+ \epsilon G'\big(\bar{\rho}_{K+2}^{c}(\mathbf{y}^{qnl})\big) \cdot \Big[\rho'(Dy_{K+2}^{qnl})w'_{K+2} + 2\rho'(2Dy_{K+2}^{qnl})(w'_{K+2})\Big] \\
&+ \epsilon G'\big(\bar{\rho}_{K+2}^{qnl}(\mathbf{y}^{qnl})\big) \cdot \Big[\rho'(Dy_{K+2}^{qnl})w'_{K+2} + \rho'(Dy_{K+2}^{qnl} + Dy_{K+1}^{qnl})(w'_{K+2} + w'_{K+1})\Big] \\
&+ \epsilon G'\big(\bar{\rho}_{K+3}^{c}(\mathbf{y}^{qnl})\big) \cdot \Big[\rho'(Dy_{K+3}^{qnl})w'_{K+3} + 2\rho'(2Dy_{K+3}^{qnl})(w'_{K+3})\Big] \\
&+ \epsilon \sum_{\ell=K+3}^{N} \Big\{ G'\big(\bar{\rho}_\ell^c(\mathbf{y}^{qnl})\big) \cdot \Big[\rho'(Dy_\ell^{qnl})w'_\ell + 2\rho'(2Dy_\ell^{qnl})(w'_\ell)\Big] \\
&\qquad\qquad + G'\big(\bar{\rho}_{\ell+1}^c(\mathbf{y}^{qnl})\big) \cdot \Big[\rho'(Dy_{\ell+1}^{qnl})w'_{\ell+1} + 2\rho'(2Dy_{\ell+1}^{qnl})(w'_{\ell+1})\Big]\Big\},
\end{aligned} \tag{3.6}$$

and the negative of the pair potential force is given by

$$\begin{aligned}
\langle \delta\tilde{\mathcal{E}}^{qnl}(\mathbf{y}^{qnl}), \mathbf{w}\rangle = \ldots \\
&+ \epsilon \sum_{\ell=0}^{K} \frac{1}{2}\Big[\phi'(Dy_\ell^{qnl})w'_\ell + \phi'(Dy_\ell^{qnl} + Dy_{\ell-1}^{qnl})(w'_\ell + w'_{\ell-1}) \\
&\qquad\qquad + \phi'(Dy_{\ell+1}^{qnl})w'_{\ell+1} + \phi'(Dy_{\ell+1}^{qnl} + Dy_{\ell+2}^{qnl})(w'_{\ell+1} + w'_{\ell+2})\Big] \\
&+ \frac{\epsilon}{2}\Big[\phi'(Dy_{K+1}^{qnl})w'_{K+1} + \phi'(Dy_{K+1}^{qnl} + Dy_K^{qnl})(w'_{K+1} + w'_K)\Big] \\
&\quad + \frac{\epsilon}{2}\Big[\phi'(Dy_{K+2}^{qnl})w'_{K+2} + 2\phi'(2Dy_{K+2}^{qnl})(w'_{K+2})\Big] \\
&+ \frac{\epsilon}{2}\Big[\phi'(Dy_{K+2}^{qnl})w'_{K+2} + \phi'(Dy_{K+2}^{qnl} + Dy_{K+1}^{qnl})(w'_{K+2} + w'_{K+1})\Big] \\
&\quad + \frac{\epsilon}{2}\Big[\phi'(Dy_{K+3}^{qnl})w'_{K+3} + 2\phi'(2Dy_{K+3}^{qnl})(w'_{K+3})\Big] \\
&+ \epsilon \sum_{\ell=K+3}^{N} \frac{1}{2}\Big[\phi'(Dy_\ell^{qnl})w'_\ell + 2\phi'(2Dy_\ell^{qnl})w'_\ell + \phi'(Dy_{\ell+1}^{qnl})w'_{\ell+1} + 2\phi'(2Dy_{\ell+1}^{qnl})w'_{\ell+1}\Big].
\end{aligned} \tag{3.7}$$

3.3 Stability Analysis of The Atomistic and EAM-QNL Models

In this section, we will give a stability analysis for the atomistic model and the EAM-QNL model for the next-nearest neighbor case. We will use techniques similar to those presented in [21] for the atomistic and QNL method for pair potentials.

3.3.1 The Atomistic Model

The uniform deformation $\mathbf{y}_F$ is an equilibrium of the atomistic model (3.2), therefore, we say that the equilibrium $\mathbf{y}_F$ is stable in the atomistic model if and only if $\langle \delta^2 \mathcal{E}^a(\mathbf{y}_F)$ is positive definite, that is,

$$\langle \delta^2 \mathcal{E}^a(\mathbf{y}_F)\mathbf{u}, \mathbf{u}\rangle = \langle \delta^2 \hat{\mathcal{E}}^a(\mathbf{y}_F)\mathbf{u}, \mathbf{u}\rangle + \langle \delta^2 \tilde{\mathcal{E}}^a(\mathbf{y}_F)\mathbf{u}, \mathbf{u}\rangle > 0 \quad \text{for all } \mathbf{u} \in \mathcal{U} \setminus \{\mathbf{0}\}. \tag{3.8}$$

Note that $\langle \delta^2 \tilde{\mathcal{E}}_a(\mathbf{y}_F)\mathbf{u}, \mathbf{u}\rangle$ is given by formula (7) in [21]:

$$\langle \delta^2 \tilde{\mathcal{E}}^a(\mathbf{y}_F)\mathbf{u}, \mathbf{u}\rangle = \tilde{A}_F \|D\mathbf{u}\|^2_{\ell^2_\epsilon} - \epsilon^2 \phi''_{2F} \|D^{(2)}\mathbf{u}\|^2_{\ell^2_\epsilon}, \tag{3.9}$$

where

$$\tilde{A}_F := \phi''_F + 4\phi''_{2F} \quad \text{for} \quad \phi''_F := \phi''(F) \text{ and } \phi''_{2F} := \phi''(2F) \tag{3.10}$$

is the *continuum elastic modulus for the pair interaction potential*. Thus, we only need to focus on $\langle \delta^2 \hat{\mathcal{E}}^a(\mathbf{y}_F)\mathbf{u}, \mathbf{u}\rangle$, that is,

$$\begin{aligned}\langle \delta^2 \hat{\mathcal{E}}^a(\mathbf{y}_F)\mathbf{u}, \mathbf{u}\rangle = \epsilon \sum_{\ell=-N+1}^{N} \Big\{ & G''_F \left[\rho'_F(u'_\ell + u'_{\ell+1}) + \rho'_{2F}(u'_{\ell-1} + u'_\ell + u'_{\ell+1} + u'_{\ell+2})\right]^2 \\ & + G'_F \left[\rho''_F (u'_\ell)^2 + \rho''_{2F}(u'_\ell + u'_{\ell-1})^2 + \rho''_F (u'_{\ell+1})^2 \right. \\ & \left. + \rho''_{2F}(u'_{\ell+1} + u'_{\ell+2})^2\right] \Big\},\end{aligned} \tag{3.11}$$

where

$$\begin{gathered}\rho'_F := \rho'(F), \quad \rho''_F := \rho''(F), \quad \rho'_{2F} := \rho(2F), \quad \rho''_{2F} := \rho''(2F), \\ G'_F := G'(\bar{\rho}^a_\ell(\mathbf{y}_F)) = G'(\bar{\rho}^c_\ell(\mathbf{y}_F)) = G'(\bar{\rho}^{qnl}_\ell(\mathbf{y}_F)), \\ G''_F := G''(\bar{\rho}^a_\ell(\mathbf{y}_F)) = G''(\bar{\rho}^c_\ell(\mathbf{y}_F)) = G''(\bar{\rho}^{qnl}_\ell(\mathbf{y}_F)).\end{gathered}$$

We calculate the identities

$$\left(u'_\ell + u'_{\ell+1}\right)^2 = 2\left(u'_\ell\right)^2 + 2\left(u'_{\ell+1}\right)^2 - \epsilon^2 (u''_{\ell+1})^2, \tag{3.12}$$

$$\left(u'_\ell + u'_{\ell+1} + u'_{\ell+2}\right)^2 = 3\left(u'_\ell\right)^2 + 3\left(u'_{\ell+1}\right)^2 + 3\left(u'_{\ell+2}\right)^2 - 3\epsilon^2\left(u''_{\ell+1}\right)^2 - 3\epsilon^2\left(u''_{\ell+2}\right)^2 + \epsilon^4\left(u^{(3)}_{\ell+2}\right)^2.$$

$$\begin{aligned} 2\left(u'_\ell + u'_{\ell+1}\right)\cdot\left(u'_{\ell-1} + u'_\ell + u'_{\ell+1} + u'_{\ell+2}\right) \\ = 2\left[\left(u'_{\ell-1}\right)^2 + 3\left(u'_\ell\right)^2 + 3\left(u'_{\ell+1}\right)^2 + \left(u'_{\ell+2}\right)^2\right] \\ - 3\epsilon^2\left[\left(u''_\ell\right)^2 + 2\left(u''_{\ell+1}\right)^2 + \left(u''_{\ell+2}\right)^2\right] + \epsilon^4\left[\left(u^{(3)}_{\ell+1}\right)^2 + \left(u^{(3)}_{\ell+2}\right)^2\right]. \end{aligned}$$

We can now calculate explicitly the first equality below and then use (3.12) (with $\mathbf{u}'$ replaced by $\mathbf{u}''$) for the second equality to obtain

$$\begin{aligned} \left(u'_\ell + u'_{\ell+1} + u'_{\ell+2} + u'_{\ell+3}\right)^2 &= 4\left((u'_\ell)^2 + (u'_{\ell+1})^2 + (u'_{\ell+2})^2 + (u'_{\ell+3})^2\right) \\ &\quad - \epsilon^2\left(u''_{\ell+1}\right)^2 - \epsilon^2\left(u''_{\ell+2}\right)^2 - \epsilon^2\left(u''_{\ell+3}\right)^2 - \epsilon^2\left(u''_{\ell+1} + u''_{\ell+2}\right)^2 \\ &\quad - \epsilon^2\left(u''_{\ell+2} + u''_{\ell+3}\right)^2 - \epsilon^2\left(u''_{\ell+1} + u''_{\ell+2} + u''_{\ell+3}\right)^2 \\ &= 4\left((u'_\ell)^2 + (u'_{\ell+1})^2 + (u'_{\ell+2})^2 + (u'_{\ell+3})^2\right) \\ &\quad - \epsilon^2\left(6(u''_{\ell+1})^2 + 8(u''_{\ell+2})^2 + 6(u''_{\ell+3})^2\right) \\ &\quad + \epsilon^4\left(4(u^{(3)}_{\ell+2})^2 + 4(u^{(3)}_{\ell+3})^2\right) - \epsilon^6(u^{(4)}_{\ell+3})^2. \end{aligned}$$

We can then obtain from the above identities that

$$\begin{aligned} \langle \delta^2\hat{\mathcal{E}}^a(\mathbf{y}_F)\mathbf{u}, \mathbf{u}\rangle &= G''_F\cdot\Big\{\left[4\left(\rho'_F\right)^2 + 16\left(\rho'_{2F}\right)^2 + 16\rho'_F\rho'_{2F}\right]\|D\mathbf{u}\|^2_{\ell^2_\epsilon} \\ &\qquad -\epsilon^2\left[\left(\rho'_F\right)^2 + 20\left(\rho'_{2F}\right)^2 + 12\rho'_F\rho'_{2F}\right]\|D^{(2)}\mathbf{u}\|^2_{\ell^2_\epsilon} \\ &\qquad +\epsilon^4\left[8\left(\rho'_{2F}\right)^2 + 2\rho'_F\rho'_{2F}\right]\|D^{(3)}\mathbf{u}\|^2_{\ell^2_\epsilon} - \epsilon^6\left(\rho'_{2F}\right)^2\|D^{(4)}\mathbf{u}\|^2_{\ell^2_\epsilon}\Big\} \\ &\quad + G'_F\cdot\left\{\left(2\rho''_F + 8\rho''_{2F}\right)\|D\mathbf{u}\|^2_{\ell^2_\epsilon} - 2\epsilon^2\rho''_{2F}\|D^{(2)}\mathbf{u}\|^2_{\ell^2_\epsilon}\right\} \\ &= \left\{4G''_F\left(\rho'_F + 2\rho'_{2F}\right)^2 + 2G'_F\left(\rho''_F + 4\rho''_{2F}\right)\right\}\|D\mathbf{u}\|^2_{\ell^2_\epsilon} \\ &\quad - \epsilon^2\left\{G''_F\left[\left(\rho'_F\right)^2 + 20\left(\rho'_{2F}\right)^2 + 12\rho'_F\rho'_{2F}\right] + G'_F\,2\rho''_{2F}\right\}\|D^{(2)}\mathbf{u}\|^2_{\ell^2_\epsilon} \\ &\quad + \epsilon^4 G''_F\left[8\left(\rho'_{2F}\right)^2 + 2\rho'_F\rho'_{2F}\right]\|D^{(3)}\mathbf{u}\|^2_{\ell^2_\epsilon} \\ &\quad - \epsilon^6 G''_F\left(\rho'_{2F}\right)^2\|D^{(4)}\mathbf{u}\|^2_{\ell^2_\epsilon}. \end{aligned} \tag{3.13}$$

We define the *continuum elastic modulus for the embedding energy* to be

$$\hat{A}_F := 4G''_F\left(\rho'_F + 2\rho'_{2F}\right)^2 + 2G'_F\left(\rho''_F + 4\rho''_{2F}\right). \tag{3.14}$$

and

$$A_F := \hat{A}_F + \tilde{A}_F, \quad B_F := -\left[\phi''_{2F} + G''_F\big((\rho'_F)^2 + 20(\rho'_{2F})^2 + 12\rho'_F\rho'_{2F}\big) + G'_F\left(2\rho''_{2F}\right)\right],$$
$$C_F := G''_F\left(8(\rho'_{2F})^2 + 2\rho'_F\rho'_{2F}\right), \quad \text{and} \quad D_F := -G''_F\left(\rho'_{2F}\right)^2.$$

Then (3.8) becomes

$$\langle \delta^2\mathcal{E}^a(\mathbf{y}_F)\mathbf{u},\mathbf{u}\rangle = A_F\|D\mathbf{u}\|^2_{\ell^2_\epsilon} + \epsilon^2 B_F\|D^{(2)}\mathbf{u}\|^2_{\ell^2_\epsilon} + \epsilon^4 C_F\|D^{(3)}\mathbf{u}\|^2_{\ell^2_\epsilon} + \epsilon^6 D_F\|D^{(4)}\mathbf{u}\|^2_{\ell^2_\epsilon}. \tag{3.15}$$

We will analyze the stability of $\langle \delta^2\mathcal{E}^a(\mathbf{y}_F)\mathbf{u},\mathbf{u}\rangle$ by using the Fourier representation [42]

$$Du_\ell = \sum_{\substack{k=-N+1\\ k\neq 0}}^{N} \frac{c_k}{\sqrt{2}} \cdot \exp\left(i\,k\frac{\ell}{N}\pi\right).$$

It then follows from the discrete orthogonality of the Fourier basis that

$$\begin{aligned}\langle \delta^2\mathcal{E}^a(\mathbf{y}_F)\mathbf{u},\mathbf{u}\rangle = \sum_{\substack{k=-N+1\\ k\neq 0}}^{N} |c_k|^2 \cdot \Bigg\{ & A_F + B_F\left[4\sin^2\left(\frac{k\pi}{2N}\right)\right] \\ & + C_F\left[4\sin^2\left(\frac{k\pi}{2N}\right)\right]^2 + D_F\left[4\sin^2\left(\frac{k\pi}{2N}\right)\right]^3\Bigg\}.\end{aligned} \tag{3.16}$$

We then see from (3.16) that the eigenvalues λ_k for $k = -N+1, \ldots, N$ of $\langle \delta^2\mathcal{E}^a(\mathbf{y}_F)\mathbf{u},\mathbf{u}\rangle$ with respect to the $\|D\mathbf{u}\|_{\ell^2_\epsilon}$ norm are given by

$$\lambda_k = \lambda_F(s_k) \quad \text{for} \quad s_k = 4\sin^2\left(\frac{k\pi}{2N}\right)$$

where

$$\lambda_F(s) := A_F + B_F s + C_F s^2 + D_F s^3.$$

From the pair interaction potential, electron density function, and embedding energy function given in Figure 2 in [29], we assume that

$$\phi''_F > 0,\ \phi''_{2F} < 0; \quad \rho'_F \le 0,\ \rho'_{2F} \le 0; \quad \rho''_F \ge 0,\ \rho''_{2F} \ge 0; \quad \text{and} \quad G''_F \ge 0. \tag{3.17}$$

We then have from the assumption (3.17) that

$$C_F > 0, \quad D_F < 0, \quad \text{and} \quad 8|D_F| \le C_F. \tag{3.18}$$

We can check that (3.18) implies that $|D_F s| \leq 4|D_F| \leq C_F/2$, for $0 \leq s \leq 4$, so

$$\lambda_F'(s) = B_F + 2C_F s + 3D_F s^2 \geq B_F + \frac{C_F}{2} s \quad \text{for all} \quad 0 \leq s \leq 4. \tag{3.19}$$

We conclude from (3.19) that the condition $B_F \geq 0$ or equivalently

$$\phi_{2F}'' + G_F'' \left[\left(\rho_F'\right)^2 + 20 \left(\rho_{2F}'\right)^2 + 12\rho_F'\rho_{2F}' \right] + G_F' \, 2\rho_{2F}'' = -B_F \leq 0, \tag{3.20}$$

and the assumptions (3.17) imply that $\lambda(s)$ is increasing for $0 \leq s \leq 4$. We thus have the sharp stability result

$$\langle \delta^2 \mathcal{E}^a(\mathbf{y}_F)\mathbf{u}, \mathbf{u} \rangle \geq \lambda_F(s_1) \|D\mathbf{u}\|_{\ell^2_\epsilon}^2 \geq \left(\hat{A}_F + \tilde{A}_F \right) \|D\mathbf{u}\|_{\ell^2_\epsilon}^2 \quad \text{for all } \mathbf{u} \in \mathcal{U}. \tag{3.21}$$

We summarize this result in the following theorem:

Theorem 3.3.1 *Suppose that the hypotheses* (3.17) *and* (3.20) *hold. Then the uniform deformation* $\mathbf{y}_F$ *is stable for the atomistic model if and only if*

$$\begin{aligned}
\lambda_F(s_1) &= A_F + B_F \left[4\sin^2\left(\frac{\pi}{2N}\right) \right] + C_F \left[4\sin^2\left(\frac{\pi}{2N}\right) \right]^2 + D_F \left[4\sin^2\left(\frac{\pi}{2N}\right) \right]^3 \\
&= \hat{A}_F + \tilde{A}_F - 4\sin^2\left(\frac{\pi}{2N}\right) \left\{ \phi_{2F}'' + G_F'' \left[\left(\rho_F'\right)^2 + 20 \left(\rho_{2F}'\right)^2 + 12\rho_F'\rho_{2F}' \right] + G_F' \, 2\rho_{2F}'' \right\} \\
&\quad + 4^2 \sin^4\left(\frac{\pi}{2N}\right) G_F'' \left[\eta \left(\rho_{2F}'\right)^2 + 2\rho_F'\rho_{2F}' \right] - 4^3 \sin^6\left(\frac{\pi}{2N}\right) G_F'' \left(\rho_{2F}'\right)^2 > 0.
\end{aligned}$$

Remark 3.3.1 *The role of the assumption* (3.20) *is to guarantee that* $u_\ell' = \sin(\epsilon\ell\pi)$ *is the eigenfunction corresponding to the smallest eigenvalue of* $\langle \delta^2 \mathcal{E}^a(\mathbf{y}_F)\mathbf{u}, \mathbf{u} \rangle$ *with respect to the norm* $\|D\mathbf{u}\|_{\ell^2_\epsilon}$. *In fact, we can see from the above Fourier analysis that* $u_\ell' = \sin(\epsilon\ell\pi)$ *is not the smallest eigenvalue of* $\langle \delta^2 \mathcal{E}^a(\mathbf{y}_F)\mathbf{u}, \mathbf{u} \rangle$ *with respect to the norm* $\|D\mathbf{u}\|_{\ell^2_\epsilon}$ *for sufficiently large N if* (3.20) *does not hold since then* $\lambda'(0) < 0$.

The assumption (3.20) *on the the pair interaction potential, electron density function, and embedding energy function cannot be expected to generally hold for physical embedded atom models since the nearest neighbor term* $G_F''(\rho_F')^2 > 0$ *dominates. We note, however, that generally* $G_F' < 0$ *for* $F < 1$ *[30], in which case* $G_F' \, 2\rho_{2F}'' < 0$; *so* (3.20) *is more likely to hold for compressive strains* $F < 1$.

3.3.2 The EAM-QNL Model

Now we will analyze the stability of the EAM-QNL model for next-nearest neighbor interactions. The Fourier techniques used to analyze the stability of the atomistic

model cannot be used for the EAM-QNL model because the Fourier modes are no longer eigenfunctions. Recall that the total atomistic interaction energy of the QNL model is $\mathcal{E}^{qnl}(\mathbf{y}) := \hat{\mathcal{E}}^{qnl}(\mathbf{y}) + \tilde{\mathcal{E}}^{qnl}(\mathbf{y}) = \epsilon \sum_{\ell=-N+1}^{N} \mathcal{E}_\ell^{qnl}(\mathbf{y})$, where $\mathcal{E}_\ell^{qnl}(\mathbf{y})$ is symmetric in $\ell \in \{-N+1, \ldots, N\}$ and is given by

$$\mathcal{E}_\ell^{qnl}(\mathbf{y}) := \begin{cases} \mathcal{E}_\ell^{a}(\mathbf{y}) & \text{for} \quad 0 \le \ell < K+1, \\ \mathcal{E}_{K+1}^{qnl}(\mathbf{y}) & \text{for} \quad \ell = K+1, \\ \mathcal{E}_{K+2}^{qnl}(\mathbf{y}) & \text{for} \quad \ell = K+2, \\ \mathcal{E}_\ell^{c}(\mathbf{y}) & \text{for} \quad K+2 < \ell < N. \end{cases}$$

Since the QNL energy is consistent (see the consistency error analysis in Section 3.4), $\mathbf{y}_F$ is still an equilibrium of $\mathcal{E}^{qnl}(\mathbf{y})$ [4]. Therefore, we will focus on $\langle \delta^2 \mathcal{E}^{qnl}(\mathbf{y}_F)\mathbf{u}, \mathbf{u}\rangle$ to estimate the stability. The second variation of $\mathcal{E}^{qnl}(\mathbf{y})$ evaluated at $\mathbf{y} = \mathbf{y}_F$ is given by

$$\langle \delta^2 \mathcal{E}^{qnl}(\mathbf{y}_F)\mathbf{u}, \mathbf{u}\rangle = \langle \delta^2 \hat{\mathcal{E}}^{qnl}(\mathbf{y}_F)\mathbf{u}, \mathbf{u}\rangle + \langle \delta^2 \tilde{\mathcal{E}}^{qnl}(\mathbf{y}_F)\mathbf{u}, \mathbf{u}\rangle. \tag{3.22}$$

We first compute the second term of (3.22) and get

$$\begin{aligned} &\langle \delta^2 \tilde{\mathcal{E}}^{qnl}(\mathbf{y}_F)\mathbf{u}, \mathbf{u}\rangle \\ &\quad = \epsilon \sum_{\ell=-K}^{K} \frac{1}{2} \left\{ \phi_F'' \left[\left(u_\ell'\right)^2 + \left(u_{\ell+1}'\right)^2 \right] + \phi_{2F}'' \left[\left(u_\ell' + u_{\ell-1}'\right)^2 + \left(u_{\ell+1}' + u_{\ell+2}'\right)^2 \right] \right\} \\ &\qquad + \frac{\epsilon}{2} \left\{ \phi_F'' \left[\left(u_{K+1}'\right)^2 + \left(u_{K+2}'\right)^2 \right] + \phi_{2F}'' \left[\left(u_{K+1}' + u_K'\right)^2 + 4\left(u_{K+2}'\right)^2 \right] \right\} \\ &\qquad + \frac{\epsilon}{2} \left\{ \phi_F'' \left[\left(u_{K+2}'\right)^2 + \left(u_{K+3}'\right)^2 \right] + \phi_{2F}'' \left[\left(u_{K+2}' + u_{K+1}'\right)^2 + 4\left(u_{K+3}'\right)^2 \right] \right\} \\ &\quad + \cdots + \epsilon \sum_{\ell=K+3}^{N} \frac{1}{2} \left\{ \phi_F'' \left[\left(u_\ell'\right)^2 + \left(u_{\ell+1}'\right)^2 \right] + \phi_{2F}'' \left[4\left(u_\ell'\right)^2 + 4\left(u_{\ell+1}'\right)^2 \right] \right\}. \end{aligned} \tag{3.23}$$

Here we omit the terms whose indices $\ell \in \{-N+1, \ldots, -(K+3)\}$ since the QNL energy is symmetric. Then we compute the first term, which is given by the following

expression:

$$
\begin{aligned}
&\langle \delta^2 \hat{\mathcal{E}}^{qnl}(\mathbf{y}_F)\mathbf{u},\mathbf{u}\rangle = \dots \\
&+\epsilon \sum_{\ell=0}^{K} \Big\{ G_F'' \left[\rho_F'(u_\ell' + u_{\ell+1}') + \rho_{2F}'(u_{\ell-1}' + u_\ell' + u_{\ell+1}' + u_{\ell+2}')\right]^2 \\
&+ G_F' \left[\rho_F''(u_\ell')^2 + \rho_{2F}''(u_\ell' + u_{\ell-1}')^2 + \rho_F''(u_{\ell+1}')^2 + \rho_{2F}''(u_{\ell+1}' + u_{\ell+2}')^2\right] \Big\} \\
&+ 2\epsilon G_F'' \left[\rho_F' u_{K+1}' + \rho_{2F}'\left(u_{K+1}' + u_K'\right)\right]^2 + \epsilon G_F' \left[\rho_F''(u_{K+1}')^2 + \rho_{2F}''\left(u_{K+1}' + u_K'\right)^2\right] \\
&+ 2\epsilon G_F'' \left(\rho_F' + 2\rho_{2F}'\right)^2 (u_{K+2}')^2 + \epsilon G_F' \left(\rho_F'' + 4\rho_{2F}''\right)(u_{K+2}')^2 \\
&+ 2\epsilon G_F'' \left[\rho_F' u_{K+2}' + \rho_{2F}'\left(u_{K+2}' + u_{K+1}'\right)\right]^2 + \epsilon G_F' \left[\rho_F''(u_{K+2}')^2 + \rho_{2F}''\left(u_{K+2}' + u_{K+1}'\right)^2\right] \\
&+ 2\epsilon G_F'' \left(\rho_F' + 2\rho_{2F}'\right)^2 (u_{K+3}')^2 + \epsilon G_F' \left(\rho_F'' + 4\rho_{2F}''\right)(u_{K+3}')^2 \\
&+ \epsilon \sum_{\ell=K+3}^{N} \left[2G_F'' \left(\rho_F' + 2\rho_{2F}'\right)^2 + G_F' \left(\rho_F'' + 4\rho_{2F}''\right)\right] \left[(u_\ell')^2 + (u_{\ell+1}')^2\right]. \qquad (3.24)
\end{aligned}
$$

Now we use (3.12) again to rewrite (3.24) in the following form

$$
\begin{aligned}
&\langle \delta^2 \hat{\mathcal{E}}^{qnl}(\mathbf{y}_F)\mathbf{u},\mathbf{u}\rangle \\
&\quad = \epsilon \sum_{\ell=-N+1}^{N} \left[2G_F'' \left(\rho_F' + 2\rho_{2F}'\right)^2 + G_F' \left(\rho_F'' + 4\rho_{2F}''\right)\right] \left[(u_\ell')^2 + (u_{\ell+1}')^2\right] \\
&\qquad + \dots - \epsilon^3 \sum_{\ell=0}^{K} \left\{G_F'' \cdot \left[(\rho_F')^2 + 20(\rho_{2F}')^2 + 12\rho_F'\rho_{2F}'\right] + G_F' \cdot 2\rho_{2F}''\right\} \left(D^{(2)} u_\ell\right)^2 \\
&\qquad - \epsilon^3 \left\{G_F'' \cdot \left[(\rho_F')^2 + 16(\rho_{2F}')^2 + 11\rho_F'\rho_{2F}'\right] + G_F' \cdot 2\rho_{2F}''\right\} \left(D^{(2)} u_{K+1}\right)^2 \\
&\qquad - \epsilon^3 \left\{G_F'' \cdot \left[8(\rho_{2F}')^2 + 5\rho_F'\rho_{2F}'\right] + G_F' \cdot 2\rho_{2F}''\right\} \left(D^{(2)} u_{K+2}\right)^2 \\
&\qquad + \epsilon^5 \sum_{\ell=0}^{K+1} G_F'' \cdot \left[8(\rho_{2F}')^2 + 2\rho_F'\rho_{2F}'\right] \left(D^{(3)} u_\ell\right)^2 \\
&\qquad + \epsilon^5 G_F'' \cdot \left[4(\rho_{2F}')^2 + \rho_F'\rho_{2F}'\right] \left(D^{(3)} u_{K+2}\right)^2 - \epsilon^7 \sum_{\ell=0}^{K+2} G_F'' \cdot (\rho_{2F}')^2 \left(D^{(4)} u_\ell\right)^2.
\end{aligned}
$$

Combining $\langle \delta^2 \hat{\mathcal{E}}^{qnl}(\mathbf{y}_F)\mathbf{u}, \mathbf{u}\rangle$ and $\langle \delta^2 \tilde{\mathcal{E}}^{qnl}(\mathbf{y}_F)\mathbf{u}, \mathbf{u}\rangle$ together we obtain

$$\begin{aligned}
\langle \delta^2 \mathcal{E}^{qnl}(\mathbf{y}_F)\mathbf{u}, \mathbf{u}\rangle = \epsilon \sum_{\ell=-N+1}^{N} &\left(\hat{A}_F + \tilde{A}_F\right)(Du_\ell)^2 + \dots \\
&- \epsilon^3 \sum_{\ell=0}^{K} \left\{\phi''_{2F} + G''_F \cdot \left[(\rho'_F)^2 + 20(\rho'_{2F})^2 + 12\rho'_F\rho'_{2F}\right] + G'_F \cdot 2\rho''_{2F}\right\}\left(D^{(2)}u_\ell\right)^2 \\
&- \epsilon^3 \left\{\phi''_{2F} + G''_F \cdot \left[(\rho'_F)^2 + 16(\rho'_{2F})^2 + 11\rho'_F\rho'_{2F}\right] + G'_F \cdot 2\rho''_{2F}\right\}\left(D^{(2)}u_{K+1}\right)^2 \\
&- \epsilon^3 \left\{\phi''_{2F} + G''_F \cdot \left[8(\rho'_{2F})^2 + 5\rho'_F\rho'_{2F}\right] + G'_F \cdot 2\rho''_{2F}\right\}\left(D^{(2)}u_{K+2}\right)^2 \\
&+ \epsilon^5 \sum_{\ell=0}^{K+1} G''_F \cdot \left[8(\rho'_{2F})^2 + 2\rho'_F\rho'_{2F}\right]\left(D^{(3)}u_\ell\right)^2 \\
&+ \epsilon^5 G''_F \cdot \left[4(\rho'_{2F})^2 + \rho'_F\rho'_{2F}\right]\left(D^{(3)}u_{K+2}\right)^2 - \epsilon^7 \sum_{\ell=0}^{K+2} G''_F \cdot (\rho'_{2F})^2 \left(D^{(4)}u_\ell\right)^2.
\end{aligned}$$

Because of the hypotheses (3.17) and (3.20), we have that

$$\begin{aligned}
&\phi''_{2F} + G''_F \cdot \left[(\rho'_F)^2 + 16(\rho'_{2F})^2 + 11\rho'_F\rho'_{2F}\right] + G'_F \cdot 2\rho''_{2F} \le 0, \\
&\phi''_{2F} + G''_F \cdot \left[8(\rho'_{2F})^2 + 5\rho'_F\rho'_{2F}\right] + G'_F \cdot 2\rho''_{2F} \le 0.
\end{aligned}$$

Thus, using

$$\left(D^{(4)}u_\ell\right)^2 = \left[\frac{1}{\epsilon}\left(D^{(3)}u_\ell - D^{(3)}u_{\ell-1}\right)\right]^2 \le \frac{2}{\epsilon^2}\left[\left(D^{(3)}u_\ell\right)^2 + \left(D^{(3)}u_{\ell-1}\right)^2\right]$$

and noting that $G''_F \cdot (\rho'_{2F})^2 \ge 0$, we have

$$\begin{aligned}
&\epsilon^5 \sum_{\ell=0}^{K+1} G''_F \cdot \left[8(\rho'_{2F})^2 + 2\rho'_F\rho'_{2F}\right]\left(D^{(3)}u_\ell\right)^2 \\
&\quad + \epsilon^5 G''_F \cdot \left[4(\rho'_{2F})^2 + \rho'_F\rho'_{2F}\right]\left(D^{(3)}u_{K+2}\right)^2 - \epsilon^7 \sum_{\ell=0}^{K+2} G''_F \cdot (\rho'_{2F})^2 \left(D^{(4)}u_\ell\right)^2 \\
&\ge \epsilon^5 \sum_{\ell=0}^{K+1} G''_F \cdot \left[4(\rho'_{2F})^2 + 2\rho'_F\rho'_{2F}\right]\left(D^{(3)}u_\ell\right)^2 \\
&\quad + \epsilon^5 G''_F \cdot \left[2(\rho'_{2F})^2 + \rho'_F\rho'_{2F}\right]\left(D^{(3)}u_{K+2}\right)^2 \ge 0.
\end{aligned} \tag{3.25}$$

So, except in the case $K \in \{N-2, \dots, N\}$ when there is no continuum region, it follows that $\mathbf{y}_F$ is stable in the QNL model if and only if $\hat{A}_F + \tilde{A}_F > 0$.

Now we can give a sharp stability estimate for the QNL model from the above estimates and the arguments in [21, 23].

Theorem 3.3.2 *Suppose that $K < N-2$ and the hypotheses* (3.17) *and* (3.20) *hold, then the uniform deformation $\mathbf{y}_F$ is stable in the QNL model if and only if $\hat{A}_F + \tilde{A}_F > 0$.*

Remark 3.3.2 *The role of the assumption* (3.20) *in Theorem 3.3.2, as in Theorem 3.3.1, is to give a necessary condition for $u'_\ell = \sin(\epsilon\ell\pi)$ to be the eigenfunction corresponding to the smallest eigenvalue of $\langle \delta^2 \mathcal{E}^{qnl}(\mathbf{y}_F)\mathbf{u}, \mathbf{u}\rangle$ with respect to the norm $\|D\mathbf{u}\|_{\ell^2_\epsilon}$.*

Remark 3.3.3 *From Theorem 3.3.1 and Theorem 3.3.2, we conclude that the difference between the sharp stability conditions of the fully atomistic and QNL models is of order $O(\epsilon^2)$. This result is the same as for the pair potential case [11].*

Remark 3.3.4 *We noted in Remark 3.3.1 that the assumption* (3.20) *is necessary for Theorem 3.3.1. We now give an explicit example showing that the uniform deformation can be more stable for the EAM-QCL model than for the fully atomistic model when* (3.20) *fails. We recall that the EAM-QCL model is the EAM-QNL model with no atomistic region, that is,*

$$\mathcal{E}^{qcl}(\mathbf{y}) := \epsilon \sum_{\ell=-N+1}^{N} \mathcal{E}^c_\ell(\mathbf{y}).$$

We consider the case when

$$\phi''_{2F} + G''_F \left(\rho'_F + 2\rho'_{2F}\right)^2 + G'_F 2\rho''_{2F} > 0, \tag{3.26}$$

which implies that (3.20) *does not hold since it then follows from* (3.17) *that*

$$\begin{aligned}
&\phi''_{2F} + G''_F \left[\left(\rho'_F\right)^2 + 20\left(\rho'_{2F}\right)^2 + 12\rho'_F\rho'_{2F}\right] + G'_F 2\rho''_{2F} \\
&\quad = \left[\phi''_{2F} + G''_F \left(\rho'_F + 2\rho'_{2F}\right)^2 + G'_F 2\rho''_{2F}\right] + 8G''_F \left(2\left(\rho'_{2F}\right)^2 + \rho'_F\rho'_{2F}\right) \\
&\quad > 0.
\end{aligned}$$

We define the oscillatory displacement $\tilde{\mathbf{u}}$ by

$$\tilde{u}_\ell = (-1)^\ell \epsilon/(2\sqrt{2}),$$

so

$$\tilde{u}'_\ell = (-1)^\ell/(\sqrt{2}), \quad \|D\tilde{\mathbf{u}}\|_{\ell^2_\epsilon} = 1, \quad \tilde{u}''_\ell = (-1)^\ell(\sqrt{2})/\epsilon.$$

We then calculate from (3.9) *and* (3.11) *that*

$$\begin{aligned}\langle \delta^2 \mathcal{E}^a(\mathbf{y}_F)\tilde{\mathbf{u}},\tilde{\mathbf{u}}\rangle &= \langle \delta^2 \tilde{\mathcal{E}}^a(\mathbf{y}_F)\tilde{\mathbf{u}},\tilde{\mathbf{u}}\rangle + \langle \delta^2 \tilde{\mathcal{E}}^a(\mathbf{y}_F)\tilde{\mathbf{u}},\tilde{\mathbf{u}}\rangle \\ &= \epsilon \sum_{\ell=-N+1}^{N} G'_F 2\rho''_F \frac{1}{2} + \left(\phi''_F + 4\phi''_{2F}\right)\|D\tilde{\mathbf{u}}\|^2_{\ell^2_\epsilon} + (-\epsilon^2\phi''_{2F})\|D^{(2)}\tilde{\mathbf{u}}\|^2_{\ell^2_\epsilon} \\ &= G'_F 2\rho''_F + \left(\phi''_F + 4\phi''_{2F}\right) - 4\phi''_{2F} = \phi''_F + G'_F 2\rho''_F. \end{aligned} \tag{3.27}$$

Thus, we obtain that

$$\inf_{\mathbf{u}\in\mathcal{U}\setminus\{\mathbf{0}\},\, \|D\mathbf{u}\|_{\ell^2_\epsilon}=1} \langle \delta^2 \mathcal{E}^a(\mathbf{y}_F)\mathbf{u},\mathbf{u}\rangle \le \phi''_F + G'_F 2\rho''_F.$$

On the other hand, we have that

$$\inf_{\mathbf{u}\in\mathcal{U}\setminus\{\mathbf{0}\},\, \|D\mathbf{u}\|_{\ell^2_\epsilon}=1} \langle \delta^2 \mathcal{E}^{qcl}(\mathbf{y}_F)\mathbf{u},\mathbf{u}\rangle = \tilde{A}_F + \tilde{A}_F = 4\left[\phi''_{2F} + G''_F\left(\rho'_F + 2\rho'_{2F}\right)^2 + G'_F 2\rho''_{2F}\right] + \phi''_F + G'_F 2\rho''_F.$$

Therefore, from (3.26) *we have*

$$\inf_{\mathbf{u}\in\mathcal{U}\setminus\{\mathbf{0}\},\, \|D\mathbf{u}\|_{\ell^2_\epsilon}=1} \langle \delta^2 \mathcal{E}^{qcl}(\mathbf{y}_F)\mathbf{u},\mathbf{u}\rangle > \phi''_F + G'_F 2\rho''_F \ge \inf_{\mathbf{u}\in\mathcal{U}\setminus\{\mathbf{0}\},\, \|D\mathbf{u}\|_{\ell^2_\epsilon}=1} \langle \delta^2 \mathcal{E}^{a}(\mathbf{y}_F)\mathbf{u},\mathbf{u}\rangle.$$

This inequality indicates that the uniform deformation $\mathbf{y}_F$ *can be unstable for the atomistic model, but stable for the EAM-QCL model, when the assumption* (3.26) *fails.*

We cannot conclude from this argument, though, that the atomistic model is less stable than the EAM-QNL model with a nontrivial atomistic region, i.e., $K > 0$*. To see this, we consider an oscillatory displacement* $\hat{\mathbf{u}} \in \mathcal{U}$ *with support only in the atomistic region (a similar test function is used in [43]):*

$$\hat{u}_\ell = \begin{cases} \frac{(-1)^\ell \epsilon}{2\sqrt{2}}, & \ell = -(K-1), \ldots, (K-1), \\ 0, & \textit{otherwise.} \end{cases}$$

Then since $\hat{u}'_\ell = (\hat{u}_\ell - \hat{u}_{\ell-1})/\epsilon$*, we have*

$$\hat{u}'_\ell = \begin{cases} \frac{(-1)^\ell}{\sqrt{2}}, \ell = -(K-2), \ldots, (K-1), \\ \frac{(-1)^K}{2\sqrt{2}}, \ell = K, \\ \frac{(-1)^{-(K-1)}}{2\sqrt{2}}, \ell = -(K-1), \\ 0, \quad \textit{otherwise.} \end{cases}$$

We substitute the displacement $\hat{\mathbf{u}}$ *into* (3.24) *and get*

$$\begin{aligned}\langle \delta^2 \hat{\mathcal{E}}^{qnl}(\mathbf{y}_F)\hat{\mathbf{u}}, \hat{\mathbf{u}}\rangle &= \epsilon \sum_{\ell=-(K-2)}^{K-3} G'_F \rho''_F + 2\epsilon \left\{ G''_F \frac{1}{8}\left[3\left(\rho'_{2F}\right)^2 + 2\left(\rho'_F - \rho'_{2F}\right)^2\right] + G'_F\left[\frac{7}{4}\rho''_F + \frac{1}{2}\rho''_{2F}\right]\right\} \\ &= \epsilon 2(K-2) G'_F \rho''_F + O(\epsilon). \end{aligned} \tag{3.28}$$

Similarly, we substitute $\hat{\mathbf{u}}$ *into* (3.23) *and get*

$$\langle \delta^2 \tilde{\mathcal{E}}^{qnl}(\mathbf{y}_F)\hat{\mathbf{u}}, \hat{\mathbf{u}}\rangle = \epsilon \sum_{\ell=-(K-2)}^{K-3} \frac{1}{2}\phi''_F + O(\epsilon) = \epsilon(K-2)\phi''_F + O(\epsilon). \tag{3.29}$$

Therefore, we obtain that

$$\langle \delta^2 \mathcal{E}^{qnl}(\mathbf{y}_F)\hat{\mathbf{u}}, \hat{\mathbf{u}}\rangle = \langle \delta^2 \hat{\mathcal{E}}^{qnl}(\mathbf{y}_F)\hat{\mathbf{u}}, \hat{\mathbf{u}}\rangle + \langle \delta^2 \tilde{\mathcal{E}}^{qnl}(\mathbf{y}_F)\hat{\mathbf{u}}, \hat{\mathbf{u}}\rangle = \epsilon(K-2)(\phi''_F + 2G'_F\rho''_F) + O(\epsilon).$$

Note that

$$\|\hat{\mathbf{u}}'\|^2_{\ell^2_\epsilon} = \epsilon \sum_{\ell=-N+1}^{N} (u'_\ell)^2 = \epsilon(K-1) + \frac{\epsilon}{4},$$

Thus, we obtain from the above and (3.27) *that*

$$\frac{\langle \delta^2 \mathcal{E}^{qnl}(\mathbf{y}_F)\hat{\mathbf{u}}, \hat{\mathbf{u}}\rangle}{\|\hat{\mathbf{u}}'\|^2_{\ell^2_\epsilon}} = \left(\phi''_F + 2G'_F\rho''_F\right) + O\left(\frac{1}{K}\right) = \frac{\langle \delta^2 \mathcal{E}^{a}(\mathbf{y}_F)\tilde{\mathbf{u}}, \tilde{\mathbf{u}}\rangle}{\|\tilde{\mathbf{u}}'\|^2_{\ell^2_\epsilon}} + O\left(\frac{1}{K}\right).$$

This indicates that when (3.26) *holds and* K *is sufficiently large, the EAM-QNL model is also less stable than the EAM-QCL model.*

3.4 Consistency Error and Convergence of The EAM-QNL Model

Setting $\mathbf{y}^{qnl} = \mathbf{y}_F + \mathbf{u}^{qnl}$ and $\mathbf{y}^a = \mathbf{y}_F + \mathbf{u}^a$, where both $\mathbf{u}^{qnl}$ and $\mathbf{u}^a$ belong to $\mathcal{U}$, we define the quasicontinuum error to be

$$\mathbf{e}^{qnl} := \mathbf{y}^a - \mathbf{y}^{qnl} = \mathbf{u}^a - \mathbf{u}^{qnl}.$$

To simplify the error analysis, we consider the linearization of the atomistic equilibrium equations (3.3) and the associated EAM-QNL equilibrium equations (3.5) about the uniform deformation $\mathbf{y}_F$. The linearized atomistic equation is

$$-\langle \delta^2 \mathcal{E}^a\left(\mathbf{y}_F\right)\mathbf{u}^a, \mathbf{w}\rangle = \langle \delta \mathcal{F}(\mathbf{y}_F), \mathbf{w}\rangle \quad \text{for all } \mathbf{w} \in \mathcal{U}, \tag{3.30}$$

and the linearized EAM-QNL equation is

$$-\langle \delta^2 \mathcal{E}^{qnl}(\mathbf{y}_F)\,\mathbf{u}^{qnl}, \mathbf{w}\rangle = \langle \delta \mathcal{F}(\mathbf{y}_F), \mathbf{w}\rangle \quad \text{for all } \mathbf{w} \in \mathcal{U}. \tag{3.31}$$

We thus analyze the linearized error equation

$$\langle \delta^2 \mathcal{E}^{qnl}(\mathbf{y}_F)\,\mathbf{e}^{qnl}, \mathbf{w}\rangle = \langle \mathbf{T}^{qnl}, \mathbf{w}\rangle \quad \text{for all } \mathbf{w} \in \mathcal{U}, \tag{3.32}$$

where the linearized consistency error is given by

$$\begin{aligned}\langle \mathbf{T}^{qnl}, \mathbf{w}\rangle &:= \langle \delta^2 \mathcal{E}^{qnl}(\mathbf{y}_F)\,\mathbf{u}^a, \mathbf{w}\rangle - \langle \delta^2 \mathcal{E}^{a}(\mathbf{y}_F)\,\mathbf{u}^a, \mathbf{w}\rangle \\ &= \langle \delta^2 \hat{\mathcal{E}}^{qnl}(\mathbf{y}_F)\,\mathbf{u}^a, \mathbf{w}\rangle - \langle \delta^2 \hat{\mathcal{E}}^{a}(\mathbf{y}_F)\,\mathbf{u}^a, \mathbf{w}\rangle \\ &\quad + \langle \delta^2 \tilde{\mathcal{E}}^{qnl}(\mathbf{y}_F)\,\mathbf{u}^a, \mathbf{w}\rangle - \langle \delta^2 \tilde{\mathcal{E}}^{a}(\mathbf{y}_F)\,\mathbf{u}^a, \mathbf{w}\rangle.\end{aligned} \tag{3.33}$$

Now we will give an estimate of the consistency error $\mathbf{T}^{qnl}, \mathbf{w}\rangle$ in the following theorem. We first define

$$\|\mathbf{v}\|^2_{\ell^2_\epsilon(\mathcal{C})} := \epsilon \sum_{\ell \in \mathcal{C}} v_\ell^2, \quad \|\mathbf{v}\|^2_{\ell^2_\epsilon(\mathcal{I})} := \epsilon \sum_{\ell \in \mathcal{I}} v_\ell^2, \quad \text{and} \quad \|\mathbf{v}\|^2_{\ell^\infty_\epsilon(\mathcal{I})} := \max_{\ell \in \mathcal{I}} |v_\ell|, \quad \text{for } \mathbf{v} \in \mathcal{U},$$

where $\mathcal{C}$ denotes the continuum region $\{-N+1, \ldots, -(K+1)\} \bigcup \{K+1, \ldots, N\}$ and $\mathcal{I}$ denotes the interface $\{-(K+7), \ldots, -K\} \bigcup \{K, \ldots, K+7\}$.

Theorem 3.4.1 *The consistency error* $\mathbf{T}^{qnl}, \mathbf{w}\rangle$, *given in* (3.33), *satisfies the following negative norm estimate*

$$\begin{aligned}\left|\langle \mathbf{T}^{qnl}, \mathbf{w}\rangle\right| \le \Big\{ &\epsilon^2 \left[G_F'' \cdot \left((\rho_F')^2 + 12\rho_F'\rho_{2F}' + 20(\rho_{2F}')^2\right) - 2G_F' \cdot \rho_{2F}'' + |\phi_{2F}''|\right] \cdot \|D^{(3)}\mathbf{u}^a\|_{\ell^2_\epsilon(\mathcal{C})} \\ &+ \epsilon^{3/2}\left(C_1 + C_2\right)\|D^{(2)}\mathbf{u}^a\|_{\ell^\infty_\epsilon(\mathcal{I})}\Big\}\,\|D\mathbf{w}\|_{\ell^2_\epsilon} \qquad \textit{for all } \mathbf{w} \in \mathcal{U}.\end{aligned}$$

Proof We focus on the first term of (3.33)

$$\langle \delta^2 \hat{\mathcal{E}}^{qnl}(\mathbf{y}_F)\,\mathbf{u}^a, \mathbf{w}\rangle - \langle \delta^2 \hat{\mathcal{E}}^{a}(\mathbf{y}_F)\,\mathbf{u}^a, \mathbf{w}\rangle = \cdots + \mathbf{I}_0 + \mathbf{I}_1 + \mathbf{I}_2 + \mathbf{I}_3,$$

where $\mathbf{I}_0$ is associated with $\ell = 0, \ldots, K$, $\mathbf{I}_1$ is associated with $\ell = K+1$, $\mathbf{I}_2$ is associated with $\ell = K+2$ and $\mathbf{I}_3$ is associated with $\ell = K+3, \ldots, N$.

We first compute $\mathbf{I}_3$. Note that $\mathbf{u}^a$ and $\mathbf{w}$ are $2N$-periodic, so in the calculation, when the indices $\ell + i > N, i = 1, 2$, we can move these terms to the $\{-N+1, \ldots, -1\}$

part by using the periodicity as done in (6.9) in [23]. Hence, we can rearrange the terms in $\mathbf{I}_3$ to get

$$\begin{aligned}
\mathbf{I}_3 = \epsilon \sum_{\ell=K+5}^{N} G_F'' \cdot \left(\rho_F'\right)^2 \left(-Du_{\ell-1}^a + 2Du_\ell^a - Du_{\ell+1}^a\right) Dw_\ell \qquad (3.34)\\
+ \epsilon \sum_{\ell=K+5}^{N} G_F'' \cdot \left(\rho_F'\rho_{2F}'\right) \left[4\left(-Du_{\ell-1}^a + 2Du_\ell^a - Du_{\ell+1}^a\right) + 2\left(-Du_{\ell-2}^a + 2Du_\ell^a - Du_{\ell+2}^a\right)\right] Dw_\ell\\
+ \epsilon \sum_{\ell=K+5}^{N} G_F'' \cdot \left(\rho_{2F}'\right)^2 \left[3\left(-Du_{\ell-1}^a + 2Du_\ell^a - Du_{\ell+1}^a\right) + 2\left(-Du_{\ell-2}^a + 2Du_\ell^a - Du_{\ell+2}^a\right)\right.\\
\left. + \left(-Du_{\ell-3}^a + 2Du_\ell^a - Du_{\ell+3}^a\right)\right] Dw_\ell\\
+ \epsilon \sum_{\ell=K+5}^{N} 2G_F' \cdot \rho_{2F}'' \left(-Du_{\ell-1}^a + 2Du_\ell^a - Du_{\ell+1}^a\right) Dw_\ell + \mathbf{I}_{31}
\end{aligned}$$

where $\mathbf{I}_{31}$ consists of the interfacial terms, i.e., $\ell \in \{K, \ldots, K+7\}$, and is given by the following expression

$$\begin{aligned}
\mathbf{I}_{31} = \epsilon G_F''\Big\{ \left(\rho_F'\right)^2 \left[\left(Du_{K+3}^a - Du_{K+4}^a\right) w_{K+3}' + \left(-Du_{K+3}^a + 2Du_{K+4}^a - Du_{K+5}^a\right) w_{K+4}'\right]\\
+ \rho_F'\rho_{2F}' \left[-\left(Du_{K+3}^a + Du_{K+4}^a\right) w_{K+2}' + \left(6Du_{K+3}^a - Du_{K+2}^a - 3Du_{K+4}^a - 2Du_{K+5}^a\right) w_{K+3}'\right.\\
\left. + \left(12Du_{K+4}^a - Du_{K+2}^a - 3Du_{K+3}^a - 4Du_{K+5}^a - 2Du_{K+6}^a\right) w_{K+4}'\right]\\
+ \left(\rho_{2F}'\right)^2 \left[-\left(Du_{K+2}^a + Du_{K+3}^a + Du_{K+4}^a + Du_{K+5}^a\right) w_{K+2}'\right.\\
+ \left(6Du_{K+3}^a - Du_{K+2}^a - 2Du_{K+4}^a - 2Du_{K+5}^a - Du_{K+6}^a\right) w_{K+3}'\\
\left. + \left(13Du_{K+4}^a - Du_{K+2}^a - 2Du_{K+3}^a - 3Du_{K+5}^a - 2Du_{K+6}^a - Du_{K+7}^a\right) w_{K+4}'\right] \Big\}\\
+ \epsilon G_F'\rho_{2F}''\Big\{ -\left(Du_{K+2}^a + Du_{K+3}^a\right) w_{K+2}' + \left(2Du_{K+3}^a - Du_{K+2}^a - Du_{K+4}^a\right) w_{K+3}'\\
+ \left(5Du_{K+4}^a - Du_{K+3}^a - 2Du_{K+5}^a\right) w_{K+4}'\Big\}.
\end{aligned}$$

Since $\mathbf{I}_0$ is associated with $\ell = 0, \ldots, K$ where the QNL and the atomistic models coincide with each other, we have $\mathbf{I}_0 = 0$. Similarly, by direct computation we get the

following expression for the sum of $\mathbf{I}_1$ and $\mathbf{I}_2$

$$
\begin{aligned}
\mathbf{I}_1+\mathbf{I}_2=\epsilon G_F''\big\{ &\left(\rho_F'\right)^2\left[\left(Du_{K+1}^a-Du_{K+2}^a\right)\left(w_{K+1}'-w_{K+2}'\right)\right]\\
&+\rho_F'\rho_{2F}'\left[\left(Du_{K+1}^a-Du_{K+2}^a\right)w_K'+\left(2Du_{K+1}^a-2Du_{K+2}^a+Du_K^a-Du_{K+3}^a\right)w_{K+1}'\right.\\
&\quad\left.+\left(6Du_{K+2}^a-Du_K^a-2Du_{K+1}^a-Du_{K+3}^a\right)w_{K+2}'-\left(Du_{K+1}^a+Du_{K+2}^a\right)w_{K+3}'\right]\\
&+\left(\rho_{2F}'\right)^2\left[\left(Du_K^a+Du_{K+1}^a-Du_{K+2}^a-Du_{K+3}^a\right)\left(w_K'+w_{K+1}'\right)\right.\\
&\quad+\left(7Du_{K+2}^a-Du_K^a-Du_{K+1}^a-Du_{K+3}^a\right)w_{K+2}'\\
&\quad\left.\left.-\left(Du_K^a+Du_{K+1}^a+Du_{K+2}^a+Du_{K+3}^a\right)w_{K+3}'\right]\right\}\\
&+\epsilon G_F'\rho_{2F}''\left\{\left(3Du_{K+2}^a-Du_{K+3}^a\right)w_{K+2}'-\left(Du_{K+2}^a+Du_{K+3}^a\right)w_{K+3}'\right\}\\
&+\epsilon G_F''\big\{\left(\rho_F'\right)^2\left[\left(Du_{K+2}^a-Du_{K+3}^a\right)\left(w_{K+2}'-w_{K+3}'\right)\right] \qquad (3.35)\\
&+\rho_F'\rho_{2F}'\left[\left(Du_{K+2}^a-Du_{K+3}^a\right)w_{K+1}'+\left(2Du_{K+2}^a-2Du_{K+3}^a+Du_{K+1}^a-Du_{K+4}^a\right)w_{K+2}'\right.\\
&\quad\left.+\left(6Du_{K+3}^a-Du_{K+1}^a-2Du_{K+2}^a-Du_{K+4}^a\right)w_{K+3}'-\left(Du_{K+2}^a+Du_{K+3}^a\right)w_{K+4}'\right]\\
&+\left(\rho_{2F}'\right)^2\left[\left(Du_{K+1}^a+Du_{K+2}^a-Du_{K+3}^a-Du_{K+4}^a\right)\left(w_{K+1}'+w_{K+2}'\right)\right.\\
&\quad+\left(7Du_{K+3}^a-Du_{K+1}^a-Du_{K+2}^a-Du_{K+4}^a\right)w_{K+3}'\\
&\quad\left.\left.-\left(Du_{K+1}^a+Du_{K+2}^a+Du_{K+3}^a+Du_{K+4}^a\right)w_{K+4}'\right]\right\}\\
&+\epsilon G_F'\rho_{2F}''\left\{\left(3Du_{K+3}^a-Du_{K+4}^a\right)w_{K+3}'-\left(Du_{K+3}^a+Du_{K+4}^a\right)w_{K+4}'\right\}.
\end{aligned}
$$

Note that we can rewrite the second term of the second line of $\mathbf{I}_3$ as

$$
\begin{aligned}
2\left(-Du_{\ell-2}^a+2Du_\ell^a-Du_{\ell+2}^a\right)=&\,2\left(-Du_{\ell-2}^a+2Du_{\ell-1}^a-Du_\ell^a\right)+4\left(-Du_{\ell-1}^a+2Du_\ell^a-Du_{\ell+1}^a\right)\\
&+2\left(-Du_\ell^a+2Du_{\ell+1}^a-Du_{\ell+2}^a\right).
\end{aligned}
$$

Similarly, we can rewrite the third term of the third line of $\mathbf{I}_3$ as

$$
\begin{aligned}
\left(-Du_{\ell-3}^a+2Du_\ell^a-Du_{\ell+3}^a\right)=&\left(-Du_{\ell-3}^a+2Du_{\ell-2}^a-Du_{\ell-1}^a\right)+2\left(-Du_{\ell-2}^a+2Du_{\ell-1}^a-Du_\ell^a\right)\\
&+3\left(-Du_{\ell-1}^a+2Du_\ell^a-Du_{\ell+1}^a\right)+2\left(-Du_\ell^a+2Du_{\ell+1}^a-Du_{\ell+2}^a\right)\\
&+\left(-Du_{\ell+1}^a+2Du_{\ell+2}^a-Du_{\ell+3}^a\right).
\end{aligned}
$$

Then we combine $\mathbf{I}_1$, $\mathbf{I}_2$ and $\mathbf{I}_3$ together and rearrange the interfacial terms, i.e., $\ell\in\{K,\ldots,K+7\}$. We find that the coefficients of the interfacial terms $\mathbf{I}_1+\mathbf{I}_2+\mathbf{I}_{31}$ are perfectly matched so that they are of order ϵ, thus we obtain the following estimate by

the Cauchy-Schwarz inequality:

$$\begin{aligned}
&\left|\langle\delta^2\hat{\mathcal{E}}^{qnl}\left(\mathbf{y}_F\right)\mathbf{u}^a,\mathbf{w}\rangle-\langle\delta^2\hat{\mathcal{E}}^{a}\left(\mathbf{y}_F\right)\mathbf{u}^a,\mathbf{w}\rangle\right| \\
&\quad\leq\Big\{\left[G_F''\cdot\left((\rho_F')^2+12\rho_F'\rho_{2F}'+20(\rho_{2F}')^2\right)-2G_F'\cdot\rho_{2F}''\right]\epsilon^2\cdot\|D^{(3)}\mathbf{u}^a\|_{\ell^2_\epsilon(\mathcal{C})} \qquad (3.36)\\
&\qquad\quad+C_1\epsilon\cdot\|D^{(2)}\mathbf{u}^a\|_{\ell^2_\epsilon(\mathcal{I})}\Big\}\|D\mathbf{w}\|_{\ell^2_\epsilon}
\end{aligned}$$

where $\mathcal{I}$ is the interface: $\{K,\ldots,K+7\}$, and C_1 is a constant independent of ϵ. We note that

$$\|D^2\mathbf{u}^a\|^2_{\ell^2_\epsilon(\mathcal{I})}=\epsilon\sum_{\ell=K}^{K+7}\left|D^{(2)}u^a_\ell\right|^2\leq\|D^{(2)}\mathbf{u}^a\|^2_{\ell^\infty_\epsilon(\mathcal{I})}\sum_{\ell=K}^{K+7}\epsilon=8\epsilon\|D^{(2)}\mathbf{u}^a\|^2_{\ell^\infty_\epsilon(\mathcal{I})}.$$

Thus, we obtain

$$\begin{aligned}
&\left|\langle\delta^2\hat{\mathcal{E}}^{qnl}\left(\mathbf{y}_F\right)\mathbf{u}^a,\mathbf{w}\rangle-\langle\delta^2\hat{\mathcal{E}}^{a}\left(\mathbf{y}_F\right)\mathbf{u}^a,\mathbf{w}\rangle\right| \\
&\quad\leq\Big\{\epsilon^2\left[G_F''\cdot\left((\rho_F')^2+12\rho_F'\rho_{2F}'+20(\rho_{2F}')^2\right)-2G_F'\cdot\rho_{2F}''\right]\cdot\|D^{(3)}\mathbf{u}^a\|_{\ell^2_\epsilon(\mathcal{C})}\\
&\qquad\quad+\epsilon^{3/2}C_1\|D^{(2)}\mathbf{u}^a\|_{\ell^\infty_\epsilon(\mathcal{I})}\Big\}\cdot\|D\mathbf{w}\|_{\ell^2_\epsilon}.
\end{aligned}$$

We can estimate the pair potential consistency error, $\langle\delta^2\tilde{\mathcal{E}}^{qnl}\left(\mathbf{y}_F\right)\mathbf{u}^a,\mathbf{w}\rangle-\langle\delta^2\tilde{\mathcal{E}}^{a}\left(\mathbf{y}_F\right)\mathbf{u}^a,\mathbf{w}\rangle$, by considering the above estimate for an embedding energy $G(\tilde{\phi})=\tilde{\phi}/2$ to obtain

$$\begin{aligned}
&\left|\langle\delta^2\tilde{\mathcal{E}}^{qnl}\left(\mathbf{y}_F\right)\mathbf{u}^a,\mathbf{w}\rangle-\langle\delta^2\tilde{\mathcal{E}}^{a}\left(\mathbf{y}_F\right)\mathbf{u}^a,\mathbf{w}\rangle\right| \\
&\quad\leq\left\{\epsilon^2|\phi_{2F}''|\|D^{(3)}\mathbf{u}\|_{\ell^2_\epsilon(\mathcal{C})}+C_2\epsilon\|D^{(2)}\mathbf{u}^a\|_{\ell^2_\epsilon(\mathcal{I})}\right\}\|D\mathbf{w}\|_{\ell^2_\epsilon}\\
&\quad\leq\left\{\epsilon^2|\phi_{2F}''|\|D^{(3)}\mathbf{u}\|_{\ell^2_\epsilon(\mathcal{C})}+C_2\epsilon^{3/2}\|D^{(2)}\mathbf{u}^a\|_{\ell^\infty_\epsilon(\mathcal{I})}\right\}\|D\mathbf{w}\|_{\ell^2_\epsilon}.
\end{aligned}$$

Therefore, we obtain the following optimal order estimate for the consistency error (3.33)

$$\begin{aligned}
\left|\langle\mathbf{T}^{qnl},\mathbf{w}\rangle\right|&\leq\left|\langle\delta^2\hat{\mathcal{E}}^{qnl}\left(\mathbf{y}_F\right)\mathbf{u}^a,\mathbf{w}\rangle-\langle\delta^2\hat{\mathcal{E}}^{a}\left(\mathbf{y}_F\right)\mathbf{u}^a,\mathbf{w}\rangle\right|\\
&\qquad+\left|\langle\delta^2\tilde{\mathcal{E}}^{qnl}\left(\mathbf{y}_F\right)\mathbf{u}^a,\mathbf{w}\rangle-\langle\delta^2\tilde{\mathcal{E}}^{a}\left(\mathbf{y}_F\right)\mathbf{u}^a,\mathbf{w}\rangle\right|\\
&\leq\Big\{\epsilon^2\left[G_F''\cdot\left((\rho_F')^2+12\rho_F'\rho_{2F}'+20(\rho_{2F}')^2\right)-2G_F'\cdot\rho_{2F}''+|\phi_{2F}''|\right]\cdot\|D^{(3)}\mathbf{u}^a\|_{\ell^2_\epsilon(\mathcal{C})}\\
&\qquad+\epsilon^{3/2}\left(C_1+C_2\right)\|D^{(2)}\mathbf{u}^a\|_{\ell^\infty_\epsilon(\mathcal{I})}\Big\}\|D\mathbf{w}\|_{\ell^2_\epsilon}\qquad\text{for all }\mathbf{w}\in\mathcal{U}.
\end{aligned}$$

□

We can now give the convergence result for the linearized EAM-QNL model.

Theorem 3.4.2 *Suppose that $\hat{A}_F + \tilde{A}_F > 0$, where $\hat{A}_F$ and $\tilde{A}_F$ are defined in* (3.14) *and* (3.10)*, and that* (3.17) *and* (3.20) *holds. Then the linearized atomistic problem* (3.30) *as well as the linearized QNL approximation* (3.31) *have unique solutions, and they satisfy the error estimate*

$$\begin{aligned}\|D\mathbf{y}^a - D\mathbf{y}^{qnl}\|_{\ell^2_\epsilon} &= \|D\mathbf{u}^a - D\mathbf{u}^{qnl}\|_{\ell^2_\epsilon} \\ &\leq \frac{\epsilon^2\left[G''_F \cdot \left((\rho'_F)^2 + 12\rho'_F\rho'_{2F} + 20(\rho'_{2F})^2\right) - 2G'_F \cdot \rho''_{2F} + |\phi''_{2F}|\right] \cdot \|D^{(3)}\mathbf{u}^a\|_{\ell^2_\epsilon(\mathcal{C})}}{\hat{A}_F + \tilde{A}_F} \\ &\quad + \frac{\epsilon^{3/2}\left(C_1 + C_2\right)\|D^{(2)}\mathbf{u}^a\|_{\ell^\infty_\epsilon(\mathcal{I})}}{\hat{A}_F + \tilde{A}_F}.\end{aligned}$$

Proof. The error estimate for the EAM-QNL model follows from the error equation (3.32), the stability estimate in Theorem 3.3.2, and the consistency estimate in Theorem 3.4.1. □

3.5 Conclusion

We describe a one-dimensional QNL method for the EAM potential following [4], and we study the stability and convergence of a linearization of the next-nearest neighbor EAM-QNL energy. We identify conditions for the pair potential, electron density function, and embedding function so that the lattice stability of the atomistic and the EAM-QNL models are asymptotically equal. These condition are necessary to guarantee that $u'_\ell = \sin(\epsilon\ell\pi)$ is the eigenfunction corresponding to the smallest eigenvalue of $\langle\delta^2\mathcal{E}^a(\mathbf{y}_F)\mathbf{u}, \mathbf{u}\rangle$ with respect to the norm $\|D\mathbf{u}\|_{\ell^2_\epsilon}$.

We then give a negative norm estimate for the consistency error and generalize the conclusions in [27] to the EAM case. We compare the equilibria of the atomistic and EAM-QNL models and give an optimal order $\mathrm{O}(\epsilon^{3/2})$ error estimate for the ℓ^2_ϵ norm of the strain in terms of the deformation in the continuum region.

Chapter 4

The Lattice Stabilities of the Embedded Atom Method Models

4.1 Chapter Review

The nucleation and motion of lattice defects such as dislocations and cracks can occur when the configuration loses stability at a critical strain. Thus, the accurate approximation of critical strains for lattice instability is a key criterion for predictive computational modeling of material deformation. Coarse-grained continuum approximations of atomistic models are needed to compute the long-range elastic interaction of defects with surfaces. In this chapter, we present a comparison of the lattice stability for atomistic chains modeled by the embedded atom method (EAM) with their approximation by local Cauchy-Born models. The volume-based Cauchy-Born strain-energy density is given by the energy-density for a homogeneously strained lattice and is the typical strain energy density used by continuum models to coarse-grain the atomistic energy of a lattice [3]. The reconstruction-based Cauchy-Born model uses linear (and bilinear) extrapolation of local atoms (usually nearest-neighbor atoms in the reference lattice) to approximate the positions of nonlocal atoms and thus approximates a nonlocal atomistic site energy by a local atomistic site energy [4, 5]. The reconstruction-based Cauchy–Born site energy has been proposed to accurately transition between an atomistic model used in the neighborhood of a defect and the coarse-grained volume-based local model.

We find that both the volume-based local model and the reconstruction-based local

model can give O(1) errors for the critical strain when the embedding energy density is nonlinear. In the physical case of a strictly convex embedding energy density, the critical strain predicted by the volume-based model is always equal to or larger than that predicted by the atomistic model (Theorem 4.4.1), but the critical strain for reconstruction-based models can be either larger, equal, or smaller than that predicted by the atomistic model (Theorem 4.4.2). If we further restrict our model to nearest-neighbor interactions, then the critical strain for the atomistic and reconstruction-based Cauchy-Born models are equal (Corollary 4.3.1 and Corollary 4.3.2), but the critical strain for the volume-based Cauchy-Born model is O(1) larger (Theorem 4.3.3). We thus expect that reconstruction-based models are more accurate than volume-based models near lattice instabilities if nearest-neighbor interactions dominate, but we note that it is not known how to coarse-grain reconstruction-based models in three space dimensions.

4.2 The Embedded Atom Model and Its Local Approximations

In this section, we will give a short description for the next-nearest-neighbor atomistic EAM model and its local approximations .

4.2.1 The Atomistic EAM Model

Given deformations $\mathbf{y} \in \mathcal{Y}_F$, the total energy per period of the next-nearest-neighbor atomistic EAM model is

$$\mathcal{E}^a_{tot}(\mathbf{y}) := \mathcal{E}^a(\mathbf{y}) + \mathcal{F}(\mathbf{y}), \tag{4.1}$$

where $\mathcal{E}^a(\mathbf{y})$ is the total atomistic energy and $\mathcal{F}(\mathbf{y})$ is the total external potential energy. The total atomistic energy $\mathcal{E}^a(\mathbf{y})$ is the sum of the *embedding energy*, $\hat{\mathcal{E}}^a(\mathbf{y})$, and the *pair potential energy*, $\tilde{\mathcal{E}}^a(\mathbf{y})$. The energy expression is

$$\mathcal{E}^a(\mathbf{y}) := \hat{\mathcal{E}}^a(\mathbf{y}) + \tilde{\mathcal{E}}^a(\mathbf{y}) = \epsilon \sum_{\ell=-N+1}^{N} \left(\hat{\mathcal{E}}^a_\ell(\mathbf{y}) + \tilde{\mathcal{E}}^a_\ell(\mathbf{y}) \right). \tag{4.2}$$

The embedding energy per atom (per atomistic reference spacing ϵ) is defined as

$$\hat{\mathcal{E}}^a_\ell(\mathbf{y}) := G\left(\bar{\rho}^a_\ell(\mathbf{y})\right),$$

where $G(\bar{\rho})$ is the embedding energy function that represents the energy required to move atom ℓ from infinity to its current position, and $\bar{\rho}^a_\ell(\mathbf{y})$ is the total contribution to the electron charge density from the first and second neighboring atoms to atom ℓ:

$$\bar{\rho}^a_\ell(\mathbf{y}) := \rho(y'_\ell) + \rho(y'_\ell + y'_{\ell-1}) + \rho(y'_{\ell+1}) + \rho(y'_{\ell+1} + y'_{\ell+2}).$$

The function $\rho(r/\epsilon)$ is the electron density contributed by an atom at distance r.

The pair potential energy per atom (per atomistic reference spacing ϵ) is

$$\tilde{\mathcal{E}}^a_\ell(\mathbf{y}) := \frac{1}{2}\left[\phi(y'_\ell) + \phi(y'_\ell + y'_{\ell-1}) + \phi(y'_{\ell+1}) + \phi(y'_{\ell+1} + y'_{\ell+2})\right],$$

where $\phi(r/\epsilon)$ is the pair potential interaction energy [29]. Our formulation allows general nonlinear external potential energies $\mathcal{F}(\mathbf{y})$ defined for $\mathbf{y} \in \mathcal{Y}_F$, but for simplicity, we only consider the total external potential energy for $2N$-periodic dead loads $\mathbf{f}$

$$\mathcal{F}(\mathbf{y}) := -\sum_{\ell=-N+1}^{N} \epsilon f_\ell y_\ell.$$

The equilibrium solution $\mathbf{y}^a$ of the EAM-atomistic model (4.1) then satisfies

$$-\langle \delta\mathcal{E}^a(\mathbf{y}^a), \mathbf{w}\rangle = -\langle \delta\hat{\mathcal{E}}^a(\mathbf{y}^a), \mathbf{w}\rangle - \langle \delta\tilde{\mathcal{E}}^a(\mathbf{y}^a), \mathbf{w}\rangle = \langle \delta\mathcal{F}(\mathbf{y}^a), \mathbf{w}\rangle \qquad \text{for all } \mathbf{w} \in \mathcal{U}. \tag{4.3}$$

Here the negative of the embedding force of (4.3) is

$$\langle \delta\hat{\mathcal{E}}^a(\mathbf{y}^a), \mathbf{w}\rangle = \epsilon \sum_{\ell=-N+1}^{N} G'\Big(\bar{\rho}^a_\ell(\mathbf{y}^a)\Big) \cdot \Big[\rho'(Dy^a_\ell)w'_\ell + \rho'(Dy^a_\ell + Dy^a_{\ell-1})(w'_\ell + w'_{\ell-1}) + \rho'(Dy^a_{\ell+1})w'_{\ell+1} + \rho'(Dy^a_{\ell+1} + Dy^a_{\ell+2})(w'_{\ell+1} + w'_{\ell+2})\Big],$$

the negative of the pair potential force of (4.3) is given by

$$\langle \delta\tilde{\mathcal{E}}^a(\mathbf{y}^a), \mathbf{w}\rangle = \epsilon \sum_{\ell=-N+1}^{N} \frac{1}{2}\Big[\phi'(Dy^a_\ell)w'_\ell + \phi'(Dy^a_\ell + Dy^a_{\ell-1})(w'_\ell + w'_{\ell-1}) + \phi'(Dy^a_{\ell+1})w'_{\ell+1} + \phi'(Dy^a_{\ell+1} + Dy^a_{\ell+2})(w'_{\ell+1} + w'_{\ell+2})\Big],$$

and the negative of the external force is formulated as

$$\langle \delta\mathcal{F}(\mathbf{y}), \mathbf{w}\rangle = \sum_{\ell=-N+1}^{N} \frac{\partial \mathcal{F}}{\partial y_\ell}(\mathbf{y}) w_\ell = -\sum_{\ell=-N+1}^{N} \epsilon f_\ell w_\ell.$$

4.2.2 The Volume-Based Local EAM Approximation

The idea of the volume-based local approximation based on the Cauchy-Born rule was first proposed in [17, 18, 3]. This local continuum model was created to improve the efficiency of atomistic models by coarse-graining. We denote this energy by $\mathcal{E}^{c,v}(\mathbf{y})$, and we can formulate the local energy associated with each atom as

$$\begin{aligned}\mathcal{E}_\ell^{c,v}(\mathbf{y}) := \hat{\mathcal{E}}_\ell^{c,v}(\mathbf{y}) + \tilde{\mathcal{E}}_\ell^{c,v}(\mathbf{y}) =& \frac{1}{2}G\left(\bar{\rho}_\ell^{c,v}(\mathbf{y}))\right) + \frac{1}{2}G\left(\bar{\rho}_{\ell+1}^{c,v}(\mathbf{y})\right) \\ &+ \frac{1}{2}\left[\phi(y'_\ell) + \phi(2y'_\ell) + \phi(y'_{\ell+1}) + \phi(2y'_{\ell+1})\right],\end{aligned}$$

where the total local electron density at atom ℓ is

$$\bar{\rho}_\ell^{c,v}(\mathbf{y}) := 2\rho(y'_\ell) + 2\rho(2y'_\ell).$$

Then the total volume-based local energy is

$$\mathcal{E}_{tot}^{c,v}(\mathbf{y}) := \mathcal{E}^{c,v}(\mathbf{y}) + \mathcal{F}(\mathbf{y}) = \epsilon \sum_{\ell=-N+1}^{N} \mathcal{E}_\ell^{c,v}(\mathbf{y}) - \epsilon \sum_{\ell=-N+1}^{N} f_\ell y_\ell. \tag{4.4}$$

The equilibrium solution $\mathbf{y}^{c,v}$ then satisfies

$$-\langle \delta\mathcal{E}^{c,v}(\mathbf{y}^{c,v}), \mathbf{w}\rangle = -\langle \delta\hat{\mathcal{E}}^{c,v}(\mathbf{y}^{c,v}), \mathbf{w}\rangle - \langle \delta\tilde{\mathcal{E}}^{c,v}(\mathbf{y}^{c,v}), \mathbf{w}\rangle = \langle \delta\mathcal{F}(\mathbf{y}^{c,v}), \mathbf{w}\rangle \quad \text{for all } \mathbf{w} \in \mathcal{U}. \tag{4.5}$$

The negative of the embedding force of (4.5) is

$$\begin{aligned}\langle \delta\hat{\mathcal{E}}^{c,v}(\mathbf{y}^{c,v}), \mathbf{w}\rangle =& \epsilon \sum_{\ell=-N+1}^{N} \Big\{ G'\left(\bar{\rho}_\ell^{c,v}(\mathbf{y}^{c,v})\right) \cdot \left[\rho'(Dy_\ell^{c,v}) + 2\rho'(2Dy_\ell^{c,v})\right] w'_\ell \\ &+ G'\left(\bar{\rho}_{\ell+1}^{c,v}(\mathbf{y}^{c,v})\right) \cdot \left[\rho'(Dy_{\ell+1}^{c,v}) + 2\rho'(2Dy_{\ell+1}^{c,v})\right] w'_{\ell+1} \Big\},\end{aligned}$$

and the negative of the pair potential force of (4.5) is given by

$$\langle \delta\tilde{\mathcal{E}}^{c,v}(\mathbf{y}^{c,v}), \mathbf{w}\rangle = \epsilon \sum_{\ell=-N+1}^{N} \frac{1}{2}\left\{ \left[\phi'(Dy_\ell^{c,v}) + 2\phi'(2Dy_\ell^{c,v})\right] w'_\ell + \left[\phi'(Dy_{\ell+1}^{c,v}) + 2\phi'(2Dy_{\ell+1}^{c,v})\right] w'_{\ell+1} \right\}.$$

4.2.3 The Reconstruction-Based Local EAM Approximation

Using the Cauchy-Born approximation, one can also reconstruct the position of each atom [5] and compute the energy $\mathcal{E}^{c,r}(\mathbf{y})$ by the approximation

$$\mathcal{E}_\ell^{c,r}(\mathbf{y}) = \hat{\mathcal{E}}_\ell^{c,r}(\mathbf{y}) + \tilde{\mathcal{E}}_\ell^{c,r}(\mathbf{y}) = G\left(\bar{\rho}_\ell^{c,r}(\mathbf{y})\right) + \frac{1}{2}\left[\phi(y'_\ell) + \phi(2y'_\ell) + \phi(y'_{\ell+1}) + \phi(2y'_{\ell+1})\right],$$

where the reconstruction-based local electron density at atom ℓ is

$$\bar{\rho}_\ell^{c,r}(\mathbf{y}) := \rho(y'_\ell) + \rho(2y'_\ell) + \rho(y'_{\ell+1}) + \rho(2y'_{\ell+1}).$$

This local continuum model is called the reconstruction-based model. It was proposed to remove the error of the coupling models on the interface[4, 5]. Thus, the total energy of the reconstruction-based local model is

$$\begin{aligned}\mathcal{E}_{tot}^{c,r}(\mathbf{y}) :=& \hat{\mathcal{E}}^{c,r}(\mathbf{y}) + \tilde{\mathcal{E}}^{c,r}(\mathbf{y}) + \mathcal{F}(\mathbf{y}) \\ =& \epsilon \sum_{\ell=-N+1}^{N} \Big\{ G\left[\rho(y'_\ell) + \rho(2y'_\ell) + \rho(y'_{\ell+1}) + \rho(2y'_{\ell+1})\right] \\ &+ \frac{1}{2}\left[\phi(y'_\ell) + \phi(2y'_\ell) + \phi(y'_{\ell+1}) + \phi(2y'_{\ell+1})\right] \Big\} - \epsilon \sum_{\ell=-N+1}^{N} f_\ell y_\ell.\end{aligned} \tag{4.6}$$

We compute the equilibrium solution of the reconstruction-based local model (4.6) from

$$-\langle \delta\mathcal{E}^{c,r}(\mathbf{y}^{c,r}), \mathbf{w}\rangle = -\langle \delta\hat{\mathcal{E}}^{c,r}(\mathbf{y}^{c,r}), \mathbf{w}\rangle - \langle \delta\tilde{\mathcal{E}}^{c,r}(\mathbf{y}^{c,r}), \mathbf{w}\rangle = \langle \delta\mathcal{F}(\mathbf{y}^{c,r}), \mathbf{w}\rangle \quad \text{for all } \mathbf{w} \in \mathcal{U}. \tag{4.7}$$

Here the negative of the embedding force of (4.7) is

$$\begin{aligned}\langle \delta\hat{\mathcal{E}}^{c,r}(\mathbf{y}^{c,r}), \mathbf{w}\rangle = \epsilon \sum_{\ell=-N+1}^{N} G'\left(\bar{\rho}_\ell^{c,r}(\mathbf{y}^{c,r})\right) \cdot \Big[&\left(\rho'(Dy_\ell^{c,r}) + 2\rho'(2Dy_\ell^{c,r})\right) w'_\ell \\ &+ \left(\rho'(Dy_{\ell+1}^{c,r}) + 2\rho'(2Dy_{\ell+1}^{c,r})\right) w'_{\ell+1}\Big],\end{aligned}$$

and the negative of the pair potential force of (4.7) is

$$\langle \delta\tilde{\mathcal{E}}^{c,r}(\mathbf{y}^{c,r}), \mathbf{w}\rangle = \epsilon \sum_{\ell=-N+1}^{N} \frac{1}{2}\left\{\left[\phi'(Dy_\ell^{c,r}) + 2\phi'(2Dy_\ell^{c,r})\right] w'_\ell + \left[\phi'(Dy_{\ell+1}^{c,r}) + 2\phi'(2Dy_{\ell+1}^{c,r})\right] w'_{\ell+1}\right\}.$$

The pair potential energy of both local approximations are exactly the same, but the embedding parts are quite different, which leads to different critical strains for lattice instability. We will analyze the lattice stability for all of the models in the next section.

4.3 Sharp Stability Analysis of The Atomistic and Local EAM Models

In this section, we analyze and compare the conditions for lattice stability of the atomistic model and the two local approximations for the next-nearest-neighbor case. We will use techniques similar to those presented in [21] for the atomistic and quasicontinuum methods with pair potential interaction.

4.3.1 Stability of the Atomistic EAM Model

We first consider the fully atomistic model. The uniform deformation $\mathbf{y}_F$ is an equilibrium of the atomistic model (4.2) without external force. We call $\mathbf{y}_F$ stable in the atomistic model if and only if $\delta^2\mathcal{E}^a(\mathbf{y}_F)$ is positive definite, that is,

$$\langle\delta^2\mathcal{E}^a(\mathbf{y}_F)\mathbf{u},\mathbf{u}\rangle = \langle\delta^2\hat{\mathcal{E}}^a(\mathbf{y}_F)\mathbf{u},\mathbf{u}\rangle + \langle\delta^2\tilde{\mathcal{E}}^a(\mathbf{y}_F)\mathbf{u},\mathbf{u}\rangle > 0 \quad \text{for all } \mathbf{u}\in\mathcal{U}\setminus\{\mathbf{0}\}. \tag{4.8}$$

We computed $\langle\delta^2\tilde{\mathcal{E}}^a(\mathbf{y}_F)\mathbf{u},\mathbf{u}\rangle$ in [21] to obtain

$$\langle\delta^2\tilde{\mathcal{E}}^a(\mathbf{y}_F)\mathbf{u},\mathbf{u}\rangle = \tilde{A}_F\|D\mathbf{u}\|^2_{\ell^2_\epsilon} - \epsilon^2\phi''_{2F}\|D^{(2)}\mathbf{u}\|^2_{\ell^2_\epsilon}, \tag{4.9}$$

where

$$\tilde{A}_F := \phi''_F + 4\phi''_{2F} \quad \text{for} \quad \phi''_F := \phi''(F) \text{ and } \phi''_{2F} := \phi''(2F) \tag{4.10}$$

is the *continuum elastic modulus for the pair interaction potential*. Thus, we focus on $\langle\delta^2\hat{\mathcal{E}}^a(\mathbf{y}_F)\mathbf{u},\mathbf{u}\rangle$, which can be formulated as

$$\begin{aligned}\langle\delta^2\hat{\mathcal{E}}^a(\mathbf{y}_F)\mathbf{u},\mathbf{u}\rangle = \epsilon\sum_{\ell=-N+1}^{N}\Big\{ & G''_F\left[\rho'_F(u'_\ell+u'_{\ell+1})+\rho'_{2F}(u'_{\ell-1}+u'_\ell+u'_{\ell+1}+u'_{\ell+2})\right]^2 \\ & +G'_F\left[\rho''_F(u'_\ell)^2+\rho''_{2F}(u'_\ell+u'_{\ell-1})^2+\rho''_F(u'_{\ell+1})^2\right. \\ & \left.+\rho''_{2F}(u'_{\ell+1}+u'_{\ell+2})^2\right]\Big\},\end{aligned} \tag{4.11}$$

where we use the simplified notation

$$\begin{aligned}\rho'_F := \rho'(F), \quad \rho''_F := \rho''(F), \quad \rho'_{2F} := \rho'(2F), \quad \rho''_{2F} := \rho''(2F),\\ G'_F := G'(\bar{\rho}^a_\ell(\mathbf{y}_F)) = G'(\bar{\rho}^{c,v}_\ell(\mathbf{y}_F)) = G'(\bar{\rho}^{c,r}_\ell(\mathbf{y}_F)),\\ G''_F := G''(\bar{\rho}^a_\ell(\mathbf{y}_F)) = G''(\bar{\rho}^{c,v}_\ell(\mathbf{y}_F)) = G''(\bar{\rho}^{c,r}_\ell(\mathbf{y}_F)).\end{aligned}$$

We define the *continuum elastic modulus for the embedding energy* to be

$$\hat{A}_F := 4G_F'' \left(\rho_F' + 2\rho_{2F}'\right)^2 + 2G_F' \left(\rho_F'' + 4\rho_{2F}''\right), \tag{4.12}$$

and we define

$$\begin{aligned} A_F := \hat{A}_F + \tilde{A}_F, \quad B_F &:= -\left[\phi_{2F}'' + G_F''\Big((\rho_F')^2 + 20(\rho_{2F}')^2 + 12\rho_F'\rho_{2F}'\Big) + G_F'\left(2\rho_{2F}''\right)\right], \\ C_F &:= G_F''\left(8(\rho_{2F}')^2 + 2\rho_F'\rho_{2F}'\right), \quad \text{and} \quad D_F := -G_F''\left(\rho_{2F}'\right)^2. \end{aligned} \tag{4.13}$$

Then (4.8) becomes

$$\langle \delta^2 \mathcal{E}^a(\mathbf{y}_F)\mathbf{u}, \mathbf{u}\rangle = A_F \|D\mathbf{u}\|_{\ell_\epsilon^2}^2 + \epsilon^2 B_F \|D^{(2)}\mathbf{u}\|_{\ell_\epsilon^2}^2 + \epsilon^4 C_F \|D^{(3)}\mathbf{u}\|_{\ell_\epsilon^2}^2 + \epsilon^6 D_F \|D^{(4)}\mathbf{u}\|_{\ell_\epsilon^2}^2, \tag{4.14}$$

where the detailed calculation can be found in the paper [9] using equation (4.5) and (4.6) in that paper.

We will analyze the stability of $\langle \delta^2 \mathcal{E}^a(\mathbf{y}_F)\mathbf{u}, \mathbf{u}\rangle$ by using the Fourier representation [42]

$$Du_\ell = \sum_{\substack{k=-N+1 \\ k\neq 0}}^{N} \frac{c_k}{\sqrt{2}} \cdot \exp\left(i\, k \frac{\ell}{N}\pi\right). \tag{4.15}$$

We exclude $k = 0$ since $D\mathbf{u}$ must satisfy the mean zero condition $\sum_{\ell=-N+1}^{N} Du_\ell = 0$. It then follows from the discrete orthogonality of the Fourier basis that

$$\begin{aligned} \langle \delta^2 \mathcal{E}^a(\mathbf{y}_F)\mathbf{u}, \mathbf{u}\rangle = \sum_{\substack{k=-N+1 \\ k\neq 0}}^{N} |c_k|^2 \cdot \Bigg\{ & A_F + B_F\left[4\sin^2\left(\frac{k\pi}{2N}\right)\right] \\ & + C_F\left[4\sin^2\left(\frac{k\pi}{2N}\right)\right]^2 + D_F\left[4\sin^2\left(\frac{k\pi}{2N}\right)\right]^3 \Bigg\}. \end{aligned} \tag{4.16}$$

We see from (4.16) that the eigenvalues λ_k^a for $k = 1, \ldots, N$ of $\langle \delta^2 \mathcal{E}^a(\mathbf{y}_F)\mathbf{u}, \mathbf{u}\rangle$ with respect to the $\|D\mathbf{u}\|_{\ell_\epsilon^2}$ norm are given by

$$\lambda_k^a = \lambda_F^a(s_k) \quad \text{for} \quad s_k = 4\sin^2\left(\frac{k\pi}{2N}\right)$$

where

$$\lambda_F^a(s) := A_F + B_F s + C_F s^2 + D_F s^3.$$

The energy and electron densities figures in [29] and [30] satisfy the following conditions which we shall assume in our analysis

$$\phi_F'' > 0,\ \phi_{2F}'' < 0; \quad \rho_{2F}' \le 0,\ \rho_F' \le 0; \quad \rho_F'' \ge 0,\ \rho_{2F}'' \ge 0; \quad \text{and} \quad G_F'' \ge 0. \tag{4.17}$$

We can derive from the assumption (4.17) that

$$C_F \ge 0, \quad D_F \le 0, \quad \text{and} \quad 8|D_F| \le C_F. \tag{4.18}$$

However, the sign of B_F is not determined. For instance, the assumption $\phi_{2F}'' < 0$ in (4.17) implies B_F can be positive. From (4.18) we have $|D_F s| \le 4|D_F| \le C_F/2$, for $0 \le s \le 4$, so

$$\lambda_F^{a\,\prime}(s) = B_F + 2C_F s + 3D_F s^2 \ge B_F + \frac{C_F}{2} s \quad \text{for all} \quad 0 \le s \le 4. \tag{4.19}$$

We note from (4.19) that the condition $B_F \ge 0$ or equivalently

$$\phi_{2F}'' + G_F'' \left[\left(\rho_F'\right)^2 + 20 \left(\rho_{2F}'\right)^2 + 12\rho_F'\rho_{2F}' \right] + G_F' \, 2\rho_{2F}'' = -B_F \le 0, \tag{4.20}$$

implies that $\lambda_F^a(s)$ is increasing for $0 \le s \le 4$. We thus conclude that if $B_F \ge 0$, then

$$\langle \delta^2 \mathcal{E}^a(\mathbf{y}_F)\mathbf{u}, \mathbf{u} \rangle \ge \lambda_F^a(s_1) \|D\mathbf{u}\|_{\ell_\epsilon^2}^2 \ge \left(\hat{A}_F + \tilde{A}_F \right) \|D\mathbf{u}\|_{\ell_\epsilon^2}^2 \quad \text{for all } \mathbf{u} \in \mathcal{U}. \tag{4.21}$$

This result can be summarized in the following theorem:

Theorem 4.3.1 *Suppose that the hypotheses* (4.17) *and* $B_F \ge 0$ *hold. Then the uniform deformation* $\mathbf{y}_F$ *is stable for the atomistic model if and only if*

$$\begin{aligned} \lambda_F^a(s_1) &= A_F + B_F \left[4\sin^2\left(\frac{\pi}{2N}\right) \right] + C_F \left[4\sin^2\left(\frac{\pi}{2N}\right) \right]^2 + D_F \left[4\sin^2\left(\frac{\pi}{2N}\right) \right]^3 \\ &= A_F + O(\epsilon^2) > 0, \end{aligned}$$

where the coefficients A_F, B_F, C_F *and* D_F *are defined in* (4.12) *and* (4.13).

We note that the differences between s_k and s_{k-1} and between $\lambda_F^a(s_k)$ and $\lambda_F^a(s_{k-1})$ are of order $O\left(\frac{2k\pi^2}{4N^2}\right) = O\left(2k\epsilon^2\right)$ for $k = 1, \ldots, N$. When the number of atoms N is sufficiently large, $\min_{0 \le s \le 4} \lambda_F^a(s)$ can be used to approximate the discrete minimum $\min_{1 \le k \le N} \lambda_F^a(s_k)$ with error at most of order $O(\epsilon)$ since $N = 1/\epsilon$.

When $B_F < 0$ and N is sufficiently large, the minimum eigenvalue of $\delta^2 \mathcal{E}^a(\mathbf{y}_F)$ is no longer $\lambda_F^a(s_1)$ and is given by the following theorem.

Theorem 4.3.2 *Suppose that the hypotheses* (4.17) *and* $B_F < 0$ *hold, and that the number of atoms* N *is sufficiently large. Then* $\lambda_F^a(s_1)$ *will no longer be the minimum eigenvalue of the second variation* $\delta^2\mathcal{E}^a(\mathbf{y}_F)$*. Instead, the minimum eigenvalue will be given by* $\lambda_F^a(s_{k^*})$ *for some* $s_{k^*} = 4\sin^2\left(\frac{k^*\pi}{2N}\right)$ *with* $k^* \in \{2, \ldots, N\}$*, where* s_{k^*} *is either equal to* 4 *or close to the critical point of the continuous function* $\lambda_F^a(s)$*:*

$$s^* := \frac{C_F - \sqrt{C_F^2 - 3B_F D_F}}{-3D_F}$$

with difference of order $O\left(2k^*\epsilon^2\right)$*.*

Proof From (4.19), we have

$$\lambda_F^{a\,\prime}(0) = B_F < 0.$$

Therefore, $\lambda_F^a(s)$ is strictly decreasing in a neighborhood of zero and thus $\lambda_F^a(0)$ is no longer the minimum value of $\lambda_F^a(s)$ on $[0, 4]$. In this case, $\min_{0\le s\le 4}\lambda_F^a(s)$ equals $\min\{\lambda_F^a(s^* \wedge 4), \lambda_F^a(4)\}$, where s^* is the critical point of $\lambda_F^a(s)$ with positive curvature and $s^* \wedge 4$ denotes $\min\{s^*, 4\}$.

Furthermore, $s_k = 4\sin^2\left(\frac{k\pi}{2N}\right)$ with $1 \le k \le N$ divides $[0, 4]$ into $N + 1$ subintervals and each subinterval has length of order $O\left(2k\epsilon^2\right)$. Hence, if s^* is in $[s_{k^*-1}, s_{k^*}]$, then the difference with the exact discrete minimum eigenvalue $\lambda_F^a(s_{k^*})$ will be of order $O\left(2k^*\epsilon^2\right)$. $\square$

In the following, we will briefly discuss the role of the coefficient B_F and leave the rigorous discussion of $\min_{0\le s\le 4}\lambda_F^a(s)$ under the condition $B_F < 0$ to section 4.4. The assumption $B_F \ge 0$ guarantees that $u'_\ell = \sin(\epsilon\ell\pi)$ is the eigenmode corresponding to the minimum eigenvalue of $\delta^2\mathcal{E}^a(\mathbf{y}_F)$ with respect to the norm $\|D\mathbf{u}\|_{\ell^2_\epsilon}$. In fact, when $B_F < 0$, $\lambda_F^a(s)$ will be strictly decreasing on $[0, s^*]$ according to its derivative (4.19).

Remark 4.3.1 *If* N *is small, then* $\lambda_F^a(s_1)$ *may be still the minimum eigenvalue of* $\delta^2\mathcal{E}^a(\mathbf{y}_F)$ *even if* $B_F < 0$*. This is because* $\lambda_F^a(s_k)$ *is defined on the discrete domain* $1 \le k \le N$*, so the continuous function* $\lambda_F^a(s)$ *is not a good approximation unless* N *is sufficiently large.*

We note that the condition $B_F \ge 0$ cannot be expected to generally hold for EAM models when the nearest-neighbor term $G_F''(\rho_F')^2 > 0$ dominates. We note, however,

that generally $G'_F < 0$ for $F < 1$ [30], in which case $B_F \geq 0$ is more likely to hold for compressive strains $F < 1$. If we only consider nearest-neighbor interactions, that is,

$$\bar{\rho}^a_\ell(\mathbf{y}) := \rho(y'_\ell) + \rho(y'_{\ell+1}) \qquad \text{and} \qquad \tilde{\mathcal{E}}^a_\ell(\mathbf{y}) := \frac{1}{2}\left[\phi(y'_\ell) + \phi(y'_{\ell+1})\right],$$

then $C_F = D_F = 0$ and $B_F = -G''_F(\rho'_F)^2 < 0$. We thus have the following corollary.

Corollary 4.3.1 *Suppose we only consider nearest-neighbor interactions and that the hypotheses* (4.17) *holds. Then the uniform deformation* $\mathbf{y}_F$ *is stable for the atomistic EAM model if and only if*

$$A_F > 4G''_F(\rho'_F)^2. \tag{4.22}$$

4.3.2 Stability of the Volume-Based Local EAM Model

We focus on the stability of the volume-based local model under a uniform deformation $\mathbf{y}_F$. Using the equilibrium equation (4.5), we obtain the second variation $\delta^2\mathcal{E}^{c,v}(\mathbf{y}_F)$ for any $\mathbf{u} \in \mathcal{U} \setminus \{\mathbf{0}\}$ to be

Comment 4.3.1

$$\begin{aligned}
\langle \delta^2\mathcal{E}^{c,v}(\mathbf{y}_F)\mathbf{u}, \mathbf{u}\rangle =& \epsilon \sum_{\ell=-N+1}^{N} \Big\{ 2G''_F \cdot \left(\rho'_F + 2\rho'_{2F}\right)^2 \left[\left(u'_\ell\right)^2 + \left(u'_{\ell+1}\right)^2\right] \\
&\qquad + G'_F\left(\rho''_F + 4\rho''_{2F}\right)\left[\left(u'_\ell\right)^2 + \left(u'_{\ell+1}\right)^2\right]\Big\} \\
&+ \epsilon \sum_{\ell=-N+1}^{N} \frac{1}{2}\left\{\phi''_F\left[\left(u'_\ell\right)^2 + \left(u'_{\ell+1}\right)^2\right] + 4\phi''_{2F}\left[\left(u'_\ell\right)^2 + \left(u'_{\ell+1}\right)^2\right]\right\} \\
=& \left(\hat{A}_F + \tilde{A}_F\right)\|D\mathbf{u}\|^2_{\ell^2_\epsilon} = A_F\|D\mathbf{u}\|^2_{\ell^2_\epsilon},
\end{aligned}$$

$$\langle \delta^2\mathcal{E}^{c,v}(\mathbf{y}_F)\mathbf{u}, \mathbf{u}\rangle = \left(\hat{A}_F + \tilde{A}_F\right)\|D\mathbf{u}\|^2_{\ell^2_\epsilon} = A_F\|D\mathbf{u}\|^2_{\ell^2_\epsilon},$$

where $\hat{A}_F$ and $\tilde{A}_F$ are defined in (4.12) and (4.10), respectively. It follows that $\mathbf{y}_F$ is stable in the volume-based local model if and only if $A_F > 0$. We summarize this result in the following theorem.

Theorem 4.3.3 *Suppose that the hypotheses* (4.17) *hold. Then the uniform deformation* $\mathbf{y}_F$ *is stable in the volume-based local model* (4.4) *if and only if* $A_F := \hat{A}_F + \tilde{A}_F > 0$.

Remark 4.3.2 *Comparing the conclusions in Theorem 4.3.1 and Theorem 4.3.3, we observe that when $B_F \geq 0$, the difference between the minimum eigenvalues of the fully atomistic and the volume-based local models is of order $O(\epsilon^2)$. This result is the same as for the pair potential case [11].*

However, when $B_F < 0$, the volume-based local model is strictly more stable than the fully atomistic model with $O(1)$ difference between their minimum eigenvalues. In the following, we give a specific example for $B_F < 0$ that can be expected to hold for the stretching of the atomistic chain.

We consider the case

$$\phi''_{2F} + G''_F \left(\rho'_F + 2\rho'_{2F}\right)^2 + G'_F 2\rho''_{2F} > 0. \tag{4.23}$$

Then it follows from (4.17) *that*

$$\begin{aligned} -B_F &= \phi''_{2F} + G''_F \left[\left(\rho'_F\right)^2 + 20\left(\rho'_{2F}\right)^2 + 12\rho'_F\rho'_{2F}\right] + G'_F 2\rho''_{2F} \\ &= \left[\phi''_{2F} + G''_F \left(\rho'_F + 2\rho'_{2F}\right)^2 + G'_F 2\rho''_{2F}\right] + 8G''_F \left(2\left(\rho'_{2F}\right)^2 + \rho'_F\rho'_{2F}\right) > 0. \end{aligned}$$

We define an oscillatory displacement $\tilde{\mathbf{u}}$, corresponding to the $k = N$ eigenmode in the Fourier expansion (4.15)*, by*

$$\tilde{u}_\ell := (-1)^\ell \epsilon/(2\sqrt{2}).$$

Therefore,

$$\tilde{u}'_\ell = (-1)^\ell/(\sqrt{2}), \quad \|D\tilde{\mathbf{u}}\|_{\ell^2_\epsilon} = 1, \quad \tilde{u}''_\ell = (-1)^\ell(\sqrt{2})/\epsilon.$$

From (4.9) *and* (4.11) *we can get*

$$\begin{aligned} \langle \delta^2\mathcal{E}^a(\mathbf{y}_F)\tilde{\mathbf{u}}, \tilde{\mathbf{u}}\rangle &= \epsilon \sum_{\ell=-N+1}^{N} G'_F 2\rho''_F \frac{1}{2} + \left(\phi''_F + 4\phi''_{2F}\right)\|D\tilde{\mathbf{u}}\|^2_{\ell^2_\epsilon} + (-\epsilon^2\phi''_{2F})\|D^{(2)}\tilde{\mathbf{u}}\|^2_{\ell^2_\epsilon} \\ &= G'_F 2\rho''_F + \left(\phi''_F + 4\phi''_{2F}\right) - 4\phi''_{2F} = \phi''_F + G'_F 2\rho''_F. \end{aligned} \tag{4.24}$$

Thus, we can obtain

$$\inf_{\mathbf{u}\in\mathcal{U}\setminus\{\mathbf{0}\},\, \|D\mathbf{u}\|_{\ell^2_\epsilon}=1} \langle \delta^2\mathcal{E}^a(\mathbf{y}_F)\mathbf{u}, \mathbf{u}\rangle \leq \phi''_F + G'_F 2\rho''_F.$$

On the other hand, Theorem 4.3.3 gives that

$$\inf_{\mathbf{u}\in\mathcal{U}\setminus\{\mathbf{0}\},\, \|D\mathbf{u}\|_{\ell^2_\epsilon}=1} \langle \delta^2\mathcal{E}^{c,v}(\mathbf{y}_F)\mathbf{u}, \mathbf{u}\rangle \equiv A_F = 4\left[\phi''_{2F} + G''_F\left(\rho'_F + 2\rho'_{2F}\right)^2 + 2G'_F\rho''_{2F}\right] + \phi''_F + 2G'_F\rho''_F.$$

Therefore, from (4.23) *and* (4.24) *we have*

$$\inf_{\mathbf{u}\in\mathcal{U}\setminus\{\mathbf{0}\},\,\|D\mathbf{u}\|_{\ell^2_\epsilon}=1}\langle\delta^2\mathcal{E}^{c,v}(\mathbf{y}_F)\mathbf{u},\mathbf{u}\rangle > \phi''_F + G'_F 2\rho''_F \geq \inf_{\mathbf{u}\in\mathcal{U}\setminus\{\mathbf{0}\},\,\|D\mathbf{u}\|_{\ell^2_\epsilon}=1}\langle\delta^2\mathcal{E}^{a}(\mathbf{y}_F)\mathbf{u},\mathbf{u}\rangle.$$

This inequality indicates that the uniform deformation $\mathbf{y}_F$ *could be unstable for the atomistic model, but still stable for the volume-based local model.*

4.3.3 Stability of the Reconstruction-Based Local EAM Model

In this case, we do a similar calculation for the reconstruction-based local model and derive the second variation $\delta^2\mathcal{E}^{c,r}(\mathbf{y})$ from the equilibrium equation given by (4.7)

$$\begin{aligned}
\langle\delta^2\mathcal{E}^{c,r}(\mathbf{y}_F)\mathbf{u},\mathbf{u}\rangle =& \epsilon\sum_{\ell=-N+1}^{N}\left\{G''_F\left(\rho'_F+2\rho'_{2F}\right)^2\left(u'_\ell+u'_{\ell+1}\right)^2+G'_F\left(\rho''_F+4\rho''_{2F}\right)\left[\left(u'_\ell\right)^2+\left(u'_{\ell+1}\right)^2\right]\right\}\\
&+\epsilon\sum_{\ell=-N+1}^{N}\frac{1}{2}\left\{\phi''_F\left[\left(u'_\ell\right)^2+\left(u'_{\ell+1}\right)^2\right]+\phi''_{2F}\left[\left(4u'_\ell\right)^2+4\left(u'_{\ell+1}\right)^2\right]\right\}\\
=&\left[4G''_F\left(\rho'_F+2\rho'_{2F}\right)^2+2G'_F\left(\rho''_F+4\rho''_{2F}\right)+\phi''_F+4\phi''_{2F}\right]\|D\mathbf{u}\|^2_{\ell^2_\epsilon}\\
&-\epsilon^2G''_F\left(\rho'_F+2\rho'_{2F}\right)^2\|D^{(2)}\mathbf{u}\|^2_{\ell^2_\epsilon}\\
=&A_F\|D\mathbf{u}\|^2_{\ell^2_\epsilon}+\epsilon^2\tilde{B}_F\|D^{(2)}\mathbf{u}\|^2_{\ell^2_\epsilon},
\end{aligned}$$

where A_F is defined in (4.10) and $\tilde{B}_F$ is defined to be

$$\tilde{B}_F := -G''_F\left(\rho'_F+2\rho'_{2F}\right)^2\leq 0. \tag{4.25}$$

We recall that for the EAM-atomistic model, the coefficient B_F of $\|D\mathbf{u}\|^2_{\ell^2_\epsilon}$ in (4.14) is defined as

$$B_F = -\left[\phi''_{2F}+G''_F\left(\left(\rho'_F\right)^2+20\left(\rho'_{2F}\right)^2+12\rho'_F\rho'_{2F}\right)+G'_F\left(2\rho''_{2F}\right)\right].$$

Comparing B_F with $\tilde{B}_F$ defined in (4.25), we find that

$$B_F = \tilde{B}_F-\left[\phi''_{2F}+G''_F\left(16\left(\rho'_{2F}\right)^2+8\rho'_F\rho'_{2F}\right)+G'_F\left(2\rho''_{2F}\right)\right].$$

We note that B_F can be positive since $\phi''_{2F}<0$, while $\tilde{B}_F$ is always negative.

We similarly use the Fourier representation

$$Du_\ell = \sum_{\substack{k=-N+1\\k\neq 0}}^{N}\frac{c_k}{\sqrt{2}}\cdot\exp\left(i\,k\frac{\ell}{N}\pi\right)$$

to analyze the stability of $\delta^2\mathcal{E}^{c,r}(\mathbf{y}_F)$. Again, we exclude $k=0$ because of the mean zero condition of $D\mathbf{u}$. From the discrete orthogonality of the Fourier basis, we have

$$\langle \delta^2\mathcal{E}^{c,r}(\mathbf{y}_F)\mathbf{u},\mathbf{u}\rangle = \sum_{\substack{k=-N+1\\k\neq 0}}^{N} |c_k|^2 \cdot \left\{ A_F + \tilde{B}_F\left[4\sin^2\left(\frac{k\pi}{2N}\right)\right]\right\}. \tag{4.26}$$

The eigenvalues $\lambda_k^{c,r}$ of $\langle \delta^2\mathcal{E}^{c,r}(\mathbf{y}_F)\mathbf{u},\mathbf{u}\rangle$ with respect to the $\|D\mathbf{u}\|_{\ell^2_\epsilon}$ norm are given by

$$\lambda_k^{c,r} = \lambda_F^{c,r}(s_k) \quad \text{for } k=1,\dots,N,$$

where

$$s_k = 4\sin^2\left(\frac{k\pi}{2N}\right) \quad \text{and} \quad \lambda_F^{c,r}(s) := A_F + \tilde{B}_F s.$$

The assumption (4.17) implies that $\tilde{B}_F \leq 0$ always holds, so $\lambda_F^{c,r}(s)$ is decreasing for $0\leq s\leq 4$ and the minimum eigenvalue of $\delta^2\mathcal{E}^{c,r}(\mathbf{y}_F)$ is achieved at $k=N$, i.e., $s_N=4$:

$$\min_{1\leq k\leq N}\lambda_F^{c,r}(s_k) = \lambda_F^{c,r}(4) = A_F + 4\tilde{B}_F = 2G_F'\left(\rho_F'' + 4\rho_{2F}''\right) + \phi_F'' + 4\phi_{2F}''.$$

The minimum eigenmode is given by the oscillatory displacement $\hat{u}_\ell' = -\hat{u}_{\ell+1}'$ since

$$\langle \delta^2\mathcal{E}^{c,r}(\mathbf{y}_F)\hat{\mathbf{u}},\hat{\mathbf{u}}\rangle = \left[2G_F'\left(\rho_F'' + 4\rho_{2F}''\right) + \phi_F'' + 4\phi_{2F}''\right]\|D\hat{\mathbf{u}}\|^2_{\ell^2_\epsilon}.$$

We thus have the following stability result for the reconstruction-based local model.

Theorem 4.3.4 *Suppose that the hypotheses* (4.17) *hold. Then the uniform deformation* $\mathbf{y}_F$ *is stable for the reconstruction-based local model* (4.6) *if and only if*

$$A_F + 4\tilde{B}_F = 2G_F'\left(\rho_F'' + 4\rho_{2F}''\right) + \phi_F'' + 4\phi_{2F}'' > 0.$$

Remark 4.3.3 *Recall that when* $B_F \geq 0$ *the minimum eigenvalue of the atomistic model* $\delta^2\mathcal{E}^a(\mathbf{y}_F)$ *is*

$$\begin{aligned} A_F + O(\epsilon^2) =& 4\left[\phi_{2F}'' + G_F''\left(\rho_F' + 2\rho_{2F}'\right)^2 + 2G_F'\rho_{2F}''\right] + \phi_F'' + 2G_F'\rho_F'' + O(\epsilon^2)\\ >& 4\left[\phi_{2F}'' + 2G_F'\rho_{2F}''\right] + \phi_F'' + 2G_F'\rho_F''. \end{aligned}$$

Whereas, the minimum eigenvalue of the reconstruction-based local model is always

$$A_F + 4\tilde{B}_F = 4\left[\phi_{2F}'' + 2G_F'\rho_{2F}''\right] + \phi_F'' + 2G_F'\rho_F''.$$

So, the fully atomistic model is strictly more stable than the reconstruction-based local model. However, if $B_F < 0$*, the conclusion will be different, and we will rigorously analyze this case in section 4.4.*

We recall that if we only consider nearest-neighbor interactions, then $C_F = D_F = 0$ and $B_F = -G_F''(\rho_F')^2 < 0$. We thus have the following corollary, which also follows since the reconstruction-based local model is identical to the atomistic model if we restrict the model to nearest-neighbor interactions.

Corollary 4.3.2 *Suppose that we only consider nearest-neighbor interactions and that the hypotheses* (4.17) *hold. Then the uniform deformation* $\mathbf{y}_F$ *is stable for the reconstruction-based EAM model if and only if*

$$A_F > 4G_F''(\rho_F')^2. \tag{4.27}$$

4.4 Comparison of the Stability of the Atomistic and Local EAM Models

In this section, we would like to give a full discussion of the sharp stability estimates for all of the EAM models. Recall that the eigenvalue function of $\delta^2\mathcal{E}^a(\mathbf{y}_F)$ is

$$\lambda_F^a(s_k) := A_F + B_F s_k + C_F s_k^2 + D_F s_k^3 \quad \text{for} \quad s_k = 4\sin^2\left(\frac{k\pi}{2N}\right), \quad k = 1, \ldots, N,$$

where the coefficients A_F, B_F, C_F and D_F are given in the equation (4.13).

To simplify the following analyses, the number of atoms N is assumed to be sufficiently large. Thus, we use the global minimum of the continuous function $\lambda_F^a(s) := A_F + B_F s + C_F s^2 + D_F s^3$ for $0 \le s \le 4$ to approximate $\min_{1\le k\le N} \lambda_F^a(s_k)$. We note that their difference is at most of order $O\left(2k\epsilon^2\right) \le O(\epsilon)$.

We recall that

$$\min_{0\le s\le 4} \lambda_F^a(s) = \lambda_F^a(0) \quad \text{if } B_F \ge 0. \tag{4.28}$$

To find $\min_{0\le s\le 4} \lambda_F^a(s)$ when $B_F < 0$, we first evaluate $\lambda_F^a(s)$ at $s = 0, 4$:

$$\begin{aligned}
\lambda_F^a(0) =& A_F = 4G_F''\left(\rho_F' + 2\rho_{2F}'\right)^2 + 2G_F'\left(\rho_F'' + 4\rho_{2F}''\right) + \phi_F' + 4\phi_{2F}'', \\
\lambda_F^a(4) =& \phi_F'' + 2G_F'\rho_F''.
\end{aligned}$$

We next compute the first and second derivatives of $\lambda_F^a(s)$, which are

$$\begin{aligned}
\lambda_F^{a\,\prime}(s) =& B_F + 2C_F s + 3D_F s^2, \\
\lambda_F^{a\,\prime\prime}(s) =& 2C_F + 6D_F s.
\end{aligned}$$

Since $\lambda_F^a{}'(s)$ is a quadratic function, we thus have two critical points of $\lambda_F^a(s)$ when the coefficients satisfy

$$C_F^2 - 3B_F D_F \geq 0 \quad \text{or equivalently} \quad \phi_{2F}'' + 2G_F'\rho_{2F}'' \leq \frac{1}{3}G_F''\left(\rho_F' - 2\rho_{2F}'\right)^2.$$

We can summarize the case when $B_F < 0$ and $C_F^2 - 3B_F D_F \leq 0$ by

$$\min_{0\leq s\leq 4} \lambda_F^a(s) = \lambda_F^a(4) \quad \text{if } B_F < 0 \text{ and } C_F^2 - 3B_F D_F \leq 0. \tag{4.29}$$

In the case $C_F^2 - 3B_F D_F > 0$, the critical points are

$$s_1 = \frac{C_F - \sqrt{C_F^2 - 3B_F D_F}}{-3D_F} \quad \text{and} \quad s_2 = \frac{C_F + \sqrt{C_F^2 - 3B_F D_F}}{-3D_F}.$$

Since $D_F < 0$, $\lambda_F^a(s)$ will then have a local minimum at $s^* = s_1$ and a local maximum at s_2. The corresponding local minimum value is

$$\begin{aligned}\lambda_F^a(s^*) =& A_F + B_F s^* + C_F(s^*)^2 + D_F(s^*)^3 \\ =& A_F + s^*\left(\frac{B_F}{2} - \frac{D_F}{2}(s^*)^2\right),\end{aligned}$$

where we use $\lambda_F^a{}'(s^*) = 0$ to get the last equality. We can thus summarize all of the cases by

$$\begin{aligned}&\min_{0\leq s\leq 4} \lambda_F^a(s) = \lambda_F^a(0) \quad \text{if } B_F \geq 0, \\ &\min_{0\leq s\leq 4} \lambda_F^a(s) = \lambda_F^a(4) \quad \text{if } B_F < 0 \text{ and } C_F^2 - 3B_F D_F \leq 0, \\ &\min_{0\leq s\leq 4} \lambda_F^a(s) = \min\{\lambda_F^a(s^* \wedge 4), \lambda_F^a(4)\} \quad \text{if } B_F < 0 \text{ and } C_F^2 - 3B_F D_F > 0,\end{aligned} \tag{4.30}$$

with $s^* \wedge 4 := \min\{s^*, 4\}$.

We note that the minimum eigenvalues of the volume-based and the reconstruction-based local models are separately given by the following expressions

$$\begin{aligned}\lambda_F^{c,v} :=& \min_{0\leq s\leq 4} \lambda_F^{c,v}(s) = A_F = 4G_F''\left(\rho_F' + 2\rho_{2F}'\right)^2 + 2G_F'\left(\rho_F'' + 4\rho_{2F}''\right) + \phi_F'' + 4\phi_{2F}'', \\ \lambda_F^{c,r} :=& \min_{0\leq s\leq 4} \lambda_F^{c,r}(s) = A_F - 4G_F''\left(\rho_F' + 2\rho_{2F}'\right)^2 = 2G_F'\left(\rho_F'' + 4\rho_{2F}''\right) + \phi_F'' + 4\phi_{2F}''.\end{aligned} \tag{4.31}$$

We thus see from the hypothesis (4.17) that

$$\lambda_F^{c,r} < \lambda_F^{c,v}$$

and the set of stable uniform deformations for the reconstruction-based local model is a proper subset of the set of stable uniform deformations for the volume-based local model.

4.4.1 The Volume-based Local EAM versus the Atomistic EAM

We first compare the minimum eigenvalues of the volume-based local and the atomistic models. Combining the results of Theorem 4.3.1 and Theorem 4.3.2, we have the following theorem.

Theorem 4.4.1 *The relation of the stability of the volume-based local model and the atomistic model depends on the sign of*

$$B_F := -\left[\phi_{2F}'' + G_F''\Big((\rho_F')^2 + 20(\rho_{2F}')^2 + 12\rho_F'\rho_{2F}'\Big) + G_F'\left(2\rho_{2F}''\right)\right]$$

and can be summarized as follows:

$$\begin{aligned}\min_{0\le s\le 4}\lambda_F^a(s) =& \lambda_F^a(0) = \lambda_F^{c,v} \quad \textit{if} \quad B_F \ge 0,\\ \min_{0\le s\le 4}\lambda_F^a(s) <& \lambda_F^a(0) = \lambda_F^{c,v} \quad \textit{if} \quad B_F < 0.\end{aligned}$$

This observation indicates that the set of stable uniform strains for the volume-based local model always includes that for the fully atomistic EAM model.

4.4.2 The Reconstruction-based Local EAM versus the Atomistic EAM

The relation of the minimum eigenvalues for $\delta^2\mathcal{E}^a(\mathbf{y}_F)$ and $\delta^2\mathcal{E}^{c,r}(\mathbf{y}_F)$ is more complicated. We note that assumption (4.17) implies

$$\begin{aligned}\lambda_F^a(0) =& A_F = 4G_F''\left(\rho_F' + 2\rho_{2F}'\right)^2 + 2G_F'\left(\rho_F'' + 4\rho_{2F}''\right) + \phi_F'' + 4\phi_{2F}''\\ \ge& 2G_F'\left(\rho_F'' + 4\rho_{2F}''\right) + \phi_F'' + 4\phi_{2F}'' = \lambda_F^{c,r},\end{aligned}$$

and we have

$$\lambda_F^a(4) - \lambda_F^{c,r} = -4\left(\phi_{2F}'' + G_F' \cdot 2\rho_{2F}''\right).$$

We thus conclude that if

$$\phi''_{2F} + G'_F \cdot 2\rho''_{2F} \leq 0, \tag{4.32}$$

then

$$\lambda^a_F(4) \geq \lambda^{c,r}_F.$$

The equal sign is achieved if and only if $\phi''_{2F} + G'_F \cdot 2\rho''_{2F} = 0$. We also have the identity

$$\phi''_{2F} + G'_F \cdot 2\rho''_{2F} = -B_F - \left[G''_F\Big((\rho'_F)^2 + 20(\rho'_{2F})^2 + 12\rho'_F\rho'_{2F}\Big)\right].$$

We next compare $\lambda^a_F(s^*)$ and $\lambda^{c,r}_F$. The difference of these two is

$$\begin{aligned}
\lambda^a_F(s^*) - \lambda^{c,r}_F &= 4G''_F\left(\rho'_F + 2\rho'_{2F}\right)^2 + s^*\left(\frac{B_F}{2} - \frac{D_F}{2}(s^*)^2\right) \\
&= 4G''_F\left(\rho'_F + 2\rho'_{2F}\right)^2 \\
&\quad + \frac{C_F - \sqrt{C_F^2 - 3B_FD_F}}{-3D_F} \cdot \frac{6B_FD_F - 2C_F^2 + C_F\left(C_F + \sqrt{C_F^2 - 3B_FD_F}\right)}{9D_F} \\
&= 4G''_F\left(\rho'_F + 2\rho'_{2F}\right)^2 - \frac{B_FC_F}{9D_F} + \frac{2\left(C_F^2 - 3B_FD_F\right)\left(C_F - \sqrt{C_F^2 - 3B_FD_F}\right)}{27D_F^2} \\
&\geq 4G''_F\left(\rho'_F + 2\rho'_{2F}\right)^2 - \frac{B_FC_F}{9D_F}.
\end{aligned} \tag{4.33}$$

According to the assumption (4.32), we can use the definition of C_F and D_F (4.13) to get

$$\begin{aligned}
B_F &= -\left[\phi''_{2F} + G'_F \cdot 2\rho''_{2F} + G''_F\left((\rho'_F)^2 + 12\rho'_F\rho'_{2F} + 20(\rho'_{2F})^2\right)\right] \\
&\geq -G''_F\left((\rho'_F)^2 + 12\rho'_F\rho'_{2F} + 20(\rho'_{2F})^2\right).
\end{aligned}$$

We thus can obtain from the above inequality and the assumption (4.17) that

$$\begin{aligned}
\lambda^a_F(s^*) - \lambda^{c,r}_F &\geq 4G''_F\left(\rho'_F + 2\rho'_{2F}\right)^2 - \frac{B_FC_F}{9D_F} \\
&\geq 4G''_F\left(\rho'_F + 2\rho'_{2F}\right)^2 + \frac{G''_F\left(8\rho'_{2F} + 2\rho'_F\right)\left((\rho'_F)^2 + 12\rho'_F\rho'_{2F} + 20(\rho'_{2F})^2\right)}{-9\rho'_{2F}} \\
&= 2G''_F\frac{\left(\rho'_F + 2\rho'_{2F}\right)\left(2\rho'_{2F} - \rho'_F\right)^2}{9\rho'_{2F}} \geq 0.
\end{aligned}$$

Therefore, we have that

$$\begin{aligned} \min_{0\le s\le 4} \lambda_F^a(s) &= \min_{0\le s\le 4} \lambda_F^{c,r}(s) \quad \text{if} \quad \phi_{2F}'' + G_F' \cdot 2\rho_{2F}'' = 0, \\ \min_{0\le s\le 4} \lambda_F^a(s) &> \min_{0\le s\le 4} \lambda_F^{c,r}(s) \quad \text{if} \quad \phi_{2F}'' + G_F' \cdot 2\rho_{2F}'' < 0. \end{aligned} \tag{4.34}$$

Now let us turn to the case that the assumption (4.32) fails, which means

$$\phi_{2F}'' + G_F' \cdot 2\rho_{2F}'' > 0. \tag{4.35}$$

In this case we have the opposite conclusion that the fully atomistic model $\mathcal{E}^a(\mathbf{y})$ is strictly less stable than the reconstruction-based local model $\mathcal{E}^{c,r}(\mathbf{y})$. From the condition (4.35), we have

$$\lambda_F^a(4) - \lambda_F^{c,r} = -4\left(\phi_{2F}'' + G_F' \cdot 2\rho_{2F}''\right) < 0, \text{ i.e., } \lambda_F^a(4) < \lambda_F^{c,r}.$$

Hence, when the assumption (4.35) holds, we have

$$\min_{0\le s\le 4} \lambda_F^a(s) \le \lambda_F^a(4) < \min_{0\le s\le 4} \lambda_F^{c,r}(s).$$

We now combine this result with (4.34) and summarize the stability relation between the atomistic model and the reconstruction-based local model by the following theorem.

Theorem 4.4.2 *The relation between the stability of the reconstruction-based local model and the atomistic model depends on the sign of* $\phi_{2F}'' + G_F' \cdot 2\rho_{2F}''$ *and is given by*

$$\begin{aligned} \min_{0\le s\le 4} \lambda_F^a(s) &< \min_{0\le s\le 4} \lambda_F^{c,r}(s) \quad \textit{if} \quad \phi_{2F}'' + G_F' \cdot 2\rho_{2F}'' > 0, \\ \min_{0\le s\le 4} \lambda_F^a(s) &= \min_{0\le s\le 4} \lambda_F^{c,r}(s) \quad \textit{if} \quad \phi_{2F}'' + G_F' \cdot 2\rho_{2F}'' = 0, \\ \min_{0\le s\le 4} \lambda_F^a(s) &> \min_{0\le s\le 4} \lambda_F^{c,r}(s) \quad \textit{if} \quad \phi_{2F}'' + G_F' \cdot 2\rho_{2F}'' < 0. \end{aligned} \tag{4.36}$$

We note from the theorem that the reconstruction-based local model can be less stable than the atomistic model, which might cause stability problems when constructing a coupling method.

4.5 Conclusion

In this chapter, we give precise estimates for the lattice stability of atomistic chains modeled by the fully atomistic EAM model, the volume-based and the reconstruction-based local models. We identify the critical assumptions for the pair potential, the electron density function, and the embedding function to study lattice stability. We find that both the volume-based local model and the reconstruction-based local model can give O(1) errors when they are used to approximate the minimum eigenvalues of the atomistic model. This is quite different from the pair potential case since without embedding energy part, the minimum eigenvalues of all the models are close to each other with difference of order $O(\epsilon^2)$ [21, 42]. Since the critical strain of the model is propotional to its minimum eigenvalue, our results show that the critical strain predicted by the volume-based model is always larger than that predicted by the atomistic model, but the critical strain for reconstruction-based models can be either larger or smaller than the atomistic model. This observation suggests that the volume-based model can improve the stability of atomistic-to-continuum coupling methods since they require the atomistic part to capture the instability.

Further research is needed to determine the significance of these results for multidimensional lattice stability and for atomistic-to-continuum coupling methods that couple an atomistic region with a volume-based local region through a reconstruction-based local region [4, 5].

Chapter 5

Positive-Definiteness of the Blended Force-Based Quasicontinuum Method

5.1 Chapter Review

The development of consistent and stable quasicontinuum models for multi-dimensional crystalline solids remains a challenge. For example, proving stability of the force-based quasicontinuum (QCF) model [14] remains an open problem. In this chapter, we show for 1 and 2 dimensional-spaces that by *blending* atomistic and Cauchy–Born continuum forces (instead of a sharp transition as in the QCF method) one obtains positive-definite blended force-based quasicontinuum (B-QCF) models. We establish sharp conditions on the required blending width.

The remainder of the paper is split into two sections: In Section 5.2 we analyze positivity of the B-QCF operator in a 1D model, whereas in Section 5.3 we analyze a 2D model. Our methods and results are likely more widely applicable to other force-based model couplings.

5.2 Analysis of the B-QCF Operator in 1D

5.2.1 Auxiliary lemma

We will frequently use the following summation by parts identity:

Lemma 5.2.1 (Summation by parts) *Suppose* $\{f_k\}_{k=m}^{n+1}$ *and* $\{g_k\}_{k=m}^{n+1}$ *are two sequences, then*

$$\sum_{k=m}^{n} f_k \left(g_{k+1} - g_k\right) = \left[f_{n+1}g_{n+1} - f_m g_m\right] - \sum_{k=n}^{m} g_{k+1}\left(f_{k+1} - f_k\right).$$

Also for future reference, we state a discrete Poincaré inequality [44],

$$\|\mathbf{v}\|_{\ell^\infty_\epsilon} \leq \|D\mathbf{v}\|_{\ell^1_\epsilon} \quad \text{for all}\, \mathbf{v} \in \mathcal{U}.$$

5.2.2 The next-nearest-neighbor atomistic and local QC models

We consider a one-dimensional (1D) atomistic chain with periodicity $2N$, denoted $\mathbf{y} \in \mathcal{Y}$. The total atomistic energy per period of $\mathbf{y}$ is given by $\mathcal{E}^a(\mathbf{y}) - \epsilon \sum_{\ell=-N+1}^{N} f_\ell y_\ell$, where

$$\mathcal{E}^a(\mathbf{y}) = \epsilon \sum_{\ell=-N+1}^{N} \left[\phi(y'_\ell) + \phi(y'_\ell + y'_{\ell-1})\right] \tag{5.1}$$

for external forces f_ℓ and a scaled Lennard-Jones type potential [45, 46] ϕ, which satisfies the following properties:

(i) $\phi \in C^3((0,+\infty);\mathbb{R})$,

(ii) there exists $r_* > 0$ such that ϕ is convex in $(0, r_*)$ and concave in $(r_*, +\infty)$,

(iii) $\phi^{(k)}(r) \to 0$ rapidly as $r \nearrow \infty$ for $k = 0, \ldots, 3$.

The equilibrium equations are given by the force balance at each atom: $F^a_\ell + f_\ell = 0$ where

$$F^a_\ell(\mathbf{y}) := \frac{-1}{\epsilon}\frac{\partial \mathcal{E}^a(\mathbf{y})}{\partial y_\ell} = \frac{1}{\epsilon}\Big\{ \left[\phi'(y'_{\ell+1}) + \phi'(y'_{\ell+2} + y'_{\ell+1})\right] - \left[\phi'(y'_\ell) + \phi'(y'_\ell + y'_{\ell-1})\right] \Big\}. \tag{5.2}$$

To study stability, we linearize the atomistic equilibrium equations about $\mathbf{y}_F$ to obtain

$$(L^a\mathbf{u}^a)_\ell = f_\ell, \quad \text{for} \quad \ell = -N+1, \dots, N,$$

where $(L^a\mathbf{v})$ for a displacement $\mathbf{v} \in \mathcal{U}$ is given by

$$(L^a\mathbf{v})_\ell := \phi''_F \frac{(-v_{\ell+1} + 2v_\ell - v_{\ell-1})}{\epsilon^2} + \phi''_{2F} \frac{(-v_{\ell+2} + 2v_\ell - v_{\ell-2})}{\epsilon^2}.$$

Appropriate extensions of the stability results in this paper can likely be obtained for more general smooth deformations by utilizing the more technical formalism developed in, for example, [8, 41, 28]. Here and throughout we use the notation $\phi''_F := \phi''(F)$ and $\phi''_{2F} := \phi''(2F)$, where ϕ is the potential in (5.1). We assume that $\phi''_F > 0$, which holds for typical pair potentials such as the Lennard-Jones potential under physically relevant deformations.

We will later require the following characterisation of the stability of L^a.

Lemma 5.2.2 *L^a is positive definite, uniformly for $N \in \mathbb{N}$, if and only if $c_0 := \min(\phi''_F, \phi''_F + 4\phi''_{2F}) > 0$. Moreover,*

$$\langle L^a\mathbf{u}, \mathbf{u}\rangle \geq c_0 \|D\mathbf{u}\|^2_{\ell^2_\epsilon} \qquad \forall \mathbf{u} \in \mathcal{U}.$$

Proof The case $\phi''_{2F} \leq 0$ was treated in [21], hence suppose that $\phi''_{2F} > 0$. The coercivity estimate is trivial in this case, and it remains to show that it is also sharp. To that end, we note that

$$\langle L^a\mathbf{u}, \mathbf{u}\rangle = \epsilon \sum_\ell \phi''_F (u'_\ell)^2 + \epsilon \sum_\ell \phi''_{2F} (u'_{\ell-1} + u'_\ell)^2.$$

Hence, testing with $u'_\ell = (-1)^\ell$ (this is admissible since there is an even number of atoms per period), the second-neighbor terms drop out and we obtain $\langle L^a\mathbf{u}, \mathbf{u}\rangle = \phi''_F \|D\mathbf{u}\|^2_{\ell^2_\epsilon}$. □

The local QC approximation (QCL) uses the Cauchy–Born extrapolation rule [17, 4], that is, approximating $y'_\ell + y'_{\ell-1}$ in (5.1) by $2y'_\ell$ in our context. Thus, the QCL energy is given by

$$\mathcal{E}^{qcl}(\mathbf{y}) = \epsilon \sum_{\ell=-N+1}^{N} \left[\phi(y'_\ell) + \phi(2y'_\ell)\right]. \tag{5.3}$$

Then the local continuum forces $F^{qcl}(\mathbf{y})$ are

$$F_\ell^{qcl}(\mathbf{y}) := \frac{-1}{\epsilon}\frac{\partial \mathcal{E}^{qcl}(\mathbf{y})}{\partial y_\ell} = \frac{1}{\epsilon}\Big\{ \left[\phi'(y'_{\ell+1}) + 2\phi'(2y'_{\ell+1})\right] - \left[\phi'(y'_\ell) + 2\phi'(2y'_\ell)\right] \Big\}.$$

We can similarly obtain the linearized QCL equilibrium equations about the uniform deformation

$$\left(L^{qcl}\mathbf{u}^{qcl}\right)_\ell = f_\ell \quad \text{for} \quad \ell = -N+1, \ldots, N,$$

where the expression of $\left(L^{qcl}\mathbf{v}\right)_\ell$ with $\mathbf{v} \in \mathcal{U}$ is

$$\left(L^{qcl}\mathbf{v}\right)_\ell := \left(\phi''_F + 4\phi''_{2F}\right)\frac{(-v_{\ell+1} + 2v_\ell - v_{\ell-1})}{\epsilon^2}.$$

5.2.3 The Blended QCF Operator

The blended QCF (B-QCF) operator is obtained through smooth blending of the atomistic and local QC models. Let $\beta : \mathbb{R} \to \mathbb{R}$ be a "smooth" and 2-periodic blending function, then we define

$$F_\ell^{bqcf}(\mathbf{y}) := \beta_\ell F_\ell^a(\mathbf{y}) + (1-\beta_\ell)F_\ell^{qcl}(\mathbf{y}),$$

where F_ℓ^{qcl} is defined analogously to F_ℓ^a and $\beta_\ell := \beta(F\epsilon\ell)$. Linearization about $\mathbf{y}_F$ yields the linearized B-QCF operator

$$(L^{bqcf}\mathbf{v})_\ell := \beta_\ell (L^a\mathbf{v})_\ell + (1-\beta_\ell)(L^{qcl}\mathbf{v})_\ell.$$

In order to obtain a *practical* atomistic-to-continuum coupling scheme, we would also need to coarsen the continuum region by choosing a coarser finite element mesh. In the present work we focus exclusively on the stability of the B-QCF operator, which is a necessary ingredient in any subsequent analysis of the B-QCF method.

5.2.4 Positive-Definiteness of the B-QCF Operator

We begin by writing L^{bqcf} in the form $L^{bqcf} = \phi''_F L_1^{bqcf} + \phi''_{2F} L_2^{bqcf}$ where

$$\begin{aligned}
\left(L_1^{bqcf}\mathbf{v}\right)_\ell &= \epsilon^{-2}\left(-v_{\ell+1} + 2v_\ell - v_{\ell-1}\right), \quad \text{and} \\
\left(L_2^{bqcf}\mathbf{v}\right)_\ell &= \beta_\ell\epsilon^{-2}\left(-v_{\ell+2} + 2v_\ell - v_{\ell-2}\right) + (1-\beta_\ell)4\epsilon^{-2}\left(-v_{\ell+1} + 2v_\ell - v_{\ell-1}\right).
\end{aligned}$$

Lemma 5.2.3 *For any $\mathbf{u} \in \mathcal{U}$, the nearest neighbor and next-nearest neighbor interaction operator can be written in the form*

$$\begin{aligned}\langle L_1^{bqcf}\mathbf{u},\mathbf{u}\rangle =& \|D\mathbf{u}\|_{\ell_\epsilon^2}^2, \quad \textit{and}\\ \langle L_2^{bqcf}\mathbf{u},\mathbf{u}\rangle =& \left[4\|D\mathbf{u}\|_{\ell_\epsilon^2}^2 - \epsilon^2\|\sqrt{\beta}D^{(2)}\mathbf{u}\|_{\ell_\epsilon^2}^2\right] + \mathbf{R}+\mathbf{S}+\mathbf{T},\end{aligned} \tag{5.4}$$

where the terms $\mathbf{R}$, $\mathbf{S}$ *and* $\mathbf{T}$ *are given by*

$$\begin{aligned}\mathbf{R} = \sum_{\ell=-N+1}^{N} 2\epsilon^3 D^{(2)}\beta_\ell \left(Du_\ell\right)^2, \quad \mathbf{S} = \sum_{\ell=-N+1}^{N} \epsilon^4 D^{(2)}\beta_\ell D^{(2)} u_\ell Du_\ell\\ \textit{and} \quad \mathbf{T} = \sum_{\ell=-N+1}^{N} \epsilon^3 \left(D^{(3)}\beta_{\ell+1}\right) u_\ell Du_{\ell+1}.\end{aligned} \tag{5.5}$$

Proof Since the proof of the first identity of Lemma 5.2.3 is not difficult, we only prove the identity for L_2^{bqcf}. The main tool used here is the summation by parts formula. We note that

$$\begin{aligned}\langle L_2^{bqcf}\mathbf{u},\mathbf{u}\rangle =& \epsilon \sum_{\ell=-N+1}^{N} \beta_\ell \frac{(-u_{\ell+2}+2u_\ell-u_{\ell-2})}{\epsilon^2}u_\ell + (1-\beta_\ell)\frac{4\left(-u_{\ell+1}+2u_\ell-u_{\ell-1}\right)}{\epsilon^2}u_\ell\\ =& \epsilon \sum_{\ell=-N+1}^{N} \frac{4\left(-u_{\ell+1}+2u_\ell-u_{\ell-1}\right)}{\epsilon^2}u_\ell\\ &+ \epsilon \sum_{\ell=-N+1}^{N} \beta_\ell \frac{(-u_{\ell+2}+4u_{\ell+1}-6u_\ell+4u_{\ell-1}-u_{\ell-2})}{\epsilon^2}u_\ell\\ =& 4\|D\mathbf{u}\|_{\ell_\epsilon^2}^2\\ &+ \epsilon \sum_{\ell=-N+1}^{N} \beta_\ell \frac{\left[-\left(u_{\ell+2}-2u_{\ell+1}+u_\ell\right)+2\left(u_{\ell+1}-2u_\ell+u_{\ell-1}\right)-\left(u_\ell-2u_{\ell-1}+u_{\ell-2}\right)\right]}{\epsilon^2}u_\ell\\ =& 4\|D\mathbf{u}\|_{\ell_\epsilon^2}^2 + \sum_{\ell=-N+1}^{N} \epsilon^2\beta_\ell\left(-D^{(3)}u_{\ell+1}+D^{(3)}u_\ell\right)u_\ell.\end{aligned} \tag{5.6}$$

We then apply the summation by parts formula to the second term of (5.6) to obtain

$$\begin{aligned}&\sum_{\ell=-N+1}^{N} \beta_\ell\epsilon^2\left(-D^{(3)}u_{\ell+1}+D^{(3)}u_\ell\right)u_\ell\\ &\quad= \sum_{\ell=-N+1}^{N} \epsilon^2 D^{(3)}u_{\ell+1}\left[\beta_{\ell+1}u_{\ell+1}-\beta_\ell u_\ell\right] = \sum_{\ell=-N+1}^{N} \epsilon^3 D^{(3)}u_\ell\left[\beta_\ell Du_\ell + u_{\ell-1}D\beta_\ell\right].\end{aligned}$$

We use the summation by parts formula again and change the index according to the periodicity so that we get

$$
\begin{aligned}
&\sum_{\ell=-N+1}^{N} \epsilon^3 D^{(3)}u_\ell \left[\beta_\ell Du_\ell + u_{\ell-1}D\beta_\ell\right] \\
&\quad= \sum_{\ell=-N+1}^{N} \epsilon^2 \left(\beta_\ell Du_\ell\right)\left(D^{(2)}u_\ell - D^{(2)}u_{\ell-1}\right) + \sum_{\ell=-N+1}^{N} \epsilon^3 \left(D^{(3)}u_\ell\right) u_{\ell-1}D\beta_\ell \\
&\quad= \sum_{\ell=-N+1}^{N} \epsilon^2 \left(-D^{(2)}u_\ell\right)\left(\beta_{\ell+1}Du_{\ell+1} - \beta_\ell Du_\ell\right) + \sum_{\ell=-N+1}^{N} \epsilon^3 \left(D^{(3)}u_\ell\right) u_{\ell-1}D\beta_\ell \\
&\quad= \sum_{\ell=-N+1}^{N} \epsilon^2 \left(-D^{(2)}u_\ell\right)\left[\beta_{\ell+1}Du_{\ell+1} - \beta_\ell Du_{\ell+1} + \beta_\ell Du_{\ell+1} - \beta_\ell Du_\ell\right] \\
&\qquad\qquad + \sum_{\ell=-N+1}^{N} \epsilon^3 \left(D^{(3)}u_\ell\right) u_{\ell-1}D\beta_\ell \qquad (5.7) \\
&\quad= -\epsilon^2 \|\sqrt{\beta}D^{(2)}\mathbf{u}\|_{\ell^2_\epsilon}^2 + \sum_{\ell=-N+1}^{N} \epsilon^3 \left[-D^{(2)}u_{\ell-1}D\beta_\ell Du_\ell + D^{(3)}u_\ell\, u_{\ell-1}D\beta_\ell\right].
\end{aligned}
$$

We now focus on the second term of (5.7). We repeatedly use the summation by parts formula to obtain

$$
\begin{aligned}
&\sum_{\ell=-N+1}^{N} \epsilon^3 \left[-D^{(2)}u_{\ell-1}D\beta_\ell Du_\ell + \left(D^{(3)}u_\ell\right) u_{\ell-1}D\beta_\ell\right] \\
&\quad= \sum_{\ell=-N+1}^{N} -\epsilon^2 D\beta_\ell \left[(Du_\ell)^2 - (Du_{\ell-1})^2\right] \\
&\qquad + \sum_{\ell=-N+1}^{N} \epsilon^2 D\beta_\ell \left[\left(Du_\ell - Du_{\ell-1}\right)Du_{\ell-1} + \left(D^{(2)}u_\ell - D^{(2)}u_{\ell-1}\right)u_{\ell-1}\right] \\
&\quad= \sum_{\ell=-N+1}^{N} \epsilon^3 D^{(2)}\beta_\ell \left(Du_\ell\right)^2 + \sum_{\ell=-N+1}^{N} \epsilon^2 D\beta_\ell \left[u_{\ell-1}D^{(2)}u_\ell - u_{\ell-2}D^{(2)}u_{\ell-1}\right] \\
&\quad= \sum_{\ell=-N+1}^{N} 2\epsilon^3 D^{(2)}\beta_\ell \left(Du_\ell\right)^2 + \sum_{\ell=-N+1}^{N} \epsilon^4 D^{(2)}\beta_\ell D^{(2)}u_\ell Du_\ell + \sum_{\ell=-N+1}^{N} \epsilon^3 \left(D^{(3)}\beta_{\ell+1}\right) u_\ell Du_{\ell+1} \\
&\quad= \mathbf{R} + \mathbf{S} + \mathbf{T},
\end{aligned}
$$

where $\mathbf{R}$, $\mathbf{S}$ and $\mathbf{T}$ are defined in (5.5).

Combining all of the above equalities, we obtain (5.4). $\square$

We shall see below that the first group in (5.4) does not negatively affect the stability of the B-QCF operator. By contrast, the three terms **R**, **S**, **T** should be considered "error terms". We estimate them in the next lemma.

In order to proceed with the analysis, we define

$$\mathcal{I} := \big\{\ell \in \mathbb{Z} : 0 < \beta_{\ell+j} < 1 \text{ for some } j \in \{\pm 1, \pm 2\}\big\},$$

so that $D^{(j)}\beta_\ell = 0$ for all $\ell \in \{-N+1, \dots N\} \setminus \mathcal{I}$ and $j \in \{1, 2, 3\}$, and $K := \sharp\mathcal{I}$. It is obvious that $K < 2N$.

Lemma 5.2.4 *Let* **R**, **S** *and* **T** *be defined by* (5.5)*, then we have the following estimates:*

$$\begin{aligned} |\mathbf{R}| &\le 2\epsilon^2 \|D^{(2)}\beta\|_{\ell^\infty_\epsilon} \|D\mathbf{u}\|^2_{\ell^2_\epsilon}, \\ |\mathbf{S}| &\le 2\epsilon^2 \|D^{(2)}\beta\|_{\ell^\infty_\epsilon} \|D\mathbf{u}\|^2_{\ell^2_\epsilon}, \quad \textit{and} \\ |\mathbf{T}| &\le \epsilon^2\sqrt{2}(K\epsilon)^{1/2} \|D^{(3)}\beta\|_{\ell^\infty_\epsilon} \|D\mathbf{u}\|^2_{\ell^2_\epsilon}. \end{aligned} \tag{5.8}$$

Proof The estimate for **R** follows directly from Hölder's inequality.

To estimate **S** recall that $D^{(2)}u_\ell := \frac{Du_{\ell+1} - Du_\ell}{\epsilon}$, which implies

$$\|D^{(2)}\mathbf{u}\|^2_{\ell^2_\epsilon} \le \frac{4}{\epsilon^2}\|D\mathbf{u}\|^2_{\ell^2_\epsilon}. \tag{5.9}$$

Therefore, **S** is bounded by

$$|\mathbf{S}| = \left| \sum_{\ell=-N+1}^{N} \epsilon^4 D^{(2)}\beta_\ell D^{(2)}u_\ell Du_\ell \right| \le \epsilon^3 \|D^{(2)}\beta\|_{\ell^\infty_\epsilon} \|D^{(2)}\mathbf{u}\|_{\ell^2_\epsilon} \|D\mathbf{u}\|_{\ell^2_\epsilon} \le 2\epsilon^2 \|D^{(2)}\beta\|_{\ell^\infty_\epsilon} \|D\mathbf{u}\|^2_{\ell^2_\epsilon}.$$

Finally, we estimate **T** by

$$|\mathbf{T}| = \left| \sum_{\ell=-N+1}^{N} \epsilon^3 D^{(3)}\beta_{\ell+1} Du_{\ell+1}\, u_\ell \right| \le \epsilon^2 \|D^{(3)}\beta\|_{\ell^\infty_\epsilon} \|\mathbf{u}\|_{\ell^2_\epsilon(\mathcal{I})} \|D\mathbf{u}\|_{\ell^2_\epsilon},$$

We then apply the Hölder inequality, the Poincaré inequality and Jensen's inequality successively to $\|\mathbf{u}\|_{\ell^2_\epsilon(\mathcal{I})}$ to get

$$\|\mathbf{u}\|^2_{\ell^2_\epsilon(\mathcal{I})} \le (K\epsilon)\|\mathbf{u}\|^2_{\ell^\infty_\epsilon} \le K\epsilon \|D\mathbf{u}\|^2_{\ell^1_\epsilon} \le 2K\epsilon \|D\mathbf{u}\|^2_{\ell^2_\epsilon}.$$

Therefore, we have

$$|\mathbf{T}| \leq \epsilon^2 \|D^{(3)}\beta\|_{\ell^\infty_\epsilon} \|\mathbf{u}\|_{\ell^2_\epsilon(\mathcal{I})} \|D\mathbf{u}\|_{\ell^2_\epsilon} \leq \sqrt{2}\epsilon^2 \|D^{(3)}\beta\|_{\ell^\infty_\epsilon} (K\epsilon)^{1/2} \|D\mathbf{u}\|^2_{\ell^2_\epsilon}.$$

Combining the above estimates, we have proven the second inequality in (5.8). □

We see from the previous result that smoothness of β crucially enters the estimates on the error terms $\mathbf{R}$, $\mathbf{S}$, $\mathbf{T}$. Before we state our main result in 1D we show how quasi-optimal blending functions can be constructed to minimize these terms, which will require us to introduce the *blending width* into the analysis. The estimate (5.10) is stated for a single connected interface region, however, an analogous result holds if the interface has connected components with comparable width. A similar result can also be found in [8].

Lemma 5.2.5 *(i) Suppose that the blending region is connected, that is* $\mathcal{I} = \{1, \dots, K\}$ *without loss of generality, then* β *can be chosen such that*

$$\|D^{(j)}\beta\|_{\ell^\infty} \leq C_\beta (K\epsilon)^{-j}, \quad \text{for } j = 1, 2, 3, \tag{5.10}$$

where C_β *is independent of* K *and* ϵ.

(ii) This estimate is sharp in sense that, if β_ℓ *attains both the values* 0 *and* 1, *then*

$$\|D^{(j)}\beta\|_{\ell^\infty} \geq (K\epsilon)^{-j}, \quad \text{for } j = 1, 2, 3. \tag{5.11}$$

(iii) Suppose that $\mathcal{J} = \{1, \dots, n\} \subset \mathcal{I}$ *such that* $\beta(1) = 0$, $\beta(n) = 1$ *(or vice-versa), and* $0, n+1 \notin \mathcal{I}$, *and suppose moreover that* (5.10) *is satisfied, then*

$$\#\big\{\ell \in \mathcal{J} : D^{(3)}\beta_\ell \leq -\tfrac{1}{2}(\epsilon K)^{-3}\big\} \geq \tfrac{1}{2C_\beta} K. \tag{5.12}$$

Proof *(i)* The upper bound follows by fixing a reference blending function $B \in C^3(\mathbb{R})$, $B = 0$ in $(-\infty, 0]$ and $B = 1$ in $[1, +\infty)$, and defining $\beta(x) = B((x - 2\epsilon)/(\epsilon K'))$ for $K' = K - 4$. Then $\mathcal{I} = \{1, \dots, K\}$, and a scaling argument immediately gives (5.10).

(ii) To prove the lower bound, suppose $0 < \beta_\ell < 1$ for $\ell = 1, \dots, K_0 - 1$, and $\beta_0 = 0$ and $\beta_{K_0} = 1$. Then $\epsilon \sum_{\ell=1}^{K_0} \beta'_\ell = 1$, from which infer the existence of $K_1 \in \{1, \dots, K_0\}$ such that $\beta'_{K_1} \geq 1/(\epsilon K_0)$. This establishes the lower bound for $j = 1$. To prove it for $j = 2$ we note that, since $\beta_{K_0} = 1$, $\beta'_{K_0+1} \leq 0$, and hence we obtain

$$\epsilon \sum_{\ell=K_1+1}^{K_0} \beta''_\ell = \beta'_{K_0+1} - \beta'_{K_1} \leq -1/(\epsilon K_0).$$

We deduce that there exists K_2 such that $\beta''_{K_2} \leq -1/(\epsilon^2 K_0(K_0 - K_1)) \leq -1/(\epsilon K)^2$. This implies (5.11) for $j = 2$. We can argue similarly to obtain the result for $j = 3$.

(iii) Finally, to establish (5.12), let $m \in \mathbb{N}$ be chosen minimally such that $\beta''_m \leq -(\epsilon K)^{-2}$ and $\beta''_0 = 0$; then $m \leq n$ and we have

$$-\frac{1}{(\epsilon K)^2} \geq \beta''_m - \beta''_0 = \epsilon \sum_{\ell=1}^{m} \beta'''_\ell \geq -\frac{\epsilon k C_\beta}{(\epsilon K)^3} - \frac{\epsilon(m-k)}{2(\epsilon K)^3},$$

where $k := \#\{\ell \in \mathcal{J} : \beta'''_\ell \leq -\frac{1}{2}(\epsilon K)^{-3}\}$. Since $K \geq m - k$ by construction, we obtain together with the above inequality

$$-\frac{1}{2(\epsilon K)^2} \geq -\frac{1}{(\epsilon K)^2} + \frac{\epsilon(m-k)}{2(\epsilon K)^3} \geq -\frac{\epsilon k C_\beta}{(\epsilon K)^3} \geq -\frac{k C_\beta}{K(\epsilon K)^2},$$

and we immediately deduce that $k/K \geq 1/(2C_\beta)$, which concludes the proof of item (iii). $\square$

We can summarize the previous estimates and get the following optimal condition for the size K of the blending region provided that β is chosen in a quasi-optimal way. Formally, the result states that L^{bqcf} is positive definite if and only if $K \gg \epsilon^{-1/5}$. In particular, we conclude that the B-QCF operator is positive definite for fairly moderate blending widths.

Theorem 5.2.1 *Let $\mathcal{I}$ and K be defined as in Lemma 5.2.5, and suppose that β is chosen to satisfy the upper bound* (5.10)*. Then there exists a constant $C_1 = C_1(C_\beta)$, such that*

$$\langle L^{bqcf}\mathbf{u}, \mathbf{u}\rangle \geq \big(c_0 - C_1|\phi''_{2F}|\big[K^{-5/2}\epsilon^{-1/2}\big]\big)\|D\mathbf{u}\|^2_{\ell^2_\epsilon} \qquad \forall \mathbf{u} \in \mathcal{U}, \tag{5.13}$$

where $c_0 = \min(\phi''_F, \phi''_F + 4\phi''_{2F})$ is the atomistic stability constant of Lemma 5.2.2.

Moreover, if β_ℓ takes both the values 0 and 1, then there exist constants $C_2, C_3 > 0$, independent of $\mathcal{I}$, N, ϕ''_F and ϕ''_{2F}, such that

$$\inf_{\substack{\mathbf{u}\in\mathcal{U} \\ \|D\mathbf{u}\|_{\ell^2_\epsilon}=1}} \langle L^{bqcf}\mathbf{u}, \mathbf{u}\rangle \leq \phi''_F + C_2|\phi''_{2F}| - C_3|\phi''_{2F}|\big[K^{-5/2}\epsilon^{-1/2}\big]. \tag{5.14}$$

Remark 5.2.1 *Estimates* (5.13) *and* (5.14) *establish the asymptotic optimality of the blending width $K \eqsim \epsilon^{-1/5}$ in the limit as $\epsilon \to 0$:* (5.13) *implies that, if $c_0 > 0$ and $K \gg \epsilon^{-1/5}$, then L^{bqcf} is coercive, while* (5.14) *shows that, if $K \ll \epsilon^{-1/5}$ then L^{bqcf} is necessarily indefinite.* $\square$

Proof We first prove the lower bound. The blended force-based operator satisfies L^{bqcf}

$$\langle L^{bqcf}\mathbf{u},\mathbf{u}\rangle = A_F\|D\mathbf{u}\|_{\ell^2_\epsilon}^2 - \epsilon^2\phi''_{2F}\|\sqrt{\beta}D^{(2)}\mathbf{u}\|_{\ell^2_\epsilon}^2 + \phi''_{2F}(\mathbf{R}+\mathbf{S}+\mathbf{T})$$

where $A_F := \phi''_F + 4\phi''_{2F}$. From Lemma 5.2.4, we have

$$|\mathbf{R}+\mathbf{S}+\mathbf{T}| \leq \epsilon^2\left[4\|D^{(2)}\beta\|_{\ell^\infty_\epsilon} + (K\epsilon)^{1/2}\|D^{(3)}\beta\|_{\ell^\infty_\epsilon}\right]\|D\mathbf{u}\|_{\ell^2_\epsilon}^2.$$

Since $\|D^{(j)}\beta\|_{\ell^\infty_\epsilon} \leq C_\beta(K\epsilon)^{-j}$, so we have

$$|\mathbf{R}+\mathbf{S}+\mathbf{T}| \leq C\epsilon^2\left[4(K\epsilon)^{-2} + (K\epsilon)^{1/2}(K\epsilon)^{-3}\right]\|D\mathbf{u}\|_{\ell^2_\epsilon}^2 \leq C_3\left[K^{-5/2}\epsilon^{-1/2}\right]\|D\mathbf{u}\|_{\ell^2_\epsilon}^2,$$

where we used the fact that $K^{-2} \leq K^{-5/2}\epsilon^{-1/2}$.

If $\phi''_{2F} \leq 0$, then we obtain

$$\langle L^{bqcf}\mathbf{u},\mathbf{u}\rangle \geq \left(A_F - C_1|\phi''_{2F}|\left[K^{-5/2}\epsilon^{-1/2}\right]\right)\|D\mathbf{u}\|_{\ell^2_\epsilon}^2.$$

If $\phi''_{2F} > 0$, then by applying (5.9)

$$\begin{aligned}\langle L^{bqcf}\mathbf{u},\mathbf{u}\rangle =&\ A_F\|D\mathbf{u}\|_{\ell^2_\epsilon}^2 - \epsilon^2\phi''_{2F}\|\sqrt{\beta}D^{(2)}\mathbf{u}\|_{\ell^2_\epsilon}^2 + \phi''_{2F}(\mathbf{R}+\mathbf{S}+\mathbf{T})\\ \geq&\ \left(\phi''_F - C_3|\phi''_{2F}|\left[K^{-5/2}\epsilon^{-1/2}\right]\right)\|D\mathbf{u}\|_{\ell^2_\epsilon}^2,\end{aligned}$$

which is the corresponding result.

To prove the opposite bound, let $\mathcal{J}$ be defined as in Lemma 5.2.5 (iii). We can assume this without loss of generality upon possibly shifting and inverting the blending function. We define $\mathcal{J}' := \{\ell \in \mathcal{J} : D^{(3)}\beta_\ell \leq -\frac{1}{2}(\epsilon K)^{-3}\}$ and $L := \epsilon\#\mathcal{J}' = \alpha\epsilon K$ for some $\alpha \geq 1/(2C_\beta)$, and a test function $\mathbf{v} \in \mathcal{U}$ through $v_0 = \frac{1}{2}$ and

$$v'_\ell = \begin{cases} L^{-1/2}, & \ell \in \mathcal{J}' \\ 0, & \ell \in \mathcal{I}\setminus\mathcal{J}', \end{cases} \tag{5.15}$$

and extending v'_ℓ outside of $\mathcal{I}$ in such a way that $\|D\mathbf{v}\|_{\ell^2_\epsilon}$ is bounded uniformly in $\mathcal{I}$ and N, and such that $\mathbf{v}$ is $2N$-periodic (see [12] for details of this construction).

With these definitions we obtain

$$\begin{aligned}\mathbf{T} =&\ \epsilon^3\sum_{\ell=-N+1}^{N} D^{(3)}\beta_{\ell+1}Dv_{\ell+1}\,v_\ell = \epsilon^3\sum_{\ell\in\mathcal{J}'} D^{(3)}\beta_{\ell-1}v'_\ell v_{\ell-1}\\ \leq&\ -\frac{\epsilon^2 LL^{-1/2}}{4(\epsilon K)^3} = -\frac{(\alpha\epsilon K)^{1/2}}{4\epsilon K^3} = -\tfrac{\alpha^{1/2}}{4}K^{-5/2}\epsilon^{-1/2}.\end{aligned}$$

Recall that, by contrast, we have

$$|\mathbf{R} + \mathbf{S}| \leq C_2 K^{-2} \|D\mathbf{v}\|_{\ell^2_\epsilon}^2.$$

Combining these estimates, and using the fact that $\|D\mathbf{v}\|_{\ell^2_\epsilon}$ is bounded independently of $\mathcal{I}$ and N, yields (5.14). $\square$

5.3 Positive-Definiteness of the B-QCF Operator in 2D

5.3.1 The triangular lattice

For some integer $N \in \mathbb{N}$ and $\epsilon := 1/N$, we define the scaled 2D triangular lattice

$$\mathbb{L} := \mathtt{A}_6 \mathbb{Z}^2, \quad \text{where} \quad \mathtt{A}_6 := [a_1, a_2] := \epsilon \begin{bmatrix} 1 & 1/2 \\ 0 & \sqrt{3}/2 \end{bmatrix},$$

where a_i, $i = 1, 2$ are the scaled lattice vectors. Throughout our analysis, we use the following definition of the periodic reference cell

$$\Omega := \mathtt{A}_6(-N, N]^2 \quad \text{and} \quad \mathcal{L} := \mathbb{L} \cap \Omega.$$

We furthermore set $a_3 = (-1/2\epsilon, \sqrt{3}/2\epsilon)^\mathtt{T}$, $a_4 := -a_1, a_5 := -a_2$ and $a_6 := -a_3$; then the set of *nearest-neighbor directions* is given by

$$\mathcal{N}_1 := \{\pm a_1, \pm a_2, \pm a_3\}.$$

The set of *next nearest-neighbor directions* is given by

$$\mathcal{N}_2 := \{\pm b_1, \pm b_2, \pm b_3\}, \quad \text{where} \quad b_1 := a_1 + a_2, \quad b_2 := a_2 + a_3 \quad \text{and} \quad b_3 = a_3 - a_1.$$

We use the notation $\mathcal{N} := \mathcal{N}_1 \cup \mathcal{N}_2$ to denote the directions of the neighboring bonds in the interaction range of each atom (see Figure 5.1).

We identify all lattice functions $\mathbf{v} : \mathbb{L} \to \mathbb{R}^2$ with their continuous, piecewise affine interpolants with respect to the canonical triangulation $\mathcal{T}$ of $\mathbb{R}^2$ with nodes $\mathbb{L}$.

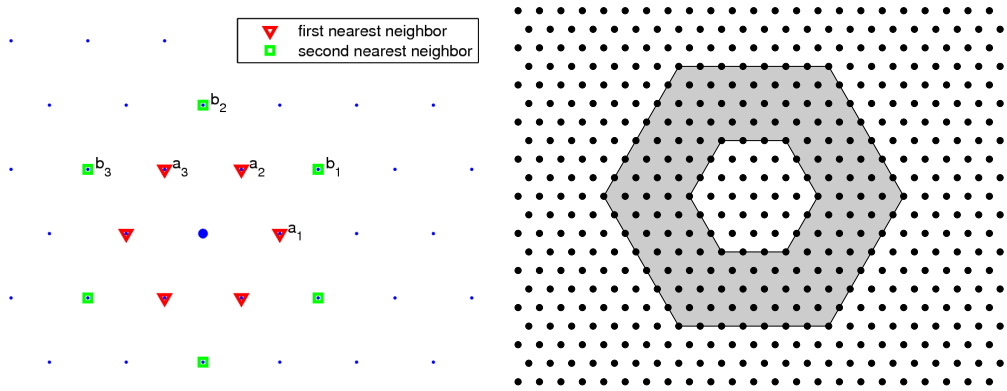

(a) Neighbor Set (b) Domain Decomposition

Figure 5.1: (a) The 12 neighboring bonds of each atom. (b) The atomistic region is $\Omega_a = \texttt{Hex}(\epsilon R_a)$. The blending region is $\Omega_b = \texttt{Hex}(\epsilon R_b) \setminus \Omega_a$. Here, $R_a = 3$, $R_b = 7$ and $K = 4$.

5.3.2 The atomistic, continuum and blending regions

Let $\texttt{Hex}(r)$ denote the closed hexagon centered at the origin, with sides aligned with the lattice directions a_1, a_2, a_3, and diameter $2r$.

For $R_a < R_b \in \mathbb{N}$, we define the atomistic, blending and continuum regions, respectively, as

$$\Omega_a := \texttt{Hex}(\epsilon R_a), \quad \Omega_b := \texttt{Hex}(\epsilon R_b) \setminus \Omega_a, \quad \text{and} \quad \Omega_c := \operatorname{clos}\left(\Omega \setminus (\Omega_a \cup \Omega_b)\right).$$

We denote the blending width by $K := R_b - R_a$. Moreover, we define the corresponding lattice sites

$$\mathcal{L}^a := \mathcal{L} \cap \Omega_a, \qquad \mathcal{L}^b := \mathcal{L} \cap \Omega_b, \qquad \text{and} \qquad \mathcal{L}^c := \mathcal{L} \cap \Omega_c.$$

For simplicity, we will again use $\mathcal{L}$ as the finite element nodes, that is, every atom is a repatom.

For a map $\mathbf{v} : \mathbb{L} \to \mathbb{R}^2$ and bond directions $r, s \in \mathcal{N}$, we define the finite difference operators

$$D_r v(x) := \frac{v(x+r) - v(x)}{\epsilon} \quad \text{and} \quad D_r D_s v(x) := \frac{D_s v(x+r) - D_s v(x)}{\epsilon}.$$

We define the space of all admissible displacements, $\mathcal{U}$, as all discrete functions $\mathbb{L} \to \mathbb{R}^2$ which are Ω-periodic and satisfy the mean zero condition on the computational

domain:

$$\mathcal{U} := \Big\{ \mathbf{u} : \mathbb{L} \to \mathbb{R}^2 : u(x) \text{ is } \Omega\text{-periodic and } \textstyle\sum_{x\in\mathcal{L}} u(x) = 0 \Big\}.$$

For a given matrix $B \in \mathbb{R}^{2\times 2}$, $\det(B) > 0$, we admit deformations $\mathbf{y}$ from the space

$$\mathcal{Y}_B := \big\{ \mathbf{y} : \mathbb{L} \to \mathbb{R}^2 : y(x) = Bx + u(x),\ \forall x \in \mathbb{L} \text{ for some } \mathbf{u} \in \mathcal{U} \big\}.$$

For a displacement $\mathbf{u} \in \mathcal{U}$ and its discrete directional derivatives, we employ the weighted discrete ℓ^2_ϵ and ℓ^∞_ϵ norms given by

$$\|\mathbf{u}\|_{\ell^2_\epsilon} := \left(\epsilon^2 \sum_{x\in\mathcal{L}} |u(x)|^2 \right)^{1/2}, \quad \|\mathbf{u}\|_{\ell^\infty_\epsilon} := \max_{x\in\mathcal{L}} |u(x)|, \quad \text{and}$$

$$\|D\mathbf{u}\|_{\ell^2_\epsilon} := \left(\epsilon^2 \sum_{x\in\mathcal{L}} \sum_{i=1}^{3} |D_{a_i} u(x)|^2 \right)^{1/2}.$$

The inner product associated with ℓ^2_ϵ is

$$\langle \mathbf{u}, \mathbf{w} \rangle := \epsilon^2 \sum_{x\in\mathcal{L}} u(x) \cdot w(x).$$

5.3.3 The B-QCF operator

The total scaled atomistic energy for a periodic computational cell Ω is

$$\mathcal{E}^a(\mathbf{y}) = \frac{\epsilon^2}{2} \sum_{x\in\mathcal{L}} \sum_{r\in\mathcal{N}} \phi(D_r y(x)) = \epsilon^2 \sum_{x\in\mathcal{L}} \sum_{i=1}^{3} \big[\phi(D_{a_i} y(x)) + \phi(D_{b_i} y(x)) \big], \tag{5.16}$$

where $\phi \in C^2(\mathbb{R}^2)$, for the sake of simplicity. Typically, one assumes $\phi(r) = \varphi(|r|)$; the more general form we use gives rise to a simplified notation; see also [41]. We define $\phi'(r) \in \mathbb{R}^2$ and $\phi''(r) \in \mathbb{R}^{2\times 2}$ to be, respectively, the gradient and hessian of ϕ.

The equilibrium equations are given by the force balance at each atom,

$$F^a(x; y) + f(x; y) = 0, \quad \text{for} \quad x \in \mathcal{L}, \tag{5.17}$$

where $f(x; y)$ are the external forces and $F^a(x; y)$ are the atomistic forces (per unit volume ϵ^2)

$$\begin{aligned} F^a(x; y) &:= -\frac{1}{\epsilon^2} \frac{\partial \mathcal{E}^a(\mathbf{y})}{\partial y(x)} \\ &= -\frac{1}{\epsilon} \sum_{i=1}^{3} \Big[\phi' \left(D_{a_i} y(x) \right) + \phi' \left(D_{-a_i} y(x) \right) \Big] - \frac{1}{\epsilon} \sum_{i=1}^{3} \Big[\phi' \left(D_{b_i} y(x) \right) + \phi' \left(D_{-b_i} y(x) \right) \Big]. \end{aligned}$$

Again, since $\mathbf{u} = \mathbf{y} - \mathbf{y}_B$, where $y_B(x) = Bx$, is assumed to be small we can linearize the atomistic equilibrium equation (5.17) about $\mathbf{y}_B$:

$$(L^a \mathbf{u}^a)(x) = f(x), \quad \text{for} \quad x \in \mathcal{L},$$

where $(L^a \mathbf{u})(x)$, for a displacement $\mathbf{u}$, is given by

$$(L^a \mathbf{u})(x) = -\sum_{i=1}^{3} \phi''(Ba_i) D_{a_i} D_{a_i} u(x - a_i) - \sum_{i=1}^{3} \phi''(Bb_i) D_{b_i} D_{b_i} u(x - b_i), \quad \text{for} \quad x \in \mathcal{L}.$$

The QCL approximation uses the Cauchy–Born extrapolation rule to approximate the nonlocal atomistic model by a local continuum model [17, 18, 3]. According to the bond density lemma [41, Lemma 3.2] (see also [22]), we can write the total QCL energy as a sum of the bond density integrals

$$\mathcal{E}^c(\mathbf{y}) = \int_\Omega \sum_{r \in \mathcal{N}} \phi(\partial_r y)\, dx = \sum_{x \in \mathcal{L}} \sum_{r \in \mathcal{N}} \int_0^1 \phi\big(\partial_r y(x + tr)\big) dt, \tag{5.18}$$

where $\partial_r y(x) = \frac{d}{dt} y(x + tr)|_{t=0}$ denotes the directional derivative. We compute the continuum force $F^c(x; y) = -\frac{1}{\epsilon^2} \frac{\partial \mathcal{E}^c}{\partial y(x)}$, and linearize the force equation about the uniform deformation $\mathbf{y}_B$ to obtain

$$(L^c \mathbf{u}^c)(x) = f(x), \quad \text{for} \quad x \in \mathcal{L}.$$

To formulate the B-QCF method, let the blending function $\beta(s) : \mathbb{R}^2 \to [0, 1]$ be a "smooth", Ω-periodic function. We shall suppose throughout that R_a, R_b are chosen in such a way that

$$\operatorname{supp}(D_{a_{i_1}} D_{a_{i_2}} D_{a_{i_3}} \beta) \subset \Omega_b \qquad \forall (i_1, i_2, i_3) \in \{1, \ldots, 6\}^3. \tag{5.19}$$

Then, the (nonlinear) B-QCF forces are given by

$$F^{bqcf}(x; y) := \beta(x) F^a(x; y) + (1 - \beta(x)) F^c(x; y),$$

and linearizing the equilibrium equation $F^{bqcf} + f = 0$ about y_B yields

$$\begin{aligned} &(L^{bqcf} \mathbf{u}^{bqcf})(x) = f(x), \quad \text{for } x \in \mathcal{L}, \\ &\text{where} \quad (L^{bqcf} \mathbf{u})(x) = \beta(x)(L^a \mathbf{u})(x) + (1 - \beta(x))(L^c \mathbf{u})(x). \end{aligned} \tag{5.20}$$

Since the nearest neighbor terms in the atomistic and the QCL models are the same, we will focus on the second-neighbor interactions. We rewrite the operator L^{bqcf} in the form

$$\begin{aligned}(L^{bqcf}\mathbf{u})(x) = &\sum_{r\in\mathcal{N}}(L_r^{bqcf}\mathbf{u})(x),\\ \text{where}\quad L_r^{bqcf}\mathbf{u}(x) = &\ \beta(x)(L_r^a\mathbf{u})(x) + (1-\beta(x))(L_r^c\mathbf{u})(x),\end{aligned}$$

where the nearest-neighbor operators are given by

$$L_{a_j}^a\mathbf{u}(x) = L_{a_j}^c\mathbf{u}(x) = -\phi''(Ba_j)D_{a_j}D_{a_j}u(x-a_j),$$

and the second-neighbor operators, stated for convenience only for $b_1 = a_1 + a_2$, by

$$\begin{aligned}\left(L_{b_1}^a\mathbf{u}\right)(x) =& -\phi''(Bb_1)D_{b_1}D_{b_1}u(x-b_1), \quad \text{while}\\ \left(L_{b_1}^c\mathbf{u}\right)(x) =& -\phi''(Bb_1)\big[D_{a_1}D_{a_1}u(x-a_1) + D_{a_2}D_{a_2}u(x-a_2)\\ &+ D_{a_1}D_{a_2}u(x-a_1) + D_{a_1}D_{a_2}u(x-a_2)\big].\end{aligned}$$

5.3.4 Auxiliary results

The following is the 2D counterpart of the summation by parts formula. The proof is straightforward.

Lemma 5.3.1 (Summation by parts) *For any $\mathbf{u}\in\mathcal{U}$ and any direction $r\in\mathcal{L}$, we have*

$$\sum_{x\in\mathcal{L}} D_rD_ru(x-r)\cdot u(x) = -\sum_{x\in\mathcal{L}} D_ru(x-r)\cdot D_ru(x-r). \tag{5.21}$$

The second auxiliary result we require is a trace- or Poincaré-type inequality to bound $\|\mathbf{u}\|_{\ell^2_\epsilon(\Omega_b)}$ in terms of global norms. As a first step we establish a continuous version of the inequality we are seeking. The key technical ingredient in its proof is a sharp trace inequality, which is stated in Section **??**.

Lemma 5.3.2 *Let $r_a < r_b \in (0, 1/2]$, and let $H := \mathtt{Hex}(r_b)\setminus\mathtt{Hex}(r_a)$; then there exists a constant C that is independent of r_a, r_b such that*

$$\|u\|^2_{L^2(H)} \le C\big[(r_b-r_a)r_b|\log r_b|\big]\|\partial u\|^2_{L^2(\Omega)} \qquad \forall u\in H^1(\Omega), \int_\Omega u dx = 0. \tag{5.22}$$

Proof Let $\Sigma := \partial\texttt{Hex}(1)$, and let dS denote the surface measure, then

$$\|u\|^2_{L^2(H)} = \int_{r=r_a}^{r_b} \int_{r\Sigma} |u|^2 dS\, dr.$$

Applying (A.1) with $r_0 = r$ and $r_1 = 1$ to each surface integral, we obtain

$$\|u\|^2_{L^2(H)} \leq (r_b - r_a)\big(C_0\|u\|^2_{L^2(\Omega)} + C_1\|\partial u\|^2_{L^2(\Omega)}\big),$$

where $C_0 \leq 8r_b$ and $C_1 = 2r_b|\log r_b|$. An application of Poincaré's inequality yields (5.22). $\square$

In our analysis, we require a result as (5.22) for discrete norms. We establish this next, using straightforward norm-equivalence arguments.

Lemma 5.3.3 *Suppose that $R_b \leq N/2$, then*

$$\|\mathbf{u}\|^2_{\ell^2_\epsilon(\mathcal{L}^b)} \leq C\,(C_P^{a,b})^2\|D\mathbf{u}\|^2_{\ell^2_\epsilon} \qquad \forall \mathbf{u} \in \mathcal{U}. \tag{5.23}$$

where C is a generic constant, and $C_P^{a,b} := \big[(\epsilon K)(\epsilon R_b)|\log(\epsilon R_b)|\big]^{1/2}$.

Proof Recall the identification of $\mathbf{u}$ with its corresponding P_1-interpolant. Let $T \in \mathcal{T}$ with corners x_j, $j = 1, 2, 3$, then

$$\int_T u\, dx = \frac{|T|}{3}\sum_{j=1}^{3} u(x_j), \quad \text{and hence} \quad \int_\Omega u\, dx = 0 \quad \forall \mathbf{u} \in \mathcal{U}.$$

Let $r_a := \epsilon R_a$ and $r_b := \epsilon R_b$, then H defined in Lemma 5.3.2 is identical to Ω_b. For any element $T \subset \Omega_b$ it is straightforward to show that

$$\|\mathbf{u}\|_{\ell^2_\epsilon(T)} \leq C\|u\|_{L^2(T)}.$$

This immediately implies

$$\|\mathbf{u}\|_{\ell^2_\epsilon(\mathcal{L}^b)} \leq C\|u\|_{L^2(H)}, \tag{5.24}$$

for a constant C that is independent of ϵ, R_a, K and $\mathbf{u}$. Applying (5.22) yields

$$\|\mathbf{u}\|^2_{\ell^2_\epsilon(\mathcal{L}^b)} \leq C\big[(r_b - r_a)r_b|\log r_b|\big]\|\partial u\|^2_{L^2(\Omega)}.$$

Fix $T \in \mathcal{T}$ and let $x_j \in T$ such that $x_j + a_j \in T$ as well. Employing [41, Eq. (2.1)] we obtain

$$\sum_{j=1}^{3}\big|D_{a_j}u(x_j)\big|^2 = \sum_{j=1}^{3}\big|(\partial u|_T)a_j\big|^2 = \tfrac{3}{2}\big|\partial u|_T\big|^2,$$

and summing over $T \in \mathcal{T}, T \subset \bar{\Omega}$ we obtain that $\|\partial u\|_{L^2(\Omega)} \leq C\|D\mathbf{u}\|_{\ell^2_\epsilon}$. This concludes the proof. $\square$

5.3.5 Bounds on $L_{b_1}^{bqcf}$

We focus only on the b_1-bonds, however, by symmetry analogous results hold for all second-neighbor bonds. As in the 1D case, we begin by converting the quadratic form $\langle L_{b_1}^{bqcf}\mathbf{u},\mathbf{u}\rangle$ into divergence form. To that end it is convenient to define the bond-dependent symmetric bilinear forms and quadratic forms (although we write them like a norm they are typically indefinite)

$$\langle r,s\rangle_b := r^{\mathrm{T}}\phi''(Bb)s, \quad \text{and} \quad |r|_b^2 := \langle r,r\rangle_b, \qquad \text{for } r,s,b\in\mathbb{R}^2.$$

Lemma 5.3.4 *For any displacement $\mathbf{u}\in\mathcal{U}$, we have*

$$\langle L_{b_1}^{bqcf}\mathbf{u},\mathbf{u}\rangle = \langle L_{b_1}^{c}\mathbf{u},\mathbf{u}\rangle - \epsilon^4\sum_{x\in\mathcal{L}}\beta(x-a_2)|D_{a_1}D_{a_2}u(x-a_1-a_2)|_{b_1}^2 + \mathbf{R}_{b_1} + \mathbf{S}_{b_1}, \quad (5.25)$$

where

$$\begin{aligned}\mathbf{R}_{b_1} :=& -\epsilon^4\sum_{x\in\mathcal{L}}\big\{D_{a_1}\beta(x-2a_1)\big\langle D_{a_1}u(x-2a_1), D_{a_2}D_{a_2}u(x-a_1-a_2)\big\rangle_{b_1}\\ &\qquad + D_{a_2}\beta(x-a_2)\big\langle D_{a_1}u(x-a_1), D_{a_1}D_{a_2}u(x-a_1-a_2)\big\rangle_{b_1}\big\}, \quad \textit{and}\\ \mathbf{S}_{b_1} :=& -\epsilon^4\sum_{x\in\mathcal{L}}D_{a_1}D_{a_1}\beta(x-2a_1)\big\langle u(x-a_1), D_{a_2}D_{a_2}u(x-a_1-a_2)\big\rangle_{b_1}.\end{aligned} \quad (5.26)$$

Proof For this purely algebraic proof we may assume without loss of generality that $\phi''(Bb_1) = \mathrm{I}$. In general, one may simply replace all Euclidean inner products with $\langle\cdot,\cdot\rangle_{b_1}$.

Starting from (5.20), we have

$$\begin{aligned}\langle L_{b_1}^{bqcf}\mathbf{u},\mathbf{u}\rangle =& \langle L_{b_1}^{c}\mathbf{u},\mathbf{u}\rangle + \langle L_{b_1}^{a}\mathbf{u} - L_{b_1}^{c}\mathbf{u}, \beta\mathbf{u}\rangle\\ =& \langle L_{b_1}^{c}\mathbf{u},\mathbf{u}\rangle - \epsilon^2\sum_{x\in\mathcal{L}}\beta(x)u(x)\cdot\big[D_{b_1}D_{b_1}u(x-b_1) - D_{a_1}D_{a_1}u(x-a_1)\\ &\qquad - D_{a_2}D_{a_2}u(x-a_2) - D_{a_1}D_{a_2}u(x-a_1) - D_{a_1}D_{a_2}u(x-a_2)\big].\end{aligned}$$

We will focus our analysis on $\langle L_{b_1}^{a}\mathbf{u} - L_{b_1}^{c}\mathbf{u}, \beta\mathbf{u}\rangle$.

Noting that $b_1 = a_1 + a_2$, one can recast $D_{b_1} D_{b_1} u(x - b_1)$ as

$$\begin{aligned}
&D_{b_1} D_{b_1} u(x - b_1) \\
&= \frac{1}{\epsilon^2} \left[u(x + b_1) - 2u(x) + u(x - b_1) \right] \\
&= D_{a_1} D_{a_2} u(x) + D_{a_1} D_{a_1} u(x - a_1) + D_{a_2} D_{a_2} u(x - a_2) + D_{a_1} D_{a_2} u(x - a_1 - a_2).
\end{aligned}$$

Applying the summation by parts formula (5.21) to $\langle L^a_{b_1} \mathbf{u} - L^c_{b_1} \mathbf{u}, \beta \mathbf{u} \rangle$, we get

$$\begin{aligned}
\langle L^a_{b_1} \mathbf{u} - L^c_{b_1} \mathbf{u}, \beta \mathbf{u} \rangle &= -\epsilon^3 \sum_{x \in \mathcal{L}} \beta(x) u(x) \cdot \Big[D_{a_1} D_{a_1} D_{a_2} u(x - a_1) - D_{a_1} D_{a_1} D_{a_2} u(x - a_1 - a_2) \Big] \\
&= -\epsilon^4 \sum_{x \in \mathcal{L}} \beta(x) u(x) \cdot D_{a_1} D_{a_1} D_{a_2} D_{a_2} u(x - a_1 - a_2) \\
&= \epsilon^4 \sum_{x \in \mathcal{L}} D_{a_1} D_{a_2} D_{a_2} u(x - a_1 - a_2) \cdot D_{a_1} \Big(\beta(x - a_1) u(x - a_1) \Big) \\
&= \epsilon^4 \sum_{x \in \mathcal{L}} D_{a_1} D_{a_2} D_{a_2} u(x - a_1 - a_2) \cdot \Big[\beta(x) D_{a_1} u(x - a_1) + u(x - a_1) D_{a_1} \beta(x - a_1) \Big].
\end{aligned}$$

Another application of the summation by parts formula (5.21) converts $\langle L^a_{b_1} \mathbf{u} - L^c_{b_1} \mathbf{u}, \beta \mathbf{u} \rangle$ into

$$\begin{aligned}
\langle L^a_{b_1} \mathbf{u} - L^c_{b_1} \mathbf{u}, \beta \mathbf{u} \rangle =& \epsilon^4 \sum_{x \in \mathcal{L}} D_{a_1} D_{a_2} D_{a_2} u(x - a_1 - a_2) \cdot \big(u(x - a_1) D_{a_1} \beta(x - a_1) \big) \\
&- \epsilon^4 \sum_{x \in \mathcal{L}} D_{a_1} D_{a_2} u(x - a_1 - a_2) \cdot \big(D_{a_2} \beta(x - a_2) D_{a_1} u(x - a_1) \big) \\
&- \epsilon^4 \sum_{x \in \mathcal{L}} D_{a_1} D_{a_2} u(x - a_1 - a_2) \cdot \big(\beta(x - a_2) D_{a_1} D_{a_2} u(x - a_1 - a_2) \big).
\end{aligned}$$

The first two terms on the right-hand side can be rewritten as

$$\begin{aligned}
&\epsilon^4 \sum_{x \in \mathcal{L}} \big\{ D_{a_1} D_{a_2} D_{a_2} u(x - a_1 - a_2) \cdot \big(u(x - a_1) D_{a_1} \beta(x - a_1) \big) \\
&\qquad - D_{a_1} D_{a_2} u(x - a_1 - a_2) \cdot \big(D_{a_2} \beta(x - a_2) D_{a_1} u(x - a_1) \big) \big\} \\
&= -\epsilon^4 \sum_{x \in \mathcal{L}} \Big(u(x - a_1) D_{a_1} D_{a_1} \beta(x - 2a_1) \Big) \cdot D_{a_2} D_{a_2} u(x - a_1 - a_2) \\
&\qquad - \epsilon^4 \sum_{x \in \mathcal{L}} \big\{ D_{a_1} \beta(x - 2a_1) D_{a_1} u(x - 2a_1) \cdot D_{a_2} D_{a_2} u(x - a_1 - a_2) \\
&\qquad\qquad + D_{a_2} \beta(x - a_2) D_{a_1} u(x - a_1) \cdot D_{a_1} D_{a_2} u(x - a_1 - a_2) \big\} \\
&= \mathbf{S}_{b_1} + \mathbf{R}_{b_1}.
\end{aligned}$$

Thus, we obtain (5.25) and (5.26). $\square$

Next, we will bound the singular terms $\mathbf{R}_{b_1}$ and $\mathbf{S}_{b_1}$, for which we introduce the notation

$$\|D^{(2)}\beta\|_{\ell^\infty_\epsilon} := \max_{1\le i,j\le 6} \|D_{a_i}D_{a_j}\beta\|_{\ell^\infty_\epsilon}, \quad \text{and} \quad \|D^{(3)}\beta\|_{\ell^\infty_\epsilon} := \max_{1\le i,j,k\le 6} \|D_{a_i}D_{a_j}D_{a_k}\beta\|_{\ell^\infty_\epsilon}.$$

Lemma 5.3.5 *The terms $\mathbf{R}_{b_1}$ and $\mathbf{S}_{b_1}$ defined in* (5.26) *are bounded by*

$$|\mathbf{R}_{b_1}| \le 4\epsilon^2 |\phi''(Bb_1)|\, \|D\beta\|_{\ell^\infty_\epsilon} \|D\mathbf{u}\|^2_{\ell^2_\epsilon}, \quad \textit{and} \tag{5.27}$$

$$|\mathbf{S}_{b_1}| \le C\epsilon^2 |\phi''(Bb_1)| \Big[\|D^{(2)}\beta\|_{\ell^\infty_\epsilon} + \|D^{(3)}\beta\|_{\ell^\infty_\epsilon} C_P^{a,b} \Big] \|D\mathbf{u}\|^2_{\ell^2_\epsilon}, \tag{5.28}$$

where C is a generic constant and $C_P^{a,b}$ is defined in Lemma 5.3.3.

Proof According to the expression of $\mathbf{R}_{b_1}$ given in (5.26) and noting that

$$\|D_{a_2}D_{a_2}\mathbf{u}\|^2_{\ell^2_\epsilon} \le \frac{4}{\epsilon^2}\|D\mathbf{u}\|^2_{\ell^2_\epsilon} \quad \text{and} \quad \|D_{a_1}D_{a_2}\mathbf{u}\|^2_{\ell^2_\epsilon} \le \frac{4}{\epsilon^2}\|D\mathbf{u}\|^2_{\ell^2_\epsilon},$$

we immediately obtain the first inequality of (5.27).

We first rewrite $\mathbf{S}_{b_1}$ as

$$\begin{aligned}
\mathbf{S}_{b_1} =& -\epsilon^4 \sum_{x\in\mathcal{L}} D_{a_1}D_{a_1}\beta(x-2a_1)\big\langle D_{a_2}D_{a_2}u(x-a_1-a_2), u(x-a_1)\big\rangle_{b_1} \\
=& -\epsilon^4 \sum_{x\in\mathcal{L}} D_{a_1}D_{a_1}\beta(x-2a_1)D_{a_2}\big\langle D_{a_2}u(x-a_1-a_2), u(x-a_1-a_2)\big\rangle_{b_1} \\
&+\epsilon^4 \sum_{x\in\mathcal{L}} D_{a_1}D_{a_1}\beta(x-2a_1)\big\langle D_{a_2}u(x-a_1-a_2), D_{a_2}u(x-a_1-a_2)\big\rangle_{b_1} \\
=& \epsilon^4 \sum_{x\in\mathcal{L}} D_{a_2}D_{a_1}D_{a_1}\beta(x-2a_1-a_2)\big\langle D_{a_2}u(x-a_1-a_2)\cdot u(x-a_1-a_2)\big\rangle_{b_1} \\
&+\epsilon^4 \sum_{x\in\mathcal{L}} D_{a_1}D_{a_1}\beta(x-2a_1)\big|D_{a_2}u(x-a_1-a_2)\big|^2_{b_1}.
\end{aligned} \tag{5.29}$$

For the second term in (5.29), we have

$$\Big|\epsilon^4 \sum_{x\in\mathcal{L}} D_{a_1}D_{a_1}\beta(x-2a_1)\big|D_{a_2}u(x-a_1-a_2)\big|^2_{b_1}\Big| \le \epsilon^2|\phi''(Bb_1)|\|D^{(2)}\beta\|_{\ell^\infty_\epsilon}\|D\mathbf{u}\|^2_{\ell^2_\epsilon}.$$

For the first term, we have

$$\begin{aligned}
&\Big|\epsilon^4 \sum_{x\in\mathcal{L}} D_{a_2}D_{a_1}D_{a_1}\beta(x-2a_1-a_2)\big\langle D_{a_2}u(x-a_1-a_2), u(x-a_1-a_2)\big\rangle_{b_1}\Big| \\
&\quad \le \epsilon^2\,|\phi''(Bb_1)|\,\|\mathbf{u}\,D_{a_2}D_{a_1}D_{a_1}\beta\|_{\ell^2_\epsilon}\|D\mathbf{u}\|_{\ell^2_\epsilon} \le \epsilon^2\,|\phi''(Bb_1)|\,\|D^{(3)}\beta\|_{\ell^\infty_\epsilon}\,\|\mathbf{u}\|_{\ell^2_\epsilon(\mathcal{L}^b)}\,\|D\mathbf{u}\|_{\ell^2_\epsilon}.
\end{aligned}$$

The last inequality comes from the assumption (5.19), which ensures that $\mathrm{supp}(D_{a_2} D_{a_1} D_{a_1} \beta) \subset \Omega_b$.

Applying Lemma 5.3.3 yields the bound for $\mathbf{S}_{b_1}$. $\square$

To summarize the estimates of this section we define a self-adjoint operator $\tilde{L}$ by

$$\langle \tilde{L}\mathbf{u}, \mathbf{u} \rangle := \langle L^c \mathbf{u}, \mathbf{u} \rangle - \epsilon^4 \sum_{j=1}^{3} \sum_{x \in \mathcal{L}} \beta(x - a_2) \big| D_{a_j} D_{a_{j+1}} u(x - a_1 - a_2) \big|_{b_1}^2; \tag{5.30}$$

then, Lemma 5.3.4 and Lemma 5.3.5 immediately yield the following result.

Corollary 5.3.1 *Suppose that R_a and R_b are defined such that* (5.19) *holds; then, for all $\mathbf{u} \in \mathcal{U}$,*

$$\langle L^{bqcf} \mathbf{u}, \mathbf{u} \rangle \geq \langle \tilde{L}\mathbf{u}, \mathbf{u} \rangle - C\, C'' \big[\epsilon^2 \|D\beta\|_{\ell^\infty} + \epsilon^2 \|D^{(2)}\beta\|_{\ell^\infty} + \epsilon^2 C_P^{a,b} \|D^{(3)}\beta\|_{\ell^\infty} \big] \|D\mathbf{u}\|_{\ell^2_\epsilon}^2, \tag{5.31}$$

where C is a generic constant, $C'' := \max_{j=1,2,3} |\phi''(Bb_j)|$ and $C_P^{a,b}$ is defined in Lemma 5.3.3.

Based on the analysis and numerical experiments in [41] for a similar linearized operator we expect that the region of stability for $\tilde{L}$ is the same as for L^a; that is, $\tilde{L}$ is positive definite for a macroscopic strain B if and only if L^a is positive definite. However, we are at this point unable to prove this result. Instead, we have the following weaker result. The proof is elementary.

Proposition 5.3.1 *Suppose that $B \in \mathbb{R}^{2\times 2}$ is such that L^c is positive definite,*

$$\langle L^c \mathbf{u}, \mathbf{u} \rangle \geq \gamma_c \|D\mathbf{u}\|_{\ell^2_\epsilon}^2 \qquad \forall \mathbf{u} \in \mathcal{U},$$

and suppose that $\phi''(Bb_j) \leq \delta \mathrm{I}$ where $\delta < \gamma_c/4$, then $\tilde{L}$ is positive definite,

$$\langle \tilde{L}\mathbf{u}, \mathbf{u} \rangle \geq \tilde{\gamma} \|D\mathbf{u}\|_{\ell^2_\epsilon}^2 \qquad \forall \mathbf{u} \in \mathcal{U}, \tag{5.32}$$

with $\tilde{\gamma} = \gamma_c - 4\delta$.

5.3.6 Positivity of the B-QCF operator in 2D

The *blending width* K is again a crucial ingredient in the stability analysis for L^{bqcf}. Due to the simple geometry we have chosen it is straightforward to generalize Lemma 5.2.5 to the two-dimensional case, using the same arguments as in 1D.

Lemma 5.3.6 *It is possible to choose β such that*

$$\|D^{(j)}\beta\|_{\ell^\infty} \leq C_\beta (K\epsilon)^{-j}, \quad \textit{for } j = 1, 2, 3. \tag{5.33}$$

Since we cannot fully characterize the stability of $\tilde{L}$ in terms of the stability of L^a or L^c we will only prove stability of L^{bqcf} subject to the assumption that $\tilde{L}$ is stable. Proposition 5.3.1 gives sufficient conditions.

Theorem 5.3.1 *Suppose that β is chosen quasi-optimally so that* (5.33) *is attained; then,*

$$\langle L^{bqcf}\mathbf{u}, \mathbf{u}\rangle \geq \gamma_{bqcf}\|D\mathbf{u}\|^2_{\ell^2_\epsilon},$$

where

$$\gamma_{bqcf} := \tilde{\gamma} - C\,C''\left[\epsilon^{-1/2}K^{-5/2}|\epsilon R_b \log(\epsilon R_b)|^{1/2}\right],$$

where C is a generic constant and C'' is defined in Corollary 5.3.1.

In particular, if $\tilde{L}$ is positive definite (5.32) *and if K is sufficiently large, then L^{bqcf} is positive definite.*

Proof From Corollary 5.3.1 and (5.33) we obtain

$$\begin{aligned}\langle L^{bqcf}\mathbf{u}, \mathbf{u}\rangle \geq & \left\{\tilde{\gamma} - C\,C''\left[\epsilon^2(\epsilon K)^{-1} + \epsilon^2(\epsilon K)^{-2} + \epsilon^2(\epsilon K)^{-5/2}|\epsilon R_b \log(\epsilon R_b)|^{1/2}\right]\right\}\|D\mathbf{u}\|^2_{\ell^2_\epsilon} \\ \geq & \left\{\tilde{\gamma} - C\,C''\left[\epsilon^{-1/2}K^{-5/2}|\epsilon R_b \log(\epsilon R_b)|^{1/2}\right]\right\}\|D\mathbf{u}\|^2_{\ell^2_\epsilon}.\end{aligned}$$

□

Remark 5.3.1 *Suppose that $\tilde{\gamma} > 0$, uniformly as $N \to \infty$ (or, $\epsilon \to 0$). In this limit, we would like to understand how to optimally scale K with R_a. (Note that R_a controls the modeling error; cf. Remark 5.3.3.) We consider three different scalings of R_a.*

Case 1: Suppose that R_a is bounded as $\epsilon \to 0$. In that case, we obtain

$$\begin{aligned}\gamma_{bqcf} - \tilde{\gamma} = & -C\,C''\,\epsilon^{-1/2}K^{-5/2}|\epsilon(R_a + K)\log(\epsilon(R_a + K))|^{1/2} \\ = & -C\,C''\,K^{-2}\left|\left(1 + \tfrac{R_a}{K}\right)\left(\log(\epsilon K) + \log(1 + \tfrac{R_a}{K})\right)\right|^{1/2} \\ \eqsim & -C\,C''\,K^{-2}|\log(\epsilon K)|^{1/2}. \end{aligned} \tag{5.34}$$

From this it is easy to see that L^{bqcf} will be positive definite provided we select $K \gg |\log\epsilon|^{1/4}$.

Case 2: Suppose that $1 \ll R_a \ll \epsilon^{-1}$*; to precise, let* $R_a \sim \epsilon^{-\alpha}$ *for some* $\alpha \in (0,1)$*. Then, a similar computation as* (5.34) *yields*

$$\gamma_{bqcf} - \tilde{\gamma} \eqsim K^{-5/2} \big| (K + \epsilon^{-\alpha})(\log \epsilon + \log(K + \epsilon^{-\alpha})) \big|^{1/2},$$

and we deduce that, in this case, L^{bqcf} *will positive definite provided we select* $K \gg \epsilon^{-\alpha/5} |\log \epsilon|^{1/5}$*.*

Case 3: Finally, the case when the atomistic region is macroscopic, i.e., $R_a = O(\epsilon^{-1})$*, can be treated precisely as the 1D case and hence we obtain that, if we select* $K \gg \epsilon^{-1/5}$*, then* L^{bqcf} *is positive.*

In summary, we have shown that, in the limit as $\epsilon \to 0$*, if* $\tilde{L}$ *is positive definite,* $R_a = O(\epsilon^{-\alpha})$ *and if we choose*

$$K \gg \begin{cases} |\log \epsilon|^{1/4}, & \alpha = 0, \\ |\log \epsilon|^{1/5} \epsilon^{-\alpha/5}, & 0 < \alpha < 1, \\ \epsilon^{-1/5}, & \alpha = 1, \end{cases} \tag{5.35}$$

then the B-QCF operator L^{bqcf} *is positive definite and* $\gamma^{bqcf} \sim \tilde{\gamma}$ *as* $\epsilon \to 0$*. We emphasize that these are very mild restrictions on the blending width.* □

It remains to show that the sufficient conditions we derived to guarantee positivity of L^{bqcf} are sharp. A result as general as (5.14) in 1D would be very technical to obtain; instead, we offer a brief formal discussion for a special case.

Remark 5.3.2 *We consider again the limit as* $\epsilon \to 0$*, and for simplicity restrict ourselves to the case where* $0 \ll K \eqsim \epsilon^{-\theta}$ *and* $0 \ll R_a \eqsim \epsilon^{-\alpha}$*, for* $0 < \theta \le \alpha \le 1$*. In particular,* $R_b \eqsim \epsilon^{-\alpha}$ *as well.*

We assume that $D_{a_3}\beta(x) = 0$ *for all* $x \in \mathcal{J} \subset \mathcal{L}^b$*, as depicted in Figure 5.2. The set* $\mathcal{J}$ *should be chosen so that its size is comparable with that of* $\mathcal{L}^b$*, but sufficiently small to still allow* β *to satisfy the bound* (5.33)*. We can now repeat the 1D argument along atomic layers to obtain that*

$$D_{a_2} D_{a_1} D_{a_1} \beta(x) \le -\tfrac{1}{2} (\epsilon K)^{-3} \eqsim -\epsilon^{-3+3\theta}$$

for all x *in a subset* $\mathcal{J}' \subset \mathcal{J}$ *containing entire atomic planes, that has comparable size to* $\mathcal{J}$*; that is,* $\# \mathcal{J}' \eqsim K R_b \eqsim \epsilon^{-\theta-\alpha}$*.*

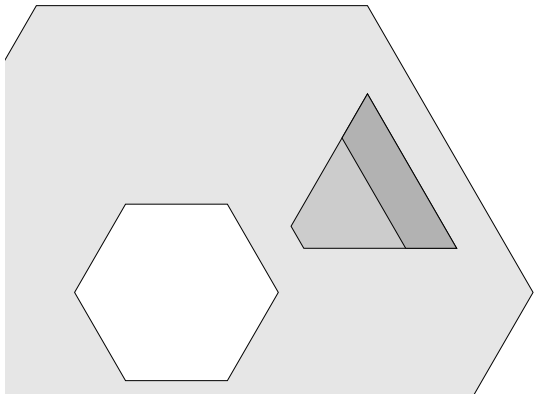

Figure 5.2: Visualization of the construction discussed in Remark 5.3.2: the white region is the atomistic domain, the light gray region the blending region, the medium gray region and dark gray regions together are the set $\mathcal{J}$ and the dark gray region is the set $\mathcal{J}'$.

Suppose now that $\phi''(Bb_1)$ has a negative eigenvalue λ with corresponding normalized eigenvector $\hat{u} \in \mathbb{R}^2$, then we seek test functions of the form $u(x) = \mu(x)\hat{u}$. It is now relatively straightforward, applying the 1D argument in normal direction and using a smooth cut-off in the tangential direction, to construct μ supported in $\mathcal{J}'$ with $D_{a_2}\mu(x) \eqsim (\epsilon^2 \# \mathcal{J}')^{-1/2}$ so that $\|D\mathbf{u}\|_{\ell^2_\epsilon} \eqsim 1$, and

$$\begin{aligned}
&\epsilon^4 \sum_{x \in \mathcal{L}} D_{a_2} D_{a_1} D_{a_1} \beta(x - 2a_1 - a_2) \big\langle D_{a_2} u(x - a_1 - a_2), u(x - a_1 - a_2) \big\rangle_{b_1} \\
&\qquad = \epsilon^4 \lambda_1 \sum_{x \in \mathcal{L}} D_{a_2} D_{a_1} D_{a_1} \beta(x - 2a_1 - a_2) D_{a_2} \mu(x - a_1 - a_2) \mu(x - a_1 - a_2) \\
&\qquad \lesssim -\epsilon^4 \lambda_1 (\# \mathcal{J}')(K\epsilon)^{-3} (\epsilon^2 \# \mathcal{J}')^{-1/2} \eqsim -\epsilon^{(5\theta - \alpha)/2}.
\end{aligned}$$

This shows that, if $K \ll \epsilon^{-\alpha/5}$, then L^{bqcf} is necessarily indefinite.

In summary, for the specific interface geometry and a particular choice of β (which does, however, lead to the quasi-optimal bound (5.33)*) we have shown that Theorem 5.3.1 is sharp up to logarithmic terms.* $\square$

Remark 5.3.3 *In practise, for the computation of different types of defects, we would first choose an appropriate scaling $R_a = \epsilon^{-\alpha}$ for the atomistic region, considering the accuracy of the B-QCF method, and then choose the blending width K in order to ensure stability.*

For instance, for a point defect in 2D with zero Burger's vector it is expected that the displacement field satisfies $u_a(x) = y_a(x) - Bx \eqsim \epsilon/r$, where r is the distance from the defect [47, 41]. Without coarse-graining, the local continuum (QCL) model has a modeling error of order $O(\epsilon^2|\partial^3 u_a|)$ (see [28, 23, 27] for proofs in 1D and [48] for a proof in arbitrary dimensions); and although we have not established it rigorously, we expect that modeling error for the B-QCF method outside the atomistic region is also of second order; see also [12].

From $u(x) \eqsim \epsilon/r$ we can make the reasonable assumption that $|\partial^3 y_a| \eqsim \epsilon/r^4$, from which we obtain (assuming also stability) that the total error is of the order

$$\|\partial(y_a - y_{bqcf})\|_{L^2} \eqsim \epsilon^2 \|\partial^3 y_a\|_{L^2(\Omega\setminus\Omega_a)} \eqsim \epsilon^3 \Big(\int_{\epsilon R_a}^1 r|r^{-4}|^2 dr \Big)^{1/2} \eqsim R_a^{-3}.$$

Hence, if we wish to obtain $\|\partial(y_a - y_{bqcf})\|_{L^2} \eqsim \epsilon^k$, $0 < k < 3$, then we need to choose

$$R_a \eqsim \epsilon^{-k/3}, \quad \text{and consequently} \quad K \gg \epsilon^{-k/15} |\log \epsilon|^{1/5}.$$

With this choice we can ensure both the stability and $O(\epsilon^k)$ accuracy of the B-QCF method; provided that our assumption that the B-QCF method has indeed a second-order modelling error is correct. $\square$

5.4 Conclusion

We have studied the stability of a blended force-based quasicontinuum (B-QCF) method. In 1D we were able to identify an asymptotically optimal condition on the width of the blending region to ensure that the linearized B-QCF operator is coercive if and only if the atomistic operator is coercive as well. In the 2D B-QCF model, we have obtained rigorous sufficient conditions and have presented a heuristic argument suggesting that they are sharp up to logarithmic terms. In 2D our proof of coercivity of L^{bqcf} relies on the coercivity of the auxiliary operator $\tilde{L}$ defined in (5.30), for which we cannot give sharp conditions at this point.

The main conclusion of this work is that the required blending width to ensure coercivity of the linearized B-QCF operator is surprisingly small.

Our analysis in this paper is the first step towards a complete a priori error analysis of the B-QCF method, which will require a coercivity analysis of the B-QCF operator

linearized about arbitrary states, as well as a consistency analysis in negative Sobolev norms.

Chapter 6

Future Work

This chapter discusses the projects that are in progress.

6.1 The development and analysis of the B-QCF method

Currently, we have studied the stability of the B-QCF model for pair-potential interactions in one and two-dimensional spaces. It would be of practical interest to extend it to multi-body potentials, such as EAM potential energies. I am also interested in establishing sharp conditions on the required blending width in three-dimensional problems and verifying our theoretical conclusions numerically. Besides the stability properties of the B-QCF method, I will study the accuracy of the B-QCF method and identify the relation between the modeling error and the blending width.

6.2 The development of Hyper Quasicontinuum method(Hyper-QC)

The multiscale methods I have investigated so far are static methods at zero temperature and hence no dynamics are involved. However, to study equilibrium behavior at finite temperature, it is necessary to adopt a dynamical approach that allows the system to evolve in time [49]. Recently, W. K. Kim, E. B. Tadmor, M. Luskin, D. Perez and A. F. Voter have proposed an accelerated finite-temperature quasicontinuum method by using hyperdynamics. This is called the Hyper-QC method [49]. They also

numerically studied the behavior of the Hyper-QC method for a one-dimensional chain of atoms interacting via a Lennard-Jones potential. I have been in the weekly Hyper-QC meeting with these authors and plan to work with them on the research project. Furthermore, I will investigate other stochastic dynamical methods, for example the well-known Parallel Replica method by A. F. Voter [50], and be involved in the development of two-dimensional computational benchmark problems to study the accuracy of these methods.

6.3 The development of multiscale methods for multi-lattices crystals

It is an open problem to develop a/c coupling methods for multi-lattices crystals like hexagonal carbon rings. In the investigation of the stable B-QCF method for single lattice crystals, we find that it is possible to extend this method to multi-lattices problems. I plan to generalize our original B-QCF method and study the stability and modeling error for multilattices.

References

[1] W. Curtin and R. Miller. Atomistic/continuum coupling in computational materials science. *Modell. Simul. Mater. Sci. Eng.*, 11(3):R33–R68, 2003.

[2] P. Lin. Convergence analysis of a quasi-continuum approximation for a two-dimensional material without defects. *SIAM J. Numer. Anal.*, 45(1):313–332 (electronic), 2007.

[3] R.E. Miller and E.B. Tadmor. The quasicontinuum method: overview, applications and current directions. *Journal of Computer-Aided Materials Design*, 9:203–239, 2003.

[4] T. Shimokawa, J.J. Mortensen, J. Schiotz, and K.W. Jacobsen. Matching conditions in the quasicontinuum method: Removal of the error introduced at the interface between the coarse-grained and fully atomistic region. *Phys. Rev. B*, 69(21):214104, 2004.

[5] W. E, J. Lu, and J.Z. Yang. Uniform accuracy of the quasicontinuum method. *Phys. Rev. B*, 74(21):214115, 2006.

[6] R. Miller and E. Tadmor. Benchmarking multiscale methods. *Modelling and Simulation in Materials Science and Engineering*, 17:053001 (51pp), 2009.

[7] X. Blanc, C. Le Bris, and F. Legoll. Analysis of a prototypical multiscale method coupling atomistic and continuum mechanics. *M2AN Math. Model. Numer. Anal.*, 39(4):797–826, 2005.

[8] Brian Van Koten and Mitchell Luskin. Analysis of energy-based blended quasicontinuum approximations. *SIAM. J. Numer. Anal.*, 49:2182–2209, 2011.

[9] Xingjie Helen Li and Mitchell Luskin. An analysis of the quasi-nonlocal quasicontinuum approximation of the embedded atom model. *International Journal for Multiscale Computational Engineering*, to appear. arXiv:1008.3628v4.

[10] Xingjie Helen Li and Mitchell Luskin. Lattice stability for atomistic chains modeled by local approximations of the embedded atom method. 2011. arXiv:1108.4473v1.

[11] M. Dobson, M. Luskin, and C. Ortner. Sharp stability estimates for force-based quasicontinuum methods. *SIAM J. Multiscale Modeling and Simulation*, 8:782–802, 2010.

[12] Matthew Dobson, Mitchell Luskin, and Christoph Ortner. Stability, instability and error of the force-based quasicontinuum approximation. *Archive for Rational Mechanics and Analysis*, 197:179–202, 2010.

[13] Jianfeng Lu and Pingbing Ming. Convergence of a force-based hybrid method for atomistic and continuum models in three dimension. arXiv:1102.2523v2.

[14] M. Dobson and M. Luskin. Analysis of a force-based quasicontinuum approximation. *M2AN Math. Model. Numer. Anal.*, 42(1):113–139, 2008.

[15] Matthew Dobson, Mitchell Luskin, and Christoph Ortner. Iterative methods for the force-based quasicontinuum approximation. *Computer Methods in Applied Mechanics and Engineering*, 200:2697–2709, 2011.

[16] M. Dobson, C. Ortner, and Alexander V. Shapeev. The spectrum of the force-based quasicontinuum operator for a homogeneous periodic chain. arXiv:1004.3435.

[17] E. B. Tadmor, M. Ortiz, and R. Phillips. Quasicontinuum analysis of defects in solids. *Philosophical Magazine A*, 73(6):1529–1563, 1996.

[18] V. B. Shenoy, R. Miller, E. B. Tadmor, D. Rodney, R. Phillips, and M. Ortiz. An adaptive finite element approach to atomic-scale mechanics–the quasicontinuum method. *J. Mech. Phys. Solids*, 47(3):611–642, 1999.

[19] M. Dobson and M. Luskin. An analysis of the effect of ghost force oscillation on the quasicontinuum error. *Mathematical Modelling and Numerical Analysis*, 43:591–604, 2009.

[20] Pingbing Ming and Jerry Zhijian Yang. Analysis of a one-dimensional nonlocal quasi-continuum method. *Multiscale Model. Simul.*, 7(4):1838–1875, 2009.

[21] Matthew Dobson, Mitchell Luskin, and Christoph Ortner. Accuracy of quasicontinuum approximations near instabilities. *Journal of the Mechanics and Physics of Solids*, 58:1741–1757, 2010.

[22] Alexander V. Shapeev. Consistent Energy-Based Atomistic/Continuum Coupling for Two-Body Potentials in One and Two Dimensions . *SIAM J. Multiscale Modeling and Simulation*, 9:905–932, 2011.

[23] Xingjie Helen Li and Mitchell Luskin. A generalized quasi-nonlocal atomistic-to-continuum coupling method with finite range interaction. *IMA Journal of Numerical Analysis*, to appear.

[24] C. Ortner and Lei Zhang. Construction and sharp consistency estimates for atomistic/continuum coupling methods with general interfaces: a 2d model problem. arXiv:1110.0168.

[25] T. Belytschko, S. P. Xiao, G. C. Schatz, and R. S. Ruoff. Atomistic simulations of nanotube fracture. *Phys. Rev B*, 65, 2002.

[26] Alexander V. Shapeev. Consistent energy-based atomistic/continuum coupling for two-body potentials in three dimensions. 2011. arXiv:1108.2991v1.

[27] M. Dobson and M. Luskin. An optimal order error analysis of the one-dimensional quasicontinuum approximation. *SIAM. J. Numer. Anal.*, 47:2455–2475, 2009.

[28] C. Ortner. A priori and a posteriori analysis of the quasinonlocal quasicontinuum method in 1D. *Math. Comp.*, 80:1265–1285, 2011.

[29] S. M. Foiles, M. I. Baskes, and M. S. Daw. Embedded-atom-method functions for the FCC metals Cu, Ag, Au, Ni, Pd, P, and their alloys. *Phys. Rev. B*, 33:7983–7911, 1986.

[30] Y. Mishin, M. J. Mehl, D. A. Papaconstantopoulos, A. F. Voter, and J. D. Kress. Structural stability and lattice defects in copper: Ab initio, tight-binding, and embedded-atom calculations. *Phys. Rev. B*, 63, 2001.

[31] R. A. Johnson and D. J. Oh. Analytic embedded atom method model for BCC metals. *JMR.*, 4:1195–1201, 1989.

[32] T. Belytschko and S. P. Xiao. Coupling methods for continuum model with molecular model. *International Journal for Multiscale Computational Engineering*, 1:115–126, 2003.

[33] Santiago Badia, Michael Parks, Pavel Bochev, Max Gunzburger, and Richard Lehoucq. On atomistic-to-continuum coupling by blending. *Multiscale Model. Simul.*, 7(1):381–406, 2008.

[34] Wing Kam Liu, Harold Park, Dong Qian, Eduard G. Karpov, Hiroshi Kadowaki, and Gregory J. Wagner. Bridging scale methods for nanomechanics and materials. *Comput. Methods Appl. Mech. Engrg.*, 195:1407–1421, 2006.

[35] S. Badia, P. Bochev, R. Lehoucq, M. L. Parks, J. Fish, M. Nuggehally, and M. Gunzburger. A force-based blending model for atomistic-to-continuum coupling. *International Journal for Multiscale Computational Engineering*, 5:387–406, 2007.

[36] Pablo Seleson and Max Gunzburger. Bridging methods for atomistic-to-continuum coupling and their implementation. *Communications in Computational Physics*, 7:831–876, 2010.

[37] Jacob Fish, Mohan A. Nuggehally, Mark S. Shephard, Catalin R. Picu, Santiago Badia, Michael L. Parks, and Max Gunzburger. Concurrent AtC coupling based on a blend of the continuum stress and the atomistic force. *Comput. Methods Appl. Mech. Engrg.*, 196(45-48):4548–4560, 2007.

[38] S. Prudhomme, H. Ben Dhia, P. T. Bauman, N. Elkhodja, and J. T. Oden. Computational analysis of modeling error for the coupling of particle and continuum models by the Arlequin method. *Comput. Methods Appl. Mech. Engrg.*, 197(41-42):3399–3409, 2008.

[39] Paul T. Bauman, Hachmi Ben Dhia, Nadia Elkhodja, J. Tinsley Oden, and Serge Prudhomme. On the application of the Arlequin method to the coupling of particle and continuum models. *Comput. Mech.*, 42(4):511–530, 2008.

[40] S. P. Xiao and T. Belytschko. A bridging domain method for coupling continua with molecular dynamics. *Comput. Methods Appl. Mech. Engrg.*, 193(17-20):1645–1669, 2004.

[41] C. Ortner and A. V. Shapeev. Analysis of an energy-based atomistic/continuum coupling approximation of a vacancy in the 2d triangular lattice. arXiv:1104.0311.

[42] Tom Hudson and Christoph Ortner. On the stability of bravais lattices and their cauchy-born approximations. 2010.

[43] P. Belik and M. Luskin. Sharp stability and optimal order error analysis of the quasi-nonlocal approximation of unconstrained linear and circular chains in 2-d. arXiv:1008.3716, 2010.

[44] C. Ortner and E. Süli. Analysis of a quasicontinuum method in one dimension. *M2AN Math. Model. Numer. Anal.*, 42(1):57–91, 2008.

[45] J.E. Jones. On the Determination of Molecular Fields. III. From Crystal Measurements and Kinetic Theory Data. *Proc. Roy. Soc. London A.*, 106:709–718, 1924.

[46] P.M. Morse. Diatomic Molecules According to the Wave Mechanics. II. Vibrational Levels. *Phys.Rev.*, 34:57–64, 1929.

[47] Robert Brooks Phillips. *Crystals, defects and microstructures: modeling across scales*. Cambridge University Press, 2001.

[48] B. Van Koten and C. Ortner. Blended atomistic/continuum hybrid methods I: Formulation and consistency. manuscript.

[49] W. K. Kim, E. B. Tadmor, M. Luskin, D. Perez, and A. F. Voter. Hyper-qc: An accelerated finite-temperature quasicontinuum method using hyperdynamics. 2011. manuscript.

[50] A. F. Voter. Parallel replica method for dynamics of infrequent events. *Phys. Rev. B*, 57:R13985R13988, 1998.

Appendix A

A Trace Inequality used in Chapter 5

In the following trace theorem, $S(1)$ denotes the unit sphere in $\mathbb{R}^d$, $r := |x|$ and $\theta := x/|x|$. Upon taking $\psi \equiv 1$ and employing standard orthogonal decompositions it is easy to check that the result is sharp. In particular, for $d = 2$, consider the case $u(x) = \log|x|$.

Lemma A.0.1 *Let $d \geq 2$, $\psi : S(1) \to (0, 1]$ be Lipschitz continuous, and $\Sigma := \{\psi(\sigma)\sigma : \sigma \in S(1)\}$. Moreover, let $0 < r_0 < r_1 \leq 1$, and $A := \bigcup_{r_0<r<r_1}(r\Sigma)$, then*

$$\|u\|^2_{L^2(r_0\Sigma)} \leq C_0\|u\|^2_{L^2(A)} + C_1\|\partial u\|^2_{L^2(A)}, \quad \forall u \in H^1(A), \tag{A.1}$$

$$\textit{where} \quad C_0 = \frac{2d}{r_1 - r_0}\Big(\frac{r_0}{r_1}\Big)^{d-1}, \quad \textit{and} \quad C_1 = \begin{cases} 2r_0|\log r_0|, & d = 2 \\ 2r_0/(d-2), & d \geq 3. \end{cases} \tag{A.2}$$

Proof Since A is a Lipschitz domain we may assume, without loss of generality that $u \in C^1(\bar{A})$. The symbol dS denotes the $(d-1)$-dimensional Hausdorff measure in $\mathbb{R}^d$.

Let $r_0 < s < r_1$, then

$$\begin{aligned} \int_{r_0\Sigma} |u|^2 dS = \; & r_0^{d-1} \int_\Sigma |u(r_0\sigma)|^2 dS_\sigma \\ = \; & r_0^{d-1} \int_\Sigma \left| u(s\sigma) - \int_{r=r_0}^{s} \frac{d}{dr} u(r\sigma) dr \right|^2 dS_\sigma \\ \leq \; & 2r_0^{d-1} \int_\Sigma \big|u(s\sigma)\big|^2 dS_\sigma + 2r_0^{d-1} \int_\Sigma \left| \int_{r=r_0}^{s} \partial u \cdot \sigma dr \right|^2 dS_\sigma. \end{aligned} \tag{A.3}$$

By hypothesis we have $|\sigma| \le 1$ for all $\sigma \in \Sigma$, hence the second term on the right-hand side can be further estimated, applying also the Cauchy–Schwartz inequality, by

$$\begin{aligned} 2r_0^{d-1} \int_\Sigma \left| \int_{r=r_0}^{s} \partial u \cdot \sigma dr \right|^2 dS_\sigma \le\ & 2r_0^{d-1} \int_\Sigma \int_{r=r_0}^{s} r^{-d+1} dr \int_{r=r_0}^{s} r^{d-1} |\partial u(r\sigma)|^2 dr\, dS_\sigma \\ =\ & 2r_0^{d-1}(J(s) - J(r_0)) \int_{r=r_0}^{s} \int_{r\Sigma} |\partial u|^2 dS\, dr \\ \le\ & 2r_0^{d-1}(J(s) - J(r_0)) \|\partial u\|^2_{L^2(A)}, \end{aligned}$$

where $J'(t) = t^{-d+1}$, that is, $J(t) = \log t$ if $d = 2$ and $J(t) = t^{-d+2}/(-d+2)$ if $d \ge 3$. Since $J(s)$ is negative and strictly increasing for $s \le 1$ we obtain

$$2r_0^{d-1} \int_\Sigma \left| \int_{r=r_0}^{s} \partial u \cdot \sigma dr \right|^2 dS_\sigma \le 2r_0^{d-1} |J(r_0)| \|\partial u\|^2_{L^2(A)}. \tag{A.4}$$

Inserting (A.4) into (A.3), multiplying the resulting inequality by s^{d-1} and integrating over $s \in (r_0, r_1)$ yields

$$\begin{aligned} \tfrac{r_1^d - r_0^d}{d} \|u\|^2_{L^2(r_0\Sigma)} =\ & \int_{s=r_0}^{r_1} s^{d-1} \int_{r_0\Sigma} |u|^2 dS\, ds \\ \le\ & 2r_0^{d-1} \int_{s=r_0}^{r_1} s^{d-1} \int_\Sigma \left|u(s\sigma)\right|^2 dS_\sigma\, ds + 2r_0^{d-1} J(r_0) \tfrac{r_1^d - r_0^d}{d} \|\partial u\|^2_{L^2(A)}. \end{aligned}$$

Dividing through by $\frac{r_1^d - r_0^d}{d}$ we obtain

$$\|u\|^2_{L^2(r_0\Sigma)} \le \tfrac{2dr_0^{d-1}}{r_1^d - r_0^d} \|u\|^2_{L^2(A)} + 2r_0^{d-1} J(r_0) \|\partial u\|^2_{L^2(A)}.$$

Finally, estimating $r_0^d - r_1^d \ge (r_1 - r_0) r_1^{d-1}$ yields the stated trace inequality. $\square$